BIOMETRIC IDENTIFICATION USING ELECTROCARDIOGRAM AND TIME FREQUENCY FEATURE MATCHING

BIOMETRIC IDENTIFICATION USING ELECTROCARDIOGRAM AND TIME FREQUENCY FEATURE MATCHING

BY

ABDULLAH BIRAN, MASc (Electrical and Computer Engineering),
Ryerson University, Ontario, Canada

A thesis
submitted to the School of Graduate Studies
of McMaster University
in partial fulfilment of the requirements
for the degree
of Doctor of Philosophy

Doctor of Philosophy (2023) McMaster University
(School of Biomedical Engineering) Hamilton, Ontario, Canada

TITLE: Biometric Identification using Electrocardiogram and time frequency feature matching

AUTHOR: Abdullah Biran
MASc. (Electrical and Computer Engineering)
Ryerson University, Toronto, Canada

SUPERVISOR: Prof. Aleksander Jeremic

NUMBER OF PAGES: xiii, 144

Abstract

The main goal of this thesis is to test the feasibility of human identification using the Electrocardiogram (ECG). Such biomedical signal has several key advantages including its intrinsic nature and liveness indicator which makes it more secure compared to some of the existing conventional and traditional biometric modalities. In compliance with the terms and regulations of McMaster University, this work has been assembled into a sandwich thesis format which consist of three journal papers. The main idea of this work is to identify individuals using distance measurement techniques and ECG feature matching. In addition, we gradually developed the content of the three papers.

In the first paper, we started with the general criteria for developing ECG based biometric systems. To explain, we proposed both fiducial and non-fiducial approaches to extract the ECG features followed by providing comparative study on the performance of both approaches. Next, we applied non-overlapped data windows to extract the ECG morphological and spectral features. The former set of features include the amplitude and slope differences between the Q, R and S peaks. The later features include extracting magnitudes of the ECG frequency components using short time Fourier Transform (STFT). In addition, we proposed a methodology for QRS detection and segmentation using STFT and binary classification of ECG fiducial features.

In the second paper, we proposed a technique for choosing overlapped data windows to extract the abovementioned features. Namely, the dynamic change in the ECG features from heart beats to heartbeat is utilized for identification purposes. To improve the performance of the proposed techniques we developed Frechet-mean based classifier for this application. These classifiers exploit correlation matrix structure that is not accounted for in classical Euclidean techniques. In

addition to considering the center of the cluster, the Frechet-mean based techniques account for the shape of the cluster as well.

In the third paper, the thesis is extended to address the variability of ECG features over multiple records. Specifically, we developed a multi-level wavelet-based filtering system which utilizes features for multiple ECGs for human identification purposes. In addition, we proposed a soft decision-making technique to combine information collected from multi-level identification channels to reach a common final class. Lastly, we evaluated the robustness of all our proposed methods over several random experiments by changing the testing data and we achieved excellent results.

The results of this thesis show that the ECG is a promising biometric modality. We evaluated the performance of the proposed methods on the public ECG ID database because it was originally recorded for biometric purposes. In addition, to make performance evaluation more realistic we used two recordings of the same person obtained under possibly different conditions. Furthermore, we randomly changed both the training and testing data which are obtained from the full ECG records for performance evaluation purposes.

However, it is worth mentioning that in all parts of the thesis, various parameters settings are presented to support the main ideas and it is subject to change according to human activity and application requirements. Finally, the thesis concludes with a comparison between all the proposed methods, and it provides suggestions on few open problems that can be considered for future research as extension to the work that has been done in this thesis. Generally, these problems are associated with the constraints on computational time, data volume and ECG clustering.

Acknowledgement

I would like to take the opportunity to thank some academic institutions and very special people; without their help this thesis would never have been written. First and foremost, I would like to thank the Biomedical Engineering Department at King Faisal University (BME KFU), the Deanship of Postgraduate Studies at KFU and the Saudi Arabian Cultural Bureau (SACB) in Ottawa for accepting me in their scholarship program, for believing in me, and for all the kinds of support they gave me during these five years.

Next, I would like to thank Dr. Aleksander Jeremic for accepting me as Ph.D. student and guiding me in both theoretical and practical knowledge of field of study. I would like to thank him for all his academic support which provided me with sources of motivation throughout my Ph.D. studies at McMaster. I would like also to thank the McMaster School of Biomedical Engineering for accepting in their Ph.D. Program which helped me to pursue my academic goals.

I would like to show my gratitude to my spouse Ms. Eman Mohammed whose presence has always been priceless. Being with such a gifted person and great mom of our daughter Nawal Biran has tremendously helped with passing the somehow gloomy days, which are an inevitable part of an international student.

Last but by no means least, I would like to thank my father and my mother for their unconditional love and consistent support through all the years, without which all my achievements have simply been impossible. They have been my sources of motivation in every academic step I took from the very first day of school up until this moment that I am finishing my Ph.D. studies. I could not wish for a better parent, and I hope I did well for all their kindness.

Contents

Lists of Figures

Lists of Tables

Declaration of Academic Achievement

This research presents analytical and computational work carried out solely by Abdullah Biran, herein referred to as “the author”, with advice and guidance provided by the academic supervisor Prof. Aleksander Jeremic. Information that is presented from outside sources which has been used towards analysis or discussion, has been cited when appropriate. All other materials are the sole work of the author.

The Impact of COVID 19 on Research Plan

The Covid 19 pandemic upended higher education, with widespread lockdowns and restrictions starting in March 2020 in Canada. Consequently, McMaster University switched to online learning in winter 2020. This unexpected move had negatively impacted some of the research objectives and led to a few changes in the research plan. As part of developing ECG based human identification system, one of the major objectives of this research was to conduct experiments to collect ECG database from human participants. This major objective of the thesis was canceled due to the strict restrictions on social gathering. The authors continued using the public ECG ID database for testing the performance of their methodologies and have successfully achieved satisfactory and promising results.

Chapter 1

1 Introduction

1.1 Background

The existing human identification systems, which aim to identify individuals using their physiological or behavioral features, have been widely applied in different fields including access control, information, finance, medicine, and communication. For example, fingerprints, face, and iris are some of the unique anatomical traits that are used in physiological based identification systems. On the other hand, voice, gait, and signature are functional characteristics that are utilized in behavioral based identification systems. Generally, both physiological and behavioral characteristics satisfy most of the requirements which define biometrics, such as universality, distinctiveness, ease in collectability, robustness, user acceptability and permanence [1] [2].

However, because of their extrinsic nature the main drawbacks of the existing biometric systems include mainly the risks of direct attack or fraud. For example, fingerprints can be falsified using gelatin materials or they can be damaged due to some state of work environment conditions. The iris can be spoofed with the use of copied contact lenses, or it can be faked using close eye picture of an authorized individual. Moreover, the personal voice can be cloned through recording and the face can be physically damaged or artificially disguised. Therefore, researchers have been working to develop robust biometrics that are more resistant to direct attacks and can be difficult to fake by unauthorized users [3] [4].

In recent years, electrocardiogram (ECG) based biometric systems have gain great attention as an alternative way for identifying humans. The uniqueness of ECG signal is supported by the fact that the physiological, morphological, and geometrical characteristics of the cardiac signal differs

from person to person. In addition, the ECG information is highly secure, safe, and private due to its intrinsic nature, which makes it hard to copy. Furthermore, the inherit nature of ECG as a life indictor measured only in living individuals makes it difficult to be forged. Therefore, ECG based biometric system have been proposed as replacement for exiting human identification systems [2] [3] [5].

1.2 The ECG as Biometric Modality

The ECG, which is a graphic display analyzed by time intervals and segment, is a measurement of the electrical activity of the heart. It typically consists of three complex waves which are known as P, QRS, and T waves (see Figure 1.1). Each of these ECG waves corresponds to different parts of the cardiac cycle and it has its own unique features and patterns. Physiologically, the P wave indicates atrial activation, the QRS complex represents the ventricular activation, and the T wave indicates the ventricular repolarization. Practically, the ECG has been extensively and widely utilized for detecting cardiac abnormalities and health monitoring. However, in the recent years there has been a growing interest in the usage of ECG as biometric modality [1] [3] [6].

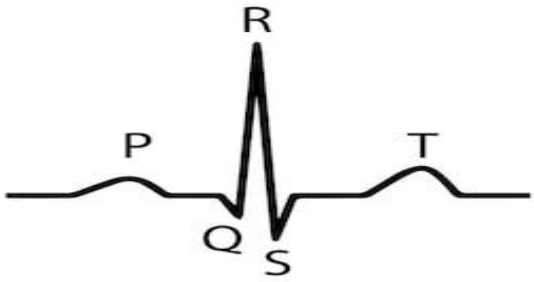

Figure 1.1: Normal wave components of a heartbeat

The ECG has a variety of significant geometrical, morphological, biological, and technical characteristics which highly advocate its usage as new approach in human authentication. To illustrate, the distinctiveness of ECG from person to person might be due to the differences in shape, amplitude, and time interval of the heartbeat components. In addition, the uniqueness of

ECG among individuals can be due to the differences in heart anatomy, position, size, relative body weight and chest configuration. Technically, the ECG can be easily collected using a single lead (e.g., by using two active electrodes and a ground electrode). Furthermore, it is difficult to fabricate the ECG because of the presence of vitality signs, which make the ECG more reliable and safer way for identification. Moreover, the intrinsic nature of ECG, the good stability and reproducibility are other factors that highly supports the feasibility of using ECG for biometric applications [1] [7] [8].

1.3 ECG-based Identification System (ECGBIS)

Generally, the ECG based identification system consists of three main stages which are preprocessing, features extraction and classification as shown in Figure 1.2. To build a robust ECGBIS, the following processes must be followed: 1) the signal must be filtered from noise components, 2) then, distinctive features have to be extracted, and 3) the appropriate classifiers for identification purposes should be utilized.

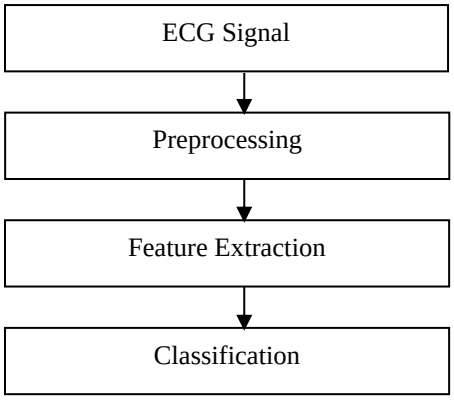

Figure 1.2: General Block Diagram of the ECG based Identification System

1.3.1 Preprocessing

The raw ECG data are difficult to deal with because they usually contain different types of noise such as baseline wander (BW) artifacts, muscle artifacts (MA), electrode motion (EM) and

power line interference (PLI). These components change the normal structure of the signal, and they must be filtered to enhance the performance of the ECGBIS. Generally, high pass, low pass, band pass and notch filters can be used to remove the ECG noises [3] [9] . Table 1.1 shows the different types, sources and frequency range of noises contained in the ECG [10].

Table 1.1: Different types, sources, and frequency range of noises in ECG signal

Noise	Source of Noise	Frequency Range
Baseline Wander (BW)	body movement and breathing	Below 1 Hz
Muscle Artifacts (MA)	motion and potentials from other muscles	20 Hz to 1000 Hz
Electrode Motion (EM)	motion of the electrode in relation to the subject's skin	1 Hz to 15 Hz
Power Line Interference (PLI)	sinusoidal current from the power grid	50 or 60 Hz

1.3.2 Feature Extraction

Feature extraction is a task of extracting significant and distinctive information from the ECG. Since it transfers the information to the classifiers, feature extraction is specifically important stage due to its great influence on the identification outcome. In addition, the uniqueness of the personal ECG highly depends on the reliability, selectivity, and accuracy of the ECG feature extraction. Based on the category of the extracted features, the existing ECG biometric systems fall into two groups which include detection of fiducial features which require segmentation of heartbeat waveforms and detection of non-fiducial features which can be defined as transform based approaches [1] [3] [9]. Table 1.2 shows the different types of fiducials and non fiducial features that can be used in ECGBIS [9].

Table 1.2: Different types of fiducials and non fiducial features of the ECG [9].

Type of features	Category	Examples
Fiducial	Temporal	1. Time intervals of the ECG waves or peaks. 2. Duration of heartbeat. 3. RR interval.
	Amplitude	1. Amplitudes of the P, Q, R, S, T peaks. 2. The ratio between peaks Amplitude's. 3. 1st or 2nd derivatives.
	Morphological	1. Heartbeat shape. 2. Area of ECG waves. 3. Slopes.
Non-Fiducial	Autocorrelation	1. Normalization the QRS (or heartbeat) shape. and length using AC techniques.
	Phase Space	1. Multi dimensional phase space analysis of ECG. 2. String Matching techniques.
	Frequency	1. Instantaneous analysis of ECG frequency data. 2. Heartbeat based frequency analysis. 3. Signal duration-based frequency analysis.

In general, fiducial-based approaches relay on locating the ECG fiducial points followed by extracting significant temporal, amplitude, and morphological features. These set of features are extracted from segmented heartbeats. The temporal features are defined as the locations and time durations of the P, Q, R, S and T points. On the other hand, the amplitude features include mainly the magnitudes of the ECG peaks. In addition, the morphological features are represented by differences in slopes, shapes, and angles between the P, QRS and T waves. Clearly, the best identification performance using fiducial approaches depends on the accuracy of detecting the P, Q, R, S and T points [1] [3] [9] [11].

In contrast, the non-fiducial-based approaches relay on extracting distinctive features without the need of heartbeat segmentation. In other words, the non-fiducial detection can be defined as transform-based approaches. Precisely, the non-fiducial ECG features are extracted from applying

methods such as Fourier transform (FT), discrete cosine transform (DCT), autocorrelation (AC) and wavelet transform (WT). Clearly, these approaches alleviate the demand to precisely detect the ECG peaks and they generally require smaller computational time [1] [9] [11].

1.3.3 Classification

In ECGBIS, data classification is a process of correctly assigning the transformed features into a specific subject (class). To achieve such goal, the ECG records are usually divided into training data and a testing data, which are mainly used for the purposes of classifier design and performance evaluation. Accordingly, many ECG samples per subject are required to achieve the best identification performance.

Generally, the classifiers used in ECGBIS are designed based on distance measurement techniques [8]. To explain, the conventional distance-based classification approaches assign unknown test sample to the nearest referencing samples in the feature space. Relatively, there are several distance functions that can be unutilized for finding the distance between feature vectors or matrices including the Euclidean distance (ED), the Fréchet distance (FD) and correlation coefficient [12] [13] [14]. Specifically, the Frechet distance is used to calculate the distance between two Gaussian distributions. Since the calculation of this distance enables inclusion of various covariates, we expect that it may be suitable for ECG based identification by accounting for the covariates between features in an efficient way. In general, the conventional distance-based approaches are robust, accurate and computationally simple.

On the other hand, classification approaches based on neural networks (NN) have been also applied [15] [16]. These methods are designed to solve non-linearly separable problems using algorithms such as the multi layer perception (MLP). In short, the basic MLP consists of at least three layers of nodes: an input layer, a hidden layer, and an output layer. Each node in these layers

is a neuron consisting of a nonlinear activation function. These multi functions are utilized to classify the unknown data to specific class [17]. The main advantage of utilizing NN based methods includes its robustness of solving complex non-linear classification problems.

In contrast to the previous methods, hierarchical based approaches (HBA), which aim to solve the data classification problems by dividing large class data into small classes, have been also applied [18] [19]. Technically, hierarchical methods apply multi level classification technique to assign the subjects into different groups. Hence, hierarchical methods can be beneficial to classify confused data; for instance, classifying subjects who can not be classified in the abovementioned classification approaches.

1.4 Challenges

There are several challenges in the potential use of ECG for human identification. First, because ECG is time variant signal, the recorded data is usually different whenever it is measured. This critical issue directly effects the reliability of the ECG features, specifically, the fiducial features. Hence, it reduces the performance of the identification systems. However, this problem can be addressed by using data normalization techniques in order to account for heart rate variability i.e. normalizing the ECG data to the heart rate or to the dynamic change of ECG features. Another challenge in developing ECGBIS is the need for large number of personal data samples which is required to further attenuate any significant changes in the measured data [2]. Although, there is no agreement in the adequate number of required measurements, it is a practical problem which can be addressed at the enrollment stage through recording the ECG on a scheduled basis. Since the size of the training set will depend on the application, the size of the required training set should be determined by performance requirements for a given application. In general, the consensus on the size of the training set is non-existent in any applications. Most importantly, the variability of

ECG during life span is a challenging problem which also requires to record the ECG on regular basis. In addition, the population size and real time identification are other challenges that yet need to be addressed. Table 1.3 summarizes the main challenges in designing ECGBIS.

Table 1.3: Summary of the main challenges for designing ECGBIS

Category	Challenges
Signal and data based	1. Defining the appropriate population size that is enrolled in ECGBIS research. 2. Collecting real ECG database for developing biometric systems. 3. Establishing standards for ECG acquisition for biometric applications.
Feature Based	1. Selecting and extracting reliable features. 2. Addressing the inter-subject and intra-subject variability of ECG features. 3. Addressing the variability of ECG during life span.
Classification and application based	1. Choosing the appropriate classifiers based on the feature characteristics. 2. Reducing the componential time for quick individual identification. 3. Defining the application fields for utilizing ECGBIS.

1.4.1 Theme and Objectives of Dissertation

In compliance with the terms and regulations of McMaster University, this dissertation has been assembled into a *sandwich thesis* format which consist of three journal papers. The articles in the dissertation follow a consistent theme that aims to expand the current knowledge in using ECG for human identification and its practical applications. The general theme of the study is designed according to the main objectives of the thesis which include:

i) To efficiently develop a simple ECG biometric model that is based on selecting both fiducial and non-fiducial features (Paper I).

ii) To effectively develop a methodology for ECGBIS that is based on addressing the dynamic change of fiducial and non-fiducial features of multiple heartbeats (Paper II).

iii) To apply different conventional distance measurements for ECG data classification (Papers I and II).

iv) To mathematically apply different conventional distance measurements for correctly classifying the ECG data based on the geometrical characteristics of the feature space (Papers II and III).

v) To effectively build a stable and robust ECGBIS through enrolling different ECG measurements and randomly selecting the ECG samples (Papers I, II and III).

vi) To efficiently propose an automatic algorithm to classify and identify the participants using multiple ECGs recorded on different days (Paper III).

vii) To mathematically implement a statistical information fusion method for reaching a common final decision (identification) (Paper III)

1.5 Summary of Enclosed Articles

The papers enclosed in this thesis are listed as follows:

1.5.1 Paper I (Chapter II)

Abdullah Biran and Aleksander Jeremic, A study based on fiducial and non-fiducial methods via applying the Short Time Fourier Transform and histograms of QRS features for ECG based human identification, European Journal of Biomedical Informatics, vol. 19, no. 1, 2023.

Preface: This paper provides a comparative study to test the feasibility of using ECG for human identification. Both fiducial and non-fiducial based algorithms have been proposed. Because the former method requires segmentation, we contributed to developing an automatic algorithm for detecting the QRS waves, which have majority of the ECG information. Then, amplitude and morphological features are extracted, normalized, and utilized for subject's identification. At the classification stage, we used the Euclidian distance to find the minimum distance between

histograms of fiducial features. In the later method, we used the Short Time Fourier Transform (STFT) to extract the non-fiducial features of multiple heart beats. Then, we proposed a normalized distance-measurement for classification purposes. Our results indicate that the non-fiducial method has shown great performance for individual identification, and it generally outperforms the fiducial based method.

1.5.2 Paper II (Chapter III)

Abdullah Biran and Aleksander Jeremic, ECG bio-identification using Fréchet classifiers: A proposed methodology based on modeling the dynamic change of the ECG features, Elsevier Journal of Biomedical Signal Processing and Control, vol. 82, 2023.

Preface: This paper expands on the concept of using the Fréchet distances as classifiers that are utilized for minimizing the distance between two feature matrices. Differently from the previous approach, this paper presents a main contribution that is based on utilizing the Short Time Fourier Transform (STFT) to capture the dynamic change in the ECG frequency components, which can be utilized as a unique characteristic. In addition, we developed a method to track the dynamic change in the QRS complex features of multiple consecutive heartbeats. Specifically, we created multiple cross feature matrices and utilized them for human identification. Most importantly, the first approach, which is based on the tracking the dynamic change in the frequency components, has shown excellent and promising results.

1.5.3 Paper III (Chapter IV)

Abdullah Biran and Aleksander Jeremic, The feasibility of human identification from multiple ECGs using Maximal Overlap Discrete Wavelet Transform (MODWT) and Weighted Majority Voting Method (WMVM), Digital Medicine and Healthcare Technology, vol. 2, 2023.

Preface: Most of the existing approaches ignored the variability of ECG features. Therefore, this paper presents a contribution that is based on addressing the variability of ECG features at the preprocessing stage by performing data filtering methods. Multiple ECGs which are recorded on two different days have been used. At each filtering level, the MODWT have been applied to create multiple filtered ECG signals followed by extracting the dynamic change in the frequency components. In addition, we proposed a new technique for data fusion at the classification stage. To reach the best identification performance, we present in this paper our scoring WMVM that is utilized to combine multiple decisions obtained from our multi-channel filtering system to reach a final common decision. Most importantly, the proposed methods in this paper have shown excellent performance on the feasibility of human identification using ECGs recorded on different days.

References

[1] S. Chauhan, A. S. Arora, and A. Kaul, "A survey of emerging biometric modalites," *Procedia Computer Science* vol. 2, pp. 213-218, 2010.

[2] X. Dong, W. Si, and W. Yu, "Identity Recognition Based on the QRS Complex Dynamics of Electrocardiogram," *in IEEE Access,* vol. 8, pp. 134373-134385, 2020.

[3] M. M. Tantawi, K. Revett, M. F. Tolba, and A. Salem, "On the use of the electrocardiogram for biometrie authentication," *The 8th International Conference on Informatics and Systems,* pp. BIO-48-BIO-54, 2012.

[4] S. C. Wu, P. L. Hung, and A. L. Swindlehurst, "ECG Biometric Recognition: Unlinkability, Irreversibility, and Security," *IEEE Internet of Things Journal,* vol. 8, no. 1, pp. 487-500, 2021.

[5] E. Alkeem *et al.*, "An Enhanced Electrocardiogram Biometric Authentication System Using Machine Learning," *in IEEE Access*, vol. 7, pp. 123069-123075, 2019.

[6] H. Ko *et al.*, "ECG-Based Advanced Personal Identification Study With Adjusted (Qi * Si)," *in IEEE Access*, vol. 7, pp. 40078-40084, 2019.

[7] D. Wang, Y. Si, W. Yang, G. Zhang, and J. Li, "A Novel Electrocardiogram Biometric Identification Method Based on Temporal-Frequency Autoencoding," *Electronics*, vol. 8, no. 6, p. 667, 2019.

[8] Y. N. Singh and S. K. Singh, "Evaluation of electrocardiogram for biometric authentication," *Journal of Information Security*, vol. 3, no. 1, pp. 39- 48, 2012.

[9] A. Fratini , S. Mario, B. Paolo, and C. Mario. "Individual Identification Via Electrocardiogram Analysis." BioMedical Engineering OnLine. (accessed.

[10] Z. F. Mohd Apandi, R. Ikeura, S. Hayakawa, and S. Tsutsum, "An Analysis of the Effects of Noisy Electrocardiogram Signal on Heartbeat Detection Performance," *Bioengineering*, vol. 7, no. 2, p. 53, 2020.

[11] D. P. Coutinho, H. Silva, H. Gamboa, A. Fred, and M. Figueiredo, "Novel fiducial and non-fiducial approaches to electrocardiogram-based biometric systems," *in IET Biometrics*, vol. 2, no. 2, pp. 64-75, February 2013.

[12] A. D. C. Chan, M. M. Hamdy, A. Badre, and V. Badee, "Wavelet Distance Measure for Person Identification Using Electrocardiograms," *in IEEE Transactions on Instrumentation and Measurement*, vol. 57, pp. 248-253, February 2008.

[13] Y. Gahi, M. Lamrani, A. Zoglat, M. Guennoun, B. Kapralos, and E. El-Khatib, "Biometric Identification System Based on Electrocardiogram Data," *New Technologies, Mobility and Security*, pp. 1-5, 2008.

[14] N. Venkatesh and S. Jayaraman, "Human Electrocardiogram for Biometrics Using DTW and FLDA," *20th International Conference on Pattern Recognition,* pp. 3838-3841, 2010.

[15] M. M. Tawfik, H. Selim, and T. Kamal, "Human identification using time normalized QT signal and the QRS complex of the ECG," *7th International Symposium on Communication Systems, Networks and Digital Signal Processing*, vol. 3, no. 1, pp. 755-759, 2010.

[16] F. Tashiro *et al.*, "Individual identification with high frequency ECG : Preprocessing and classification by neural network," *33rd Annual International Conference of the IEEE Engineering in Medicine and Biology Society,* pp. 2749-2751, 2011.

[17] V. Mai, I. Khalil, and C. Meli, "ECG biometric using multilayer perceptron and radial basis function neural networks," *33rd Annual International Conference of the IEEE Engineering in Medicine and Biology Society,* pp. 2745-2748, 2011.

[18] Y. Wang, F. Agrafioti, D. Hatzinakos, and N. K. Plataniotis, "Analysis of human electrocardiogram for biometric recognition," *EURASIP Journal on Advances in Signal Processing,* p. 1:148658, 2008.

[19] Y. Zhang and Y. Shi, "A new method for ECG biometric recognition using a hierarchical scheme classifier," *6th IEEE International Conference on Software Engineering and Service Science*, pp. 457-460, 2015.

Chapter 2

2 A study based on Fiducial and Non-Fiducial methods via applying the Short Time Fourier Transform and Histograms of QRS Features for ECG based human identification

2.1 Abstract

Biometric systems have been a subject of considerable research interest for human identification. In this paper, we present both fiducial and non-fiducial methods for individual identification. In both methods, we randomize the process of data selection and we use different referencing and testing windows to examine the stability of our methods. Our identification system randomly selects both the referencing and testing data by utilizing multiple data windows from the full ECG record. The first identification method is based on extracting multiple bivariate histograms of fiducial QRS features. Namely, these features are the amplitude and slope differences between the Q, R and S peaks. Then, we find the Euclidean distance between these multiple histograms for classification purposes. Additionally, we propose an algorithm which automatically segments the QRS waves using Short Time Fourier Transform (STFT) and single feature-based classification process. The second non-fiducial identification method is based on finding the magnitudes of the frequency components from the ECG data. Then, we utilize the normalized STFT distance between these frequency components for classification purposes. Technically, our identification process is

based on finding the minimum Euclidean distance between a single random testing data and multiple random referencing data. We tested the applicability of our methodology on 124 ECG records of 62 subjects. Our results show that the non-fiducial-based method requires less ECG samples and it outperforms the fiducial-based method. Specifically, we achieved the best performance of 99.64% average identification accuracy by selecting 50% of the ECG data length and applying the non-fiducial method. In comparison, we achieved the best performance of 96.61% average identification accuracy by selecting 85% of the ECG data length and applying the fiducial-based method. These findings indicate that the ECG is a unique signal which can be utilized as biometric modality.

2.2 Introduction

Biometric technologies which relay on individual intrinsic characteristics have several advantages compared to knowledge-based approaches and they are currently used in wide range of applications. Moreover, most of the existing biometric systems relay on the personal physical traits such as face, fingerprint, and iris. However, there are several security and privacy concerns associated with these biometric systems as they can be damaged or stolen. Therefore, biomedical signals are recently emerging as alternative biometric modalities [1]. The potential use of biomedical signals for human identification has been a considerable research topic in previous studies [1]. Specifically, the feasibility of utilizing the Electrocardiogram (ECG) for individual recognition has shown promising results in many reported studies [2] [3] [4] [5]. Namely, the universality, hidden nature and simple acquisition of the ECG make it an excellent trait for bio-identification [1]. Unlike the traditional biometric systems which are based on physical traits, the innate nature of ECG as vital sign makes it extremely hard to steal or fraud. Additionally, the ECG

can be safely and noninvasively measured. Thus, biometric systems based on ECG sufficiently decrease the privacy and security concerns.

The existing ECG based human identification system are divided into two major categories which are fiducial and non-fiducial methods [1]. The former techniques mainly depend on locating the heart waveform points, onsets and offsets. Additionally, such fiducial based methods relay on extracting several amplitude, temporal and morphological features from the ECG. The later techniques apply non-segmented based algorithms such as autocorrelation, wavelet coefficients, principal component analysis (PCA) and Fourier transform (FT) to extract significant ECG features. Generally, non-fiducial based methods have smaller computational time compared to fiducial based methods. However, due to the variability of the ECG characteristics, both approaches have been widely applied [5].

Recently, several methods for ECG based human identification have been reported. In [6] the authors proposed a non-fiducial method using spectral correlation images and convolutional neural networks (CNN). They have tested the performance of their algorithm using public data of normal and abnormal ECG recordings. In contrast, in [7]. the authors proposed fiducial points-based method to extract combined temporal and amplitude feature vectors, which are utilized for human identification by applying distance measurements.

Moreover, in our previous work [8] [9], we initially developed fiducial and non-fiducial techniques to test the feasibility of utilizing ECG as biometric modality. In this paper, we expand on our previous work by randomly selecting different data windows to test the stability of our methodology. Generally, our previous work [8] is based on performing Short Time Fourier Transform (STFT), extracting QRS features, and applying the Euclidian distance for classification purposes using a single data window for referencing and testing purposes. Similarly, in [4] the

authors have proposed both fiducial and non-fiducial approaches to examine the applicability of human identification in real time ECG based biometric systems by extracting a total of 53 features from the P-QRS-T waves. Whereas in the non-fiducial methodology [4], they used information theory tools, converting the ECG signal values into sequence of symbols (strings).

Zhang et al. [10] proposed a multiresolution convolutional neural network (MCNN) technique. The ECG segments were blindly selected and automatically analyzed using discrete wavelet transform (DWT). A multi scale autoregressive model method (MSARM) algorithm for human identification using ECG was proposed by Liu et al. [11]. Such method is based on obtaining the power spectrum features of the ECG signal at different scale levels and weights using the DWT. In [12], the authors presented heart rate dependent methodology for human identification. Individual's unique model was created by addressing the morphological changes using a combination of Gaussian mixture model (GMM), Hidden Markov model (HMM) and subject's specific thresholding criteria.

Additionally, Adrian et al. [13] have proposed a method using wavelet-based distance measure. Saiful et al. developed a method using the heartbeat morphology features [3]. Lin et al. [14] developed an algorithm based on nonlinear Lyapunov exponents, root mean square (RMS) and support vector machine (SVM), Unlike [13] [3] [4] where the ECG data were recorded under resting state, Lin et al. focused on investigating the applicability of using ECG as biometric modality during working body states. Their study involved ECGs recorded after participants performed an exercise.

Furthermore, Sidek et al. [15] investigated the feasibility of ECG signal as biometric trait in abnormal cardiac conditions such as super ventricular arrythmia, cardiac autonomy neuropathy and atrial fibrillation. Odinaka et al. [16] proposed a multibiometric system based on combining

both the electrical originating signal, the ECG, and the laser Doppler vibrometry (LDV) mechanical signal. Gutta and Cheng [2] proposed discrete cosine transform (DCT) and autocorrelation techniques for extracting non-fiducial ECG features.

In contrast, in [17] the authors developed a numerical algorithm to extract fiducial-based time and amplitude features. More work about the recent advances in utilizing the ECG for human identification can be found in [18].

In this paper, we aim to test the applicability of using the ECG for human identification by proposing both fiducial and non-fiducial-based approaches. Moreover, we aim to study the influence of changing the length the of the ECG data for achieving the best possible performance. Differently from our previous work, we randomize the process of ECG data selection. Briefly, the identification process using the non-fiducial method is based on finding the STFT of randomly selected ECG data followed by obtaining the minimum normalized Euclidean distance. In the fiducial method, the ECG data are also randomly selected; however, the identification process depends on computing four fiducial QRS features followed by finding histogram-based distances. Moreover, we present in this paper our proposed method for automatic QRS detection and segmentation.

2.3 Methods

Generally, we propose two methods for utilizing the ECG for human identification. In section 2.3.1, we introduce the public ECG ID database and we explain our preprocessing step on Automatic QRS detection and classification. In sections 2.3.2 and 2.3.3, we explain our fiducial and non-fiducial methods for ECG based identification respectively. Moreover, Figure 2.1 shows the block diagram of our proposed method for automatic QRS detection. In addition, Figure 2.2 shows the block diagram of our proposed ECG Bio-identification methods.

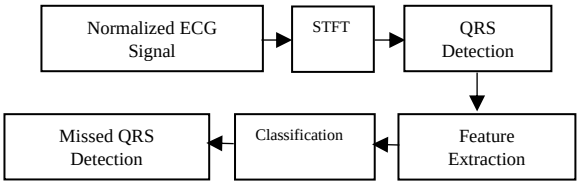

Figure 2.1: Block diagram of the proposed methodology for automatic QRS detection

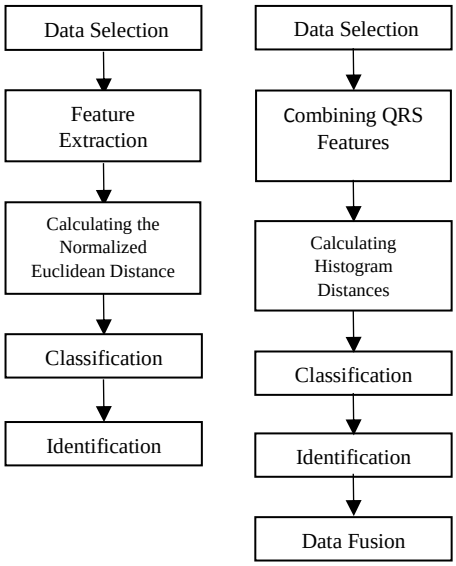

Figure 2.2: Block diagram of the proposed methodology for ECG based human identification

2.3.1 Automatic QRS detection and Classification

We present here a new automatic technique for QRS detection because it is a major step in fiducial-based identification systems [3]. Technically, this is a preprocessing step to locate the Q, R and S peaks from all the ECG records to reduce the computational time of QRS feature extraction in our fiducial method which will be explained later in this paper. Relatively, our method accurately detects the QRS waves using STFT and QRS features.

2.3.1.1 ECG Database

In this study, we used ECGs of 62 subjects from the publicly available ECG ID database [19]. The ECGs were measured using single lead at 500 Hz sampling frequency. Each of these ECG

signals was measured for a duration of 20 seconds ($n_l = 10000$ samples). In this paper, we selected two different ECG records which are measured over a six-month period. In addition, the public ECG ID database has a preprocessed version of the ECG recordings. Therefore, we use the filtered versions of the ECG ID database to simplify the algorithm implementation.

Following majority of the existing algorithms [20] for human identification, we normalize the data before applying advanced techniques. This data normalization procedure is expected to enhance the identification process because different subjects might have similar features such as the frequency components. Therefore, we use equation (2.1) to normalize the ECG database.

$$x(t) = \frac{x(t) - Min(\boldsymbol{X})}{Max(\boldsymbol{X}) - Min(\boldsymbol{X})} \quad (2.1)$$

2.3.1.2 Applying short time Fourier transform

Short Time Fourier transform is well known tool which is widely applied in signal processing field. Most importantly, STFT robustness in analyzing signals whose power spectral density change with time, makes it an excellent method to detect specific components that are contaminated in the signal [21]. In this work, we apply STFT on sub-signals that are derived from the full ECG. We subdivide each ECG into many n_w sub-signals. For the rest of this paper, we will use the notation $\boldsymbol{X_w}$ to refer to any single sub-signal obtained from the full ECG where $w = 1,2,3, \ldots . n_w$ refers to index of the sub-signal. Technically we subdivide the main ECG using a window of length n_s samples and we obtain n_w many sub-signals. Note that we set n_s approximately to a length of a full heartbeat; however, this generally depends on the personal heart rate and the ECG sampling frequency. In addition, we choose $n_o = n_s/2$ samples of overlap between the many adjoining sub-signals. Therefore, the total number of the overlapped sub-signals is calculated using equation (2.2). Consequently, we obtain the time matrix $X \in R^{n_s \times n_w}$.

$$n_w = \frac{n_l}{n_o} - 1 \quad (2.2)$$

2.3.1.3 QRS detection

The QRS complex, is the largest wave in a normal ECG and it has most of the ECG frequency components. Therefore, after we perform STFT on n_w many sub-signals, we select only the sub-signals which contain the large percentage of power. However, the actual number of QRS vary between subjects and it highly depends on the personal heart rate. Therefore, we set our proposed method to initially extract a maximum of n_{qrs} many QRS waves. Mathematically, we apply equation (2.3) to compute the frequency components:

$$FR_w(k) = \sum_{m=0}^{n_{ft}} \boldsymbol{X_w}(m) e^{-j\left(\frac{2\pi}{n_{ft}}\right)km} \tag{2.3}$$

where n_{ft} is the number of the STFT sampling points.

After applying equation (2.3), we only select the magnitude components. Since we set $n_{ft} = n_w$, we define here the symmetric amplitude matrix $A \in R^{n_w \times n_w}$. Then we perform summation:

$$e_w = \sum_{m=1}^{n_{ft}} a_{m,w} \tag{2.4}$$

where $\boldsymbol{A_w}$ has the magnitude components of all frequencies in the wth sub-signal.

Consequently, we obtain $\boldsymbol{E} \in R^{n_w}$. The QRS detection process depends on finding n_c many maximum values of $\boldsymbol{E}$. i.e., the corresponding index of each value (w), is an estimate index of $\boldsymbol{X_w}$ containing a QRS wave. However, note that because of the 50% samples overlap, one full QRS can exist in two consecutive sub-signals. In these cases, we remove the double detection of a similar QRS based on the R-R interval. Consequently, we extract $n_b \leq n_{qrs}$ many sub-signals from n_w many sub-signals. Figure 2.3 shows spectrograms of different sub-signals including QRS segments which have significant amplitudes. It shows that spectrograms of sub-signals containing

QRS waves (the top 2) have higher amplitudes than spectrograms of sub-signals containing non QRS waves (the bottom 2).

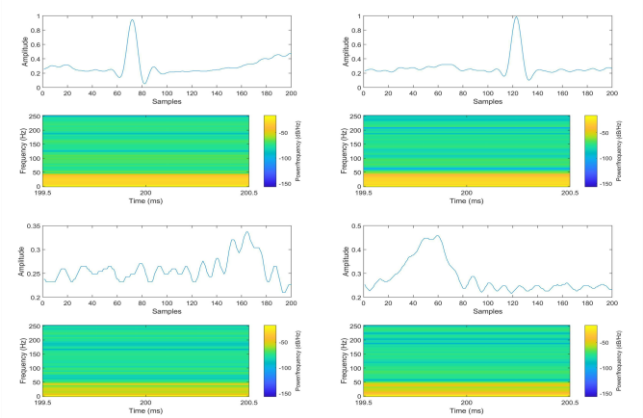

Figure 2.3: Multiple ECG sub signals and their spectrograms

2.3.1.4 Feature Extraction

The proposed algorithm classifies each of the n_b many selected sub-signals into QRS segment or non QRS segment by extracting four morphological and amplitude features. For each of these n_b many sub-signals, we assume that it has a QRS wave. Then, we find the R peak as the largest peak in the sub-signal. Relatively, we find the Q and S peaks as the minimum peaks right and left of the R peaks respectively. Namely, the four features that we extract include the amplitude difference between Q and R peaks (f_1), the amplitude difference between R and S peaks (f_2), the slope between Q and R peaks (f_3) and the slope between R and S peaks (f_4). Let $\boldsymbol{Q} \in R^{n_b}$, $\boldsymbol{R} \in R^{n_b}$ and $\boldsymbol{S} \in R^{n_b}$ consist of the Q, R and S peaks indices from X, the four features are computed using the following equations:

$$\boldsymbol{F_1} = \boldsymbol{X_R} - \boldsymbol{X_Q} \tag{2.5}$$

$$\boldsymbol{F_2} = \boldsymbol{X_R} - \boldsymbol{X_S} \tag{2.6}$$

$$\boldsymbol{F_3} = \frac{\boldsymbol{F_1}}{\boldsymbol{R-Q}} \tag{2.7}$$

$$\boldsymbol{F_4} = -\frac{\boldsymbol{F_2}}{\boldsymbol{S-R}} \tag{2.8}$$

where $\boldsymbol{X_R}$, $\boldsymbol{X_Q}$ and $\boldsymbol{X_S}$ contain the amplitude values of the Q, R and S peaks from the time domain signal X.

Note that we extract multiple sub-signals, and we estimate that each of these sub-signals contains a QRS wave. However, we expect that few of these extracted sub-signals may not contain a QRS wave. Consequently, we define here different thresholds based on the maximum and minimum values of the above obtained feature vectors. These thresholds are utilized as reference information for the QRS classification process. Technically, these thresholds are calculated using the following equation (2.9):

$$thr_i = \begin{cases} \dfrac{\max(F_i)}{2} & ,i = 1,2,3 \\ \dfrac{\min(F_i)}{2} & ,i = 4 \end{cases} \tag{2.9}$$

where i is the feature index

2.3.1.5 Classification

We introduce here the single feature-based classification (SFBC) method which is created to classify each of the n_b many sub-signals into a QRS segment or non QRS segment. Technically, using equation (2.9), we calculate four thresholds which are individually used as reference data for binary classification. The classification process in this work depends on applying majority voting algorithm. Full details of the SFBC process are explained in Table 1. Technically, given any ECG sub-signal ($\boldsymbol{X_w}$) with a total of number of (n_f) QRS features, the classification procedure is done using equation (2.10):

$$c_{\boldsymbol{X_w}} = \begin{cases} c_{qrs} & if \ \sum_{i=1}^{n_f} v_i > \dfrac{n_f}{2} \\ c_{nqrs} & if \ \sum_{i=1}^{n_f} v_i < \dfrac{n_f}{2} \end{cases} \tag{2.10}$$

where c_{qrs} refers to a QRS class, c_{nqrs} refers to non QRS class, and v_i is the binary decision found using Table 2.1.

However, when majority voting does not lead to final decision, specifically, the SFBC based decisions are equally splatted, the final decision depends on F_5 which is defined as the variance of the frequency components of the n_b many selected sub-signals. In general, f_5 is smaller in QRS segments than non QRS segments. Therefore, the larger the f_5, the larger the possibility that the relevant $\boldsymbol{X_w}$ has non QRS segment. Let $\hat{A} \in R^{n_w \times n_b}$ be the matrix that has the magnitude of frequency components of the n_b many sub-signals, f_5 is calculated using equation (2.11).

$$\boldsymbol{F_5} = \frac{1}{n_{ft}} \sum_{m=1}^{n_{ft}} (\hat{a}_{m,b} - \overline{\hat{a}_b})^2 \tag{2.11}$$

where $b = 1,2, \ldots, n_b$

Table 2.1: Feature based classification

Feature	QRS segment $v_i = 1$	Non QRS segment $v_i = 0$
F_1	If $f_1 > thr_1$	$if\ f_1 < thr_1$
F_2	If $f_2 > thr_2$	$if\ f_2 < thr_2$
F_3	If $f_3 > thr_3$	$if\ f_3 < thr_3$
F_4	If $f_4 < thr_4$	$if\ f_4 > thr_4$
F_5	If $f_5 < thr_5$	If $f_5 > thr_5$

Consequently, we then define relative the threshold of the fifth feature which is based on the average variance of the frequency components of the n_b many selected sub-signals. Technically, it is calculated using equation (2.12).

$$thr_5 = \frac{0.7}{n_b} \times \sum_{b=1}^{n_b} f_{5_b} \tag{2.12}$$

In Figure 2.4, we show an example of the SFBC process. From top, we show the main ECG signal then we show the selected sub-signals. On the middle, we show the features f_1 and f_3 of each $\boldsymbol{X_w}$ as scatter plot. On the bottom, we show the features f_2 and f_4 of each $\boldsymbol{X_w}$ as scatter plot. We can clearly see that one of the selected $\boldsymbol{X_w}$ $(w = 31)$ is a non QRS segments and its features are out of our defined thresholds range, the separation lines. In contrast, we show that features of QRS segments are within the defined thresholds range.

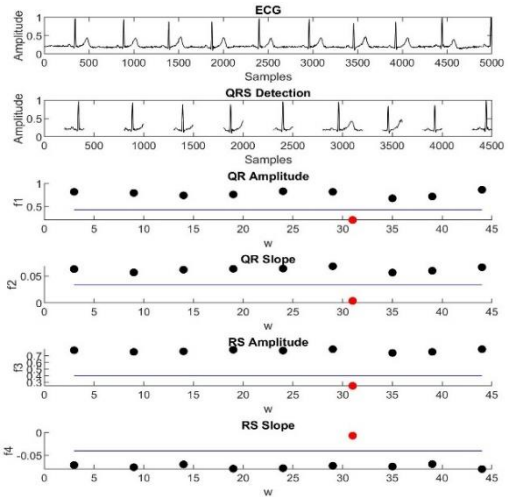

Figure 2.4: The SFBC method using QRS features

2.3.1.6 Finding missed QRS

As explained above, we initially extract a maximum number of n_b many QRS complexes, however, the actual number of heart beats depends on the heart rate. Hence, few of the QRS complexes will not be detected. Therefore, we develop a technique for automatically finding regions of missed QRS complexes. More precisely, we locate search regions of the missed QRS waves if the RR interval between any two correctly classified QRS $d_{RR} \geq 2\, min_{RR}$, where min_{RR} is the minimum RR interval between all the correctly classified QRS complexes.

Accordingly, in each of these accurately defined search regions, our proposed method automatically extracts sub-signals which are estimated to have missed QRS waves. Then, the SFBC method is utilized for classifying the additionally extracted sub-signals. In Figure 2.5 we show an example of detecting a missed QRS waves. From the top, we show a random ECG, then, we show the correctly classified QRS waves. After that, we define 2 min_{RR} as the threshold line for finding regions of missed QRS waves. Finally, we extract them.

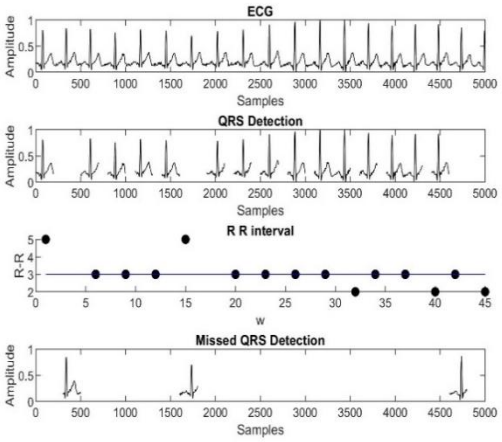

Figure 2.5: The process of finding missed QRS complexes

2.3.2. Human identification using QRS features

The QRS features are special properties which can be utilized to investigate the distinctiveness of the ECG. On other words, the QRS features provide details which describe the uniqueness of the personal ECG. Accordingly, our fiducial-based identification process is based on utilizing the above discussed QRS features.

2.3.2.1 Referencing and testing data selection

In this work, we randomly select the referencing and testing data to evaluate the performance of the proposed algorithm. We arbitrarily select multiple QRS waves and utilize their features for individual recognition. In general, the appropriate number of QRS waves required for the

referencing and testing purposes should be determined based on the type of biometric application and it should mimic realistic conditions.

Let $\boldsymbol{X}$ be an ECG recording with a total of n_l samples, we randomly choose a window of ECG data that starts from a random sample x_t to x_{t+n_r-1} such that $t \leq n_l - n_r + 1$, where n_r is the length of the selected data. Therefore, the total number of available data windows is $n_d = n_l - n_r + 1$.

As previously mentioned all the QRS waves and their features have been extracted in the preprocessing stage. Accordingly, we select here only the QRS waves which exist in the randomly chosen data window. In Figure 2.6 we show an example of the randomization in the referencing and testing data selection. We see on the top, the normalized ECG, then we can see that the proposed method has randomly selected two sets of ECG data. In addition, we see that the QRS peaks are located and labeled based on the preprocessing stage which is explained in the automatic QRS detection section.

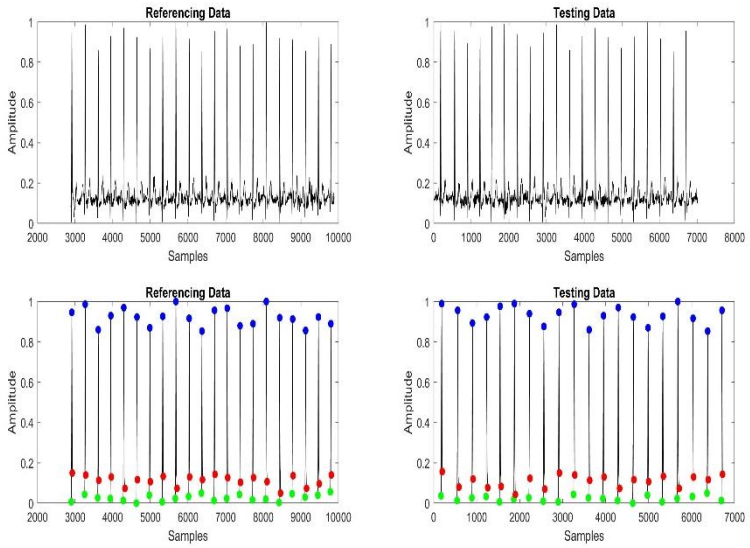

Figure 2.6: Randomization of the referencing and testing data selection

2.3.2.2 Combining the QRS features

After we select a random data of an ECG signal, we use equations (2.6) to (2.8) to calculate the

above mentioned QRS features. Namely, we find $\boldsymbol{F_1}$ to $\boldsymbol{F_4}$ of the QRS waves that fall within the selected data window (see Figure 2.6). Then, we merge these vectors into groups of two as shown in Table 2.2. Consequently, we obtain the new feature matrices F_1 to F_6.

Table 2.2: Combining the QRS features

Feature	Combined Features	Feature	Combined Features
F_1	$\boldsymbol{F_1}$, $\boldsymbol{F_2}$	F_4	$\boldsymbol{F_2}$, $\boldsymbol{F_4}$
F_2	$\boldsymbol{F_3}$, $\boldsymbol{F_4}$	F_5	$\boldsymbol{F_1}$, $\boldsymbol{F_4}$
F_3	$\boldsymbol{F_1}$, $\boldsymbol{F_3}$	F_6	$\boldsymbol{F_2}$, $\boldsymbol{F_3}$

2.3.2.3 Finding histogram distances

After pairing the QRS features and creating the new features matrices, we find the bivariate histograms H_1 to H_6 of F_1 to F_6 respectively. Technically, let $\boldsymbol{X^{ref}}$ and $\boldsymbol{X^{t}}$ be two different data windows of an ECG signal with a total of n_r samples, we obtain a total of six bivariate histograms from each data window. Figure 2.7 shows an example of creating six bivariate histograms from pairing the QRS features that are extracted from randomly selected referencing and testing data. In the left, we show histograms obtained from the referencing data and in the right we show histograms obtained from the testing data. Technically, the distance between any two relevant histograms can be computed using equation (2.13):

$$d_{h_i}^{p_i} = \sqrt{\sum_{d_m=1}^{d_p} \sum_{d_m=1}^{d_p} \left(H^{t,p_i} - H^{ref,p_j}\right)^2} \tag{2.13}$$

where $h_i = 1,2,\ldots n_h$ refers to the bivariate histogram number with a total of n_h many histograms, p_i is the index for one subject , $p_j = 1,2,\ldots.,n_p$ is the subject number with a total of n_p many subjects, and $d_m = 1,2,\ldots,d_p$ is the dimension of the bivariate histogram.

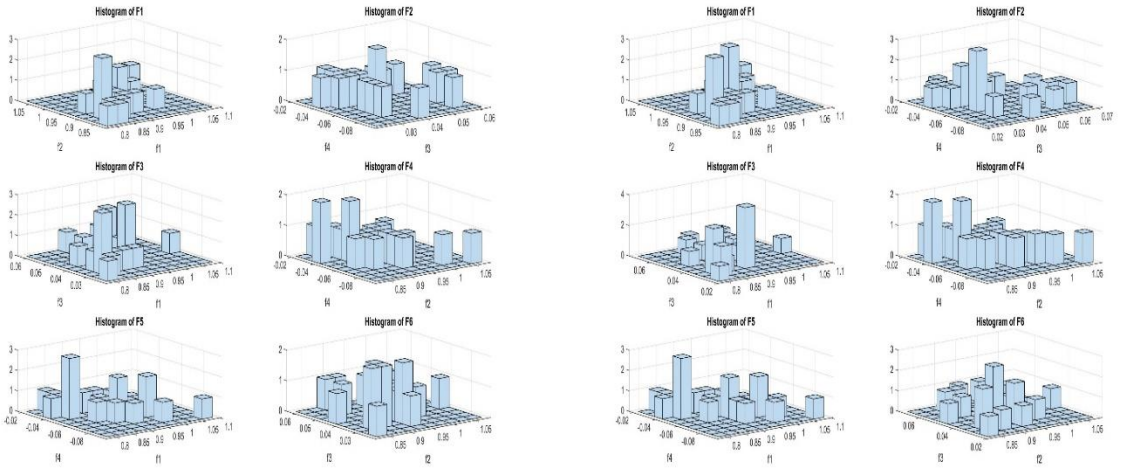

Figure 2.7: Histograms of paired QRS features that are extracted from two different data windows

2.3.2.4 Classification and identification

Namely, using one testing data window (X^t) of a random subject (p_i), we obtain n_h many distance vectors $\boldsymbol{D}_{h_i}^{p_i} \in R^{n_p}$. Obviously, each of these n_h many vectors contain the distances between the histograms of one testing data and histograms of one referencing data of all subjects involved in this study. For each subject, these multiple histograms are computed and recorded as their unique features. Consequently, for any feature pair, the classification process depends on finding the smallest distance using equation (2.14):

$$c_{h_i}^{p_i} = min_{p_j}\left(\boldsymbol{D}_{h_i}^{p_i}\middle|_{1}^{n_p}\right) \tag{2.14}$$

where $\boldsymbol{D}_{h_i}^{p_i}$ is a vector that has n_p many distances and $c_{h_i}^{p_i}$ is the class obtained using a single bivariate histogram h_i.

Accordingly, the number of classes is equivalent to the total number of subjects. Technically, the identification process relays on obtaining the smallest distance which we expect to be between the testing data and refencing data that belong to one subject. In Figure 2.8 we show the flowchart of the classification process. Namely, our classification process is based on finding the similarity between the testing data and referencing data through finding the minimum Euclidean distance.

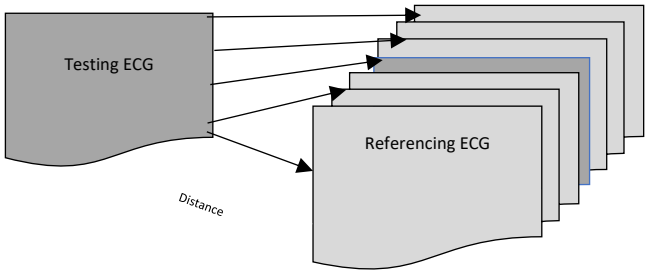

Figure 2.8: The classification process

Consequently, equation (2.14) returns n_h many classes and the final decision for any randomly selected testing data is made using majority voting algorithm, where the subject who has more votes from the six histogram-based distances will be chosen. Technically, we use equation (2.15) for obtaining the final classification:

$$c_{n_h}^{p_i} = \begin{cases} p_i & if \ \sum_{h_i=1}^{n_h} ds_{h_i} > \frac{n_h}{2} \\ else \ \ if & \sum_{h_i=1}^{n_h} ds_{h_i} < \frac{n_h}{2} \end{cases} \tag{2.15}$$

where $c_{n_h}^{p_i}$ is the final class obtained using n_h many histograms and ds_{h_i} is a binary decision that is obtained using equation (2.16) such that:

$$ds_{h_i} = \begin{cases} 0, & if \ c_{h_i}^{p_i} = p_j \\ 1, & if \ c_{h_i}^{p_i} = p_i \end{cases} \tag{2.16}$$

However, when majority voting does not yield to a classification because we have an even number of distances, we perform identification with selecting the $d_{h_i}^{p_i}$ entry with smallest distance according to the equation (2.17):

$$c^{p_i} = min_{h_i}\left(\boldsymbol{D}^{p_i}\Big|_{1}^{n_h}\right) \tag{2.17}$$

where $\boldsymbol{D}^{p_i}$ is a vector that has n_h many smallest distances

In general, the correct identification process will be reached if the smallest distances from majority of the histograms are calculated between the testing data and referencing data that belong to one subject.

2.3.3 Non-Fiducial based methodology

We introduce here a non-fiducial method for ECG based human identification. Namely, our method is based on extracting the frequency components from both the testing and referencing data. Then, we perform classification by finding the Euclidean distance between these frequency components.

2.3.3.1 Referencing and testing data selection

Similarly, we randomly select the referencing and testing data to examine the stability of our proposed method. As previously mentioned, we can choose n_d many data windows from each record of the ECG ID database. Note that the window length (n_r) should be at least equal to the length of a heartbeat to fully extract the frequency components.

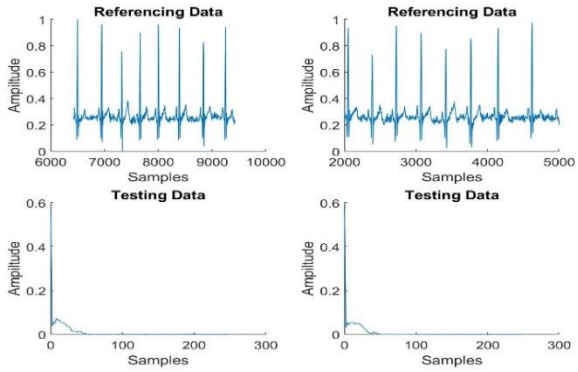

Figure 2.9: ECG frequency

2.3.3.2 Feature Extraction

STFT is a powerful tool since it provides detailed information about all the frequencies that exist in a signal [21]. Since the ECG signal is believed to be unique, we except that its frequency components may contain significant and distinguishable information between different subjects.

Namely, we find the frequency components and utilize them as unique feature. In Figure 2.9, we show the ECG frequency components that are extracted from randomly selected referencing and testing ECG data.

2.3.3.3 Classification and Identification

Similarly, to the fiducial-based method, the intrinsic value that we use for identifying subjects is the smallest distance between one testing data and one referencing data of all subjects involved in this study. Technically, let $\boldsymbol{X}$ be a random data window from the ECG record, the frequency components can be computed using equation (2.3). Note that in the QRS detection part, equation (2.3) is used on many sub-signals that are extracted from the ECG signal. However, we use equation (2.3) here on the whole randomly selected testing and referencing data. Then, we obtain the frequency components matrix FR, Then, we only choose the magnitude components. Consequently, we define here the feature matrix AF which has the magnitudes of all frequency components. Accordingly, the distance between two feature matrices can be calculated using equation (2.18):

$$d^{p_i} = \sqrt{\sum_{m=0}^{\frac{n_{ft}}{2}+1} \sum_{m=0}^{\frac{n_{ft}}{2}+1} \left(\frac{af(m)^{t,p_i}}{\sigma^t} - \frac{AF(m)^{ref,p_j}}{\sigma^{ref}} \right)^2} \tag{2.18}$$

where AF^{t,p_i} refers to the feature matrix of a testing data, AF^{ref,p_j} refers to the feature matrix of a referencing data and σ is the standard deviation calculated using equation (2.19):

$$\sigma = \sqrt{\frac{1}{n_{ft}-1} \sum_{m=0}^{n_{ft}} (af_m - \mu)^2} \tag{2.19}$$

where af_m is the magnitude of the frequency component m and μ is the mean of $\boldsymbol{AF}$:

$$\mu = \frac{1}{n_{ft}} \sum_{m=0}^{n_{ft}} af_m \tag{2.20}$$

This statistical normalization, see [18] , will further enhance the identification process as some individuals could have similar frequency components. Thus, by normalizing the values, such similarity decreases and the performance of the identification process increases. Consequently, using one testing data and equation (2.18), we obtain $D^{p_i} \in R^{n_p}$. Similarly, to the non-fiducial-based method, the classification process is performed by finding the smallest distance using equation (2.21):

$$c^{p_i} = min_{p_j}\left(\boldsymbol{D}^{p_i}\Big|_{1}^{n_p}\right) \tag{2.21}$$

where $\boldsymbol{D}^{p_i}$ is a vector that has n_p many distances and c^{p_i} is the class obtained using the feature vector of frequency components. Therefore, the identification process relays on finding the smallest distance which we expect to be between the testing data and refencing data that belong to one subject.

2.4 Results

2.4.1 Automatic QRS detection and classification

The proposed methodology has been applied on ECGs of 62 subjects from the publicly available ECG ID database. For each subject, we selected two ECG recordings that are measured in two different days. Thus, the total number of ECG signals is 124. As a result, we tested the performance of the automatic QRS detection and classification method in terms of the average QRS classification accuracy which is calculated using equation (2.22):

$$qrsacc_{ave} = \frac{1}{n_{ecg}} \sum_{ecg=1}^{n_{ecg}} acc_{ecg} \tag{2.22}$$

where $qrsacc_{ave}$ is the average QRS classification accuracy of the method, ecg is the ECG number with a total of n_{ecg} many ECGs and $qrsacc_z$ is the QRS classification accuracy of a single ECG:

$$qrsacc_z = \frac{\widehat{n_{qrs}}}{n_{qrs}} \times 100 \tag{2.23}$$

where n_{qrs} is the total number of QRS waves and $\widehat{n_{qrs}}$ is the total number of accurately detected and classified QRS waves.

Furthermore, we show in Table 2.3 the results of the QRS classification accuracy using all the 124 ECG signals. Most importantly, using equation (2.22), we achieved 99.67% average QRS classification accuracy. However, for 1 ECG signal, we obtained 86.36% QRS classification accuracy. Although we were accurately locating the regions of missed QRS, yet the proposed algorithm was not detecting three QRS waves. Relatively, the SFBC process has shown excellent performance because all the non QRS sub-signals are also accurately classified. In Figure 2.10 we show an example of detecting all QRS waves from n_b many sub-signals that consists of n_s many samples.

Table 2.3: QRS Classification Accuracy

acc_z Range	100%	95%-99%	86%-94%
No. of ECGs	116	7	1

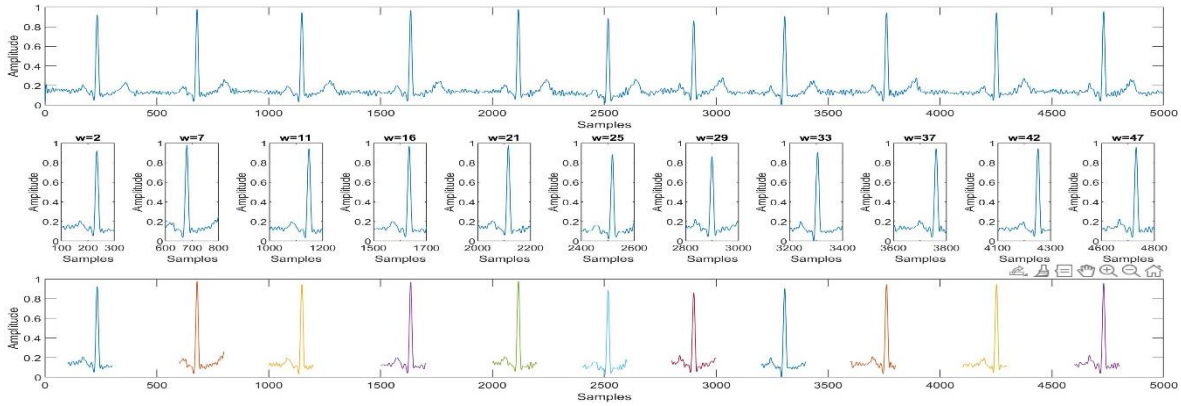

Figure 2.10: QRS detection and classification process

Furthermore, we applied equation (2.24) to compute the average personal QRS segmentation accuracy:

$$qrsacc_{p_i} = \frac{1}{n_{rec}} \sum_{rec=1}^{n_{rec}} \frac{\widehat{n_{qrs,rec}}}{n_{qrs,rec}} x100 \tag{2.24}$$

where $qrsacc_{p_i}$ is average personal QRS classification accuracy, n_{rec} is the total number of ECG signals for each person, $n_{qrs,rec}$ is the total number of QRS waves and $\widehat{n_{qrs,rec}}$ is the total number of accurately classified QRS waves.

As shown in Table 2.4, using our proposed method, we achieved excellent results because we successfully classified all the QRS waves for majority of the subjects with 100 % average personal QRS classification accuracy. Also, Figure 2.11 shows detailed information about the QRS classification accuracy for each subject. We can see that majority of the subjects (61 out of 62) have QRS classification accuracy ranging from (95 % to 100%).

Table 2.4: Average Personal QRS Segmentation Accuracy

$qrsacc_{p_i}$ Range	100%	96%-99%	91%-95%
No. of Subjects	54	7	1

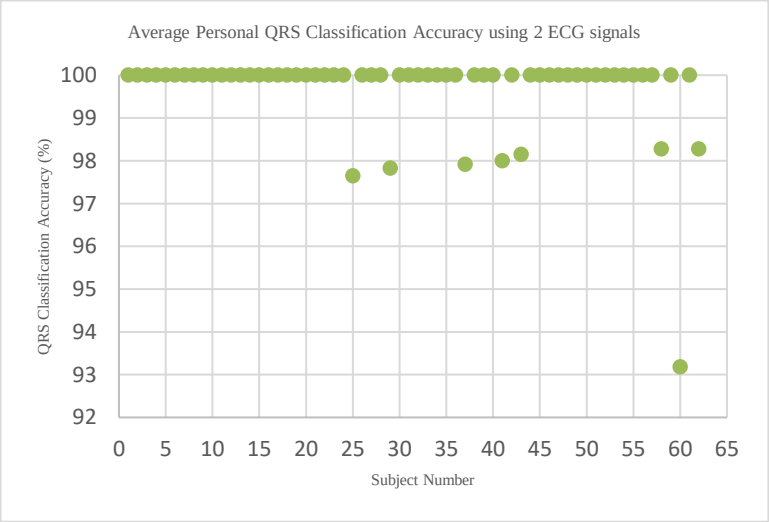

Figure 2.11: The average personal QRS classification accuracy

2.4.2 Human identification using histograms of QRS features

The performance of the proposed method for human identification using QRS histograms has been evaluated in terms of the average identification accuracy of the method and the average personal identification accuracy. In addition, we repeated the randomization process of referencing and testing data selection many times. Namely, we apply equation (2.25) to obtain the average identification accuracy of the method:

$$acc_{ave} = \frac{1}{n_p} \sum_{p_i=1}^{n_p} acc_{p_i} \tag{2.25}$$

where acc_{ave} is the average identification accuracy, n_p in the total number of subjects and acc_{p_i} is the average personal identification accuracy:

$$acc_{p_i} = \frac{n_{correct}}{n_{exp}} x100 \tag{2.26}$$

where $n_{correct}$ is the number of times each subject is correctly identified.

Most importantly, we set n_r to different values to evaluate the stability of the fiducial method by changing the length of the selected ECG samples. Consequently, the identification process using histograms of QRS features has achieved 94.58% average identification accuracy. Moreover, we repeated the identification process using ECGs measured on a different day (record 2). As a result, we achieved slightly higher performance of 96.41% average identification accuracy. However, the performance of the of fiducial method requires larger values of n_r this is expected as result of the variability of the ECG fiducial features specifically the amplitude features. Figure 2.12 shows the average personal identification accuracy of the fiducial method. We can see that majority of the subjects have a personal identification accuracy ranging from 91 % to 100%. In addition, Figure 2.13 shows the average identification accuracy of the proposed fiducial method. In both figures, we can see that as n_r increases, the performance of the identification process increases.

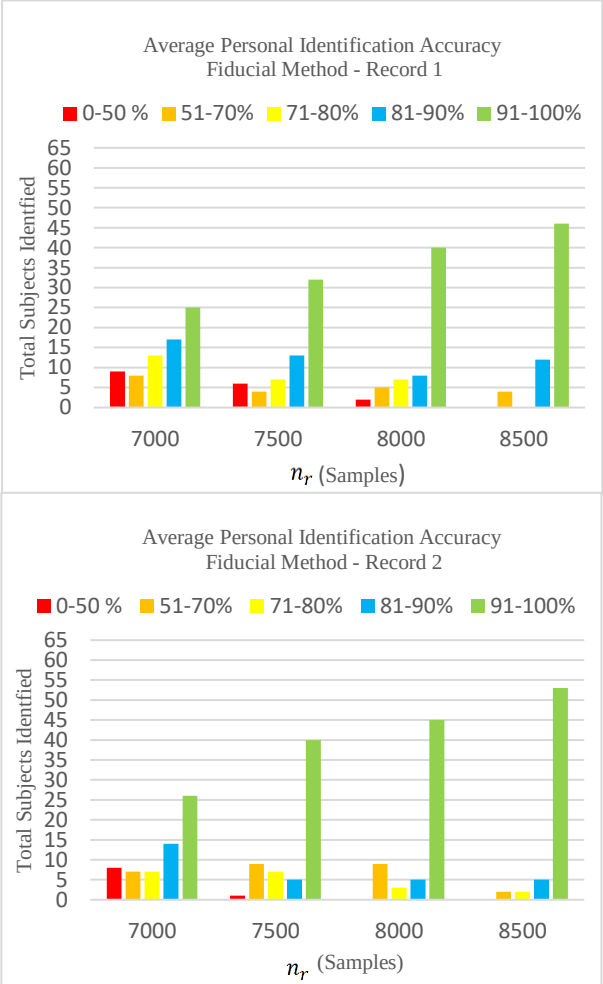

Figure 2.12: The average personal identification accuracy using proposed fiducial method

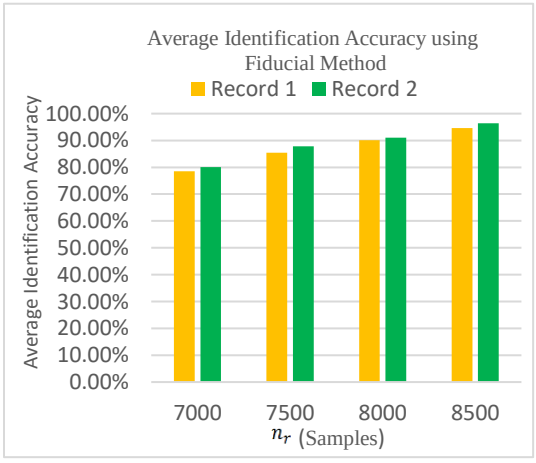

Figure 2.13: The identification accuracy of the proposed fiducial method

Furthermore, we observe the best findings at $n_r = 8500$ samples. Moreover, Table 2.5 shows detalied infromation about the personal identification accracy using different n_r values and multiple ECGs.

Table 2.5: Average personal identification accuracy of the proposed fiducial method

n_r (samples)	rec	0-50 %	51-70%	71-80%	81-90%	91-100%
7000	1	9	8	13	17	25
	2	8	7	7	14	26
7500	1	6	4	7	13	32
	2	1	9	7	5	40
8000	1	2	5	7	8	40
	2	0	9	3	5	45
8500	1	0	4	0	12	46
	2	0	2	2	5	53

2.4.3 Human identification using ECG frequency components

The identification process using the proposed non-fiducial method which requires lower values of n_r has significantly shown excellent results compared to the results of the fiducial method. Similarly, we randomized the process of referencing and testing data selection n_{exp} many times. As a result, for ECGs selected from record 1, we significantly achieved high average identification accuracy of 98.48%. In addition, we achieved slightly higher performance of 99.64% average identification accuracy using ECGs from record 2. Moreover, we used equation (25) to evaluate the performance of the method in terms of the personal identification accuracy. Consequently, Figure 2.14 and Figure 2.15 show the results with majority of the subjects having a personal identification accuracy ranging from 91 % to 100%. Most importantly, increasing n_r enhances the performance of the method and we observed the best findings at $n_r = 5000$ samples. In addition, Table 6. shows the complete results.

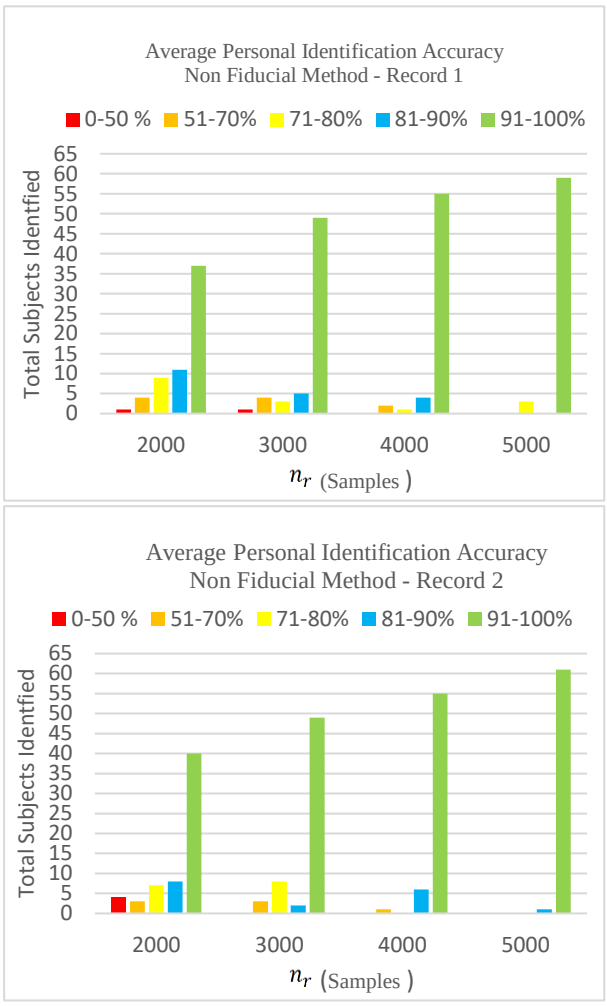

Figure 2.14: The average personal identification accuracy of the proposed non fiducial method

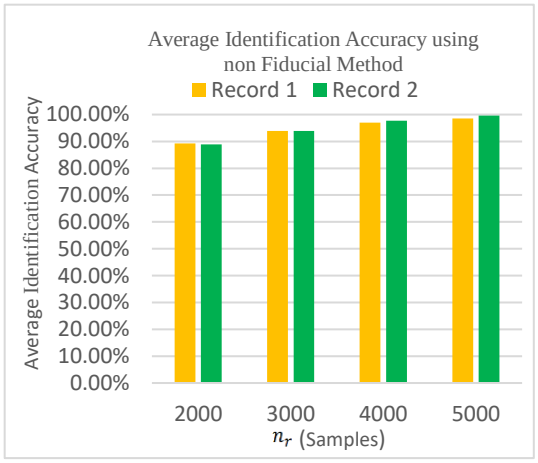

Figure 2.15: The identification accuracy of the proposed non fiducial method

As we excepted, the personal identification using the non-fiducial method is more stable than using the fiducial-based method. In general, this is because the non-fiducial features, namely the frequency components, have lower variation than the QRS amplitude and slope features [1]. Hence, this indicates that lower variation of the ECG features significantly increases the identification process.

Table 2.6: Average personal identification accuracy of the proposed Non fiducial method

n_r (samples)	rec	0-50 %	51-70%	71-80%	81-90%	91-100%
2000	1	1	4	9	11	37
	2	4	3	7	8	40
300	1	1	4	3	5	49
	2	0	3	8	2	49
4000	1	0	2	1	4	55
	2	0	1	0	6	55
5000	1	0	0	3	1	59
	2	0	0	0	0	61

2.4.4 Performance evaluation of the proposed methodology

The performance of the proposed methodology is also evaluated using the following parameters: Precision which is defined as the ratio of truly identifying subjects with total number of identifications:

$$Precision = \frac{1}{n_p} \sum_{p_i=1}^{n_p} \frac{TP_{p_i}}{TP_{p_i} + FP_{p_i}} \tag{27}$$

Where TP_{p_i} is total number of times subject p_i is correctly identified when the test data was selected from subject p_i , and FP_{p_i} is the total number of times subject p_i is falsely identified when the test data was selected from different subjects.

Recall / true positive rate (TPR) which is defined as the ratio of truly identifying subjects with total number of identification attempts:

$$Recall = \frac{1}{n_p} \sum_{p_i=1}^{n_p} \frac{TP_{p_i}}{TP_{p_i} + FN_{p_i}} \tag{28}$$

where FN_{p_i} is total number of times subject p_i is not identified when the test data was selected from subject p_i.

False Acceptance Rate (FAR) which is defined as the ratio of falsely identifying subjects with the total number of rejection attempts

$$FAR = \frac{1}{n_p} \sum_{p_i=1}^{n_p} \frac{FP_{p_i}}{TN_{p_i} + FP_{P_i}} \tag{29}$$

False Rejection Rate (FRR) which is defined the ratio of falsely not identifying subjects with the total number of identification attempts:

$$FRR = \frac{1}{n_p} \sum_{p_i=1}^{n_p} \frac{FN_{p_i}}{TP_{p_i} + FN_{P_i}} \tag{30}$$

where TN_{p_i} is total number of times subject p_i is correctly not identified when the test data was selected from different subjects.

Consequently, Table 2.7 and Table 2.8 show the precision, recall FRR and FAR of the proposed methodologies. According to both tables, increasing the length of the random data significantly increases the overall performance of the proposed methodologies. In addition, we achieved our best result of 0.9965 precision, 0.9968 recall, 0.0035 FRR and 0.001 FAR using the non-fiducial methodology at n_r= 5000 samples. Furthermore, we evaluated the performance of both approaches using the receiver operating curves (ROC) and precision recall curves (PR) which are shown in Figure 2.16, Figure 2.17, Figure 2.18 and Figure 2.19 respectively. According to

Figure 2.16 and Figure 2.17, we achieve the nearest ROC curves to the top left corner via increasing n_r. Similarly, according to Figure 2.18 and Figure 2.19 we achieve the nearest PR curves to the top right corner via increasing the random data length. These performance measures show that the proposed fiducial and non-fiducial methodologies achieve satisfactory results, and they can be utilized for ECG based human identification.

Table 2.7: Performance evaluation of the proposed fiducial method

Record Number	n_r (samples)	Precision	Recall	FRR	FAR
1	$n_{r1} = 7000$	0.7848	0.8570	0.2152	0.0035
	$n_{r2} = 7500$	0.8542	0.8955	0.1458	0.0024
	$n_{r3} = 8000$	0.9010	0.9261	0.0990	0.0016
	$n_{r4} = 8500$	0.9458	0.9567	0.0542	0.0009
2	$n_{r1} = 7000$	0.8010	0.8668	0.1990	0.0033
	$n_{r2} = 7500$	0.8787	0.9145	0.1213	0.0020
	$n_{r3} = 8000$	0.9110	0.9339	00.0890	0.0015
	$n_{r4} = 8500$	0.9642	0.9700	0.0358	0.0006

Table 2.8: Performance evaluation of the proposed non fiducial method

Record Number	n_r (samples)	Precision	Recall	FRR	FAR
1	$n_{r1} = 2000$	0.8923	0.9005	0.1077	0.0018
	$n_{r2} = 3000$	0.9384	0.9435	0.0616	0.0010
	$n_{r3} = 4000$	0.9694	0.9719	0.0306	0.0005
	$n_{r4} = 5000$	0.9848	0.9863	0.0152	0.0002
2	$n_{r1} = 2000$	0.8887	0.8937	0.1113	0.0018
	$n_{r2} = 3000$	0.9394	0.9450	0.0606	0.0010
	$n_{r3} = 4000$	0.9774	0.9793	0.0226	0.0004
	$n_{r4} = 5000$	0.9965	0.9964	0.0035	0.0001

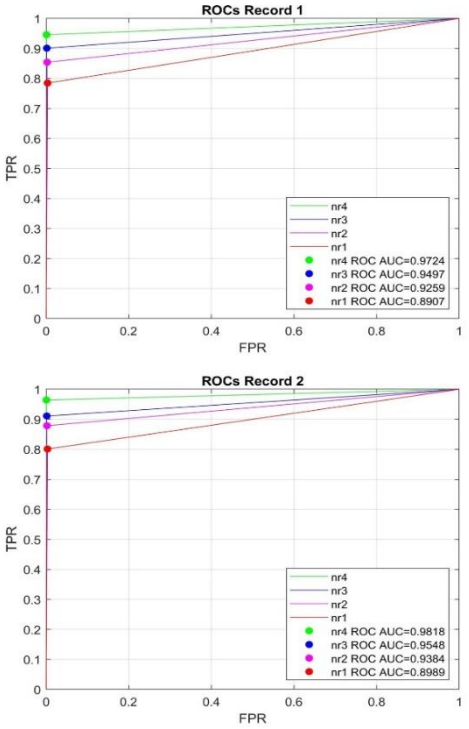

Figure 2.17: ROCs of the proposed fiducial methodology

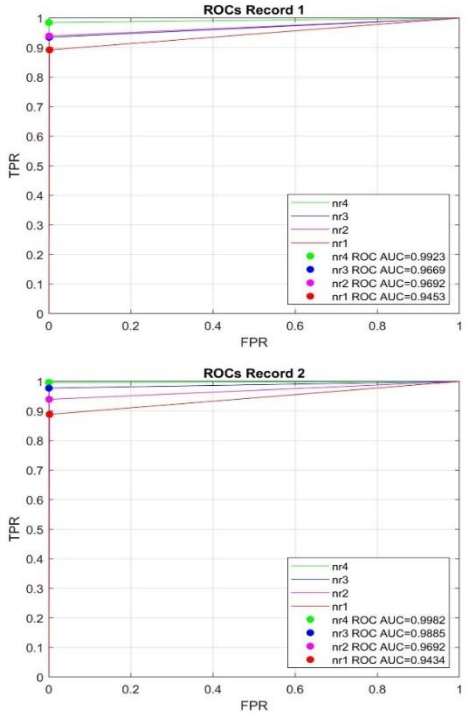

Figure 2.16: ROCs of the proposed non fiducial methodology

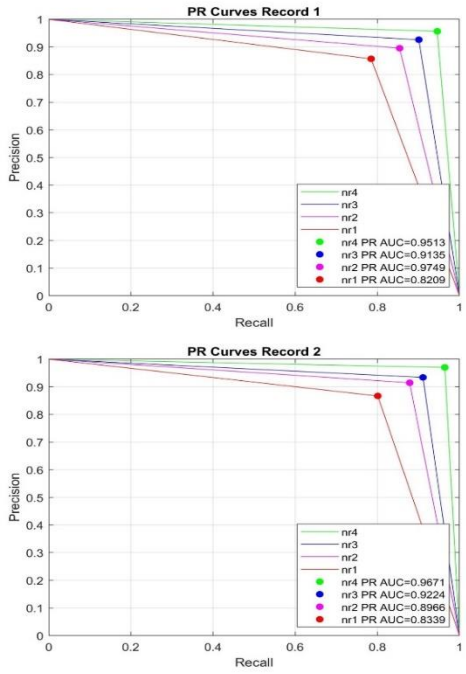

Figure 2.18: PR Curves of the proposed fiducial methodology

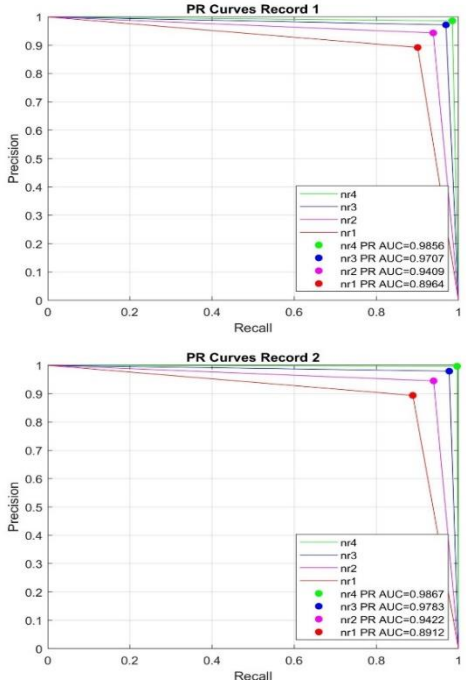

Figure 2.19: PR Curves of the proposed non fiducial methodology

2.5. Discussion and Conclusion

ECG based human identification has shown promising results in previous research [17] [22] [1] [2]. In this work, we proposed both fiducial and non-fiducial algorithms to identify 62 subjects using their ECG. Our results indicate that the non- fiducial method which is based on finding the ECG frequency components outperforms the fiducial method which is based on extracting QRS features. In addition, the former method relays on obtaining the minimum normalized Euclidean distance between ECG data while the later method relays on finding the minimum Euclidean distance between multiple bivariate histograms of ECG data. Most importantly, our method has shown higher performance than some of the work in the literature as seen in Table 2.7 [6] [13] [11].

Table 2.9: Comparison between the proposed method and approaches in the literature

Authors	Approach	Subjects	Accuracy
Bak et al [7]	Fiducial	100	94%
Abdeldayem et al [6]	Combined	20	99,.6%
Coutinho et al [4]	Fiducial	26	99.57%
Coutinho et al [4]	Non-Fiducial	26	99.94%
Islam et al [3]	Fiducial	76	99%
Wu et al [5]	Fiducial	285	97.19%
Chan et al [13]	Non-Fiducial	50	90%
Liu et al. [11]	Non-Fiducial	146	93.15%
Proposed work	Fiducial	62	93.93%
Proposed work	Non-Fiducial	62	99.64%

However, the fiducial-based method requires larger amounts of ECG samples to achieve the best identification accuracy. In contrast, the non-fiducial method requires less amounts of ECG samples to achieve high identification accuracy. Nevertheless, the ECG based personal identification process does not only relay on the length of selected ECG samples, but it also depends on the stability of the ECG features over time. It has been demonstrated that ECG features may have significant variations even in the same ECG record [18]. Generally, lower variability in ECG

features increases the identification process. In contrast, higher variability in ECG features decreases the identification process. This problem may be addressed by developing similarity measurement techniques to optimize the process of feature selection for choosing the most appropriate fiducial and non-fiducial features. Nevertheless, choosing the most appropriate distance measure for classification purposes should depend on the geometrical characteristics of ECG features because the space of such features might not be always Euclidean (e.g., finding the minimum distance between matrices) [23]. Moreover, further algorithms development is needed to reduce the length of ECG data selection specifically for real implementation of ECG bio identification systems. In conclusion, the findings of this work further proof the uniqueness of the heart signal. In addition, it indicates the feasibility of identifying human using ECG.

References

[1] J. Ribeiro Pinto, J. S. Cardoso, and A. Lourenco, "Evolution, Current Challenges, and Future Possibilities in ECG Biometrics," *in IEEE Access* vol. 6, pp. 34746-34776, 2018.

[2] S. Gutta and Q. Cheng, "Joint Feature Extraction and Classifier Design for ECG-Based Biometric Recognition," *in IEEE Journal of Biomedical and Health Informatics*, vol. 20, pp. 460-468, March 2016.

[3] S. Islam, N. Alajlan, Y. Bazi, and H. S. Hichri, "HBS: A Novel Biometric Feature Based on Heartbeat Morphology," *in IEEE transactions on Information Technology in Biomedicine*, vol. 16, pp. 445-453, May 2012.

[4] P. C. David, H. Silva, H. Gamboa, A. Fred, and M. Figueiredo, "Novel fiducial and non-fiducial approaches to electrocardiogram-based biometric systems," *in IET Biometrics*, vol. 2, no. 2, pp. 64-75, February 2013.

[5] S. Wu, P. Chen, A. L. Swindlehurst, and P. Hung, "Cancelable Biometric Recognition With ECGs: Subspace-Based Approaches," *in IEEE Transactions on Information Forensics and Security,* vol. 14, pp. 1323-1336, May 2019.

[6] S. Abdeldayem and T. Bourlai, "A Novel Approach for ECG-Based Human Identification Using Spectral Correlation and Deep Learning," *in IEEE Transcations on Biometrics, Behavior, and Identity Science,* vol. 2, no. 1, pp. 1-14, 2020.

[7] E. Bak, G. Choi, and S. B. Pan, "ECG-Based Human Identification System by Temporal-Amplitude Combined Feature Vectors," *in IEEE Access,* vol. 8, pp. 42217-42230, 2020.

[8] A. Biran and A. Jeremic, "ECG Based Human Identification using Short Time Fourier Transform and Histograms of Fiducial QRS Features," in *BIOSIGNALS,* Malta, 2020, vol. 4, pp. 324-329.

[9] A. Biran and A. Jeremic, "Automatic QRS Detection and Segmentation using Short Time Fourier Transform and Feature Fusion," in *33rd Canadian Conference on Electrical and Computer Engineering,* London, 2020, pp. 1-4.

[10] Q. Zhang , D. Zhou, and X. Zeng, "HeartID: A Multiresolution Convolutional Neural Network for ECG-Based Biometric Human Identification in Smart Health Applications," *in IEEE Access,* vol. 5, pp. 11805-11816, 2017.

[11] J. Liu, L. Yin, C. He, B. Wen, X. Hong, and Y. Li, "A Multiscale Autoregressive Model-Based Electrocardiogram Identification Method," *in IEEE Access,* pp. 18251-18263, 2018.

[12] C. L. P. Lim, W. L. Woo, S. S. Dlay, and G. Bin, "Heartrate-Dependent Heartwave Biometric Identification With Thresholding-Based GMM–HMM Methodology," *in IEEE Transactions on Industrial Informatics,* vol. 15, no. 1, pp. 45-23, 2019.

[13] A. D. C. Chan, M. M. Hamdy, A. Badre, and V. Badee, "Wavelet Distance Measure for Person Identification Using Electrocardiograms," *in IEEE Transactions on Instrumentation and Measurement,* vol. 57, pp. 248-253, February 2008.

[14] S. Lin, C. Chen, C. Lin, W. Yang, and C. Chiang, "Individual identification based on chaotic electrocardiogram signals during muscular exercise," *in IET Biometrics,* vol. 3, no. 4, pp. 257–266, 2014.

[15] K. A. Sidek, I. Khalil, and H. F. Jelinek, "ECG Biometric with Abnormal Cardiac Conditions in Remote Monitoring System," *in IEEE Transactions on Systems, Man, and Cybernetics: Systems,* vol. 44, no. 11, pp. 1498-1509, November 2014.

[16] I. Odinaka, J. A. O'Sullivan, E. J. Sirevaag, and J. W. Rohrbaugh, "Cardiovascular Biometrics: Combining Mechanical and Electrical Signals," *in IEEE Transactions on Information Forensics and Security,* vol. 10, no. 1, pp. 16-27, January 2015.

[17] J. S. Arteaga-Falconi, H. Al Osman, and A. El Saddik, "ECG Authentication for Mobile Devices," *in IEEE Transactions on Instrumentation and Measurement,* vol. 65, no. 8, pp. 591-600, March 2016.

[18] M. Ingale, R. Cordeiro, S. Thentu, Y. Park, and N. Karimian, "ECG Biometric Authentication: A Comparative Analysis," *in IEEE Access,* vol. 8, pp. 117853-117866, 2020.

[19] T. S. Lugovaya, "Biometric human identification based on electrocardiogram," Master's, Faculty of Computing Technologies and Informatics, Russian Federation, 2005.

[20] H. Li and A. Jeremic, "Semi-supervised Distributed Clustering for Bioinformatics - Comparison Study," in *Proceedings of the 10th International Joint Conference on Biomedical Engineering Systems and Technologies,* 2017, vol. 4, pp. 259-264.

[21] A. V. Oppenheim and R. W. Schafer, *Discrete-Time Signal Processing*. New Jersey: Prentie-Hall, Inc, 1989.

[22] A. Biran and A. Jeremic, "Non-Segmented ECG bio-Identification using Short Time Fourier Transfrom and Frecht Mean Distance," in *42nd Annual International Conference of the IEEE Engineering in Medicine and Biology Society*, Montreal, 2020, pp. 5506-5509.

[23] R. Bhatia and J. Holbrook, "Riemannian geometry and matrix geometric means," *Linear Algebra and its applications* vol. 413, no. 2, pp. 594-618, 2006.

Chapter 3

3 ECG Bio-Identification using Fréchet Classifiers: A proposed Methodology based on modeling the Dynamic Change of the ECG Features

3.1 Abstract

Recently, the use of electrocardiogram (ECG) for human identification has attracted great attention. Generally, most existing ECG based biometric systems relay on extracting the static fiducial or non-fiducial features of the cardiac signal. However, the recorded ECG data is more likely to be different whenever it is measured. Such problem can be addressed by utilizing the dynamic change in ECG features. This paper proposes a new methodology for human identification via ECG, based on tracking the dynamic change in ECG features and utilizing the Fréchet distance measures for multiclass classification of feature matrices. The proposed dynamic feature matrices can be utilized to model nonstationary signals because they provide continues information on feature variability. Technically, we utilize the consecutive change of ECG power spectral density as significant feature. In addition, we use the dynamic change of QRS features as a distinguishable characteristic. At the classification stage, we use equations of Fréchet distances to perform multiclass classification because the covariance matrices of the dynamic feature matrices are symmetric positive definite, and their relative geometric space is not Euclidian. The performance of our methodology was evaluated using the publicly available ECG ID database of 62 subjects. To support real world applicability of our method, we randomized the reference / test

data selection using data windowing techniques for examining the stability of our method by changing the datasets. The experimental results show that our methodology was able to achieve an identification accuracy of 97.03% with 0.971 precision, 0.999 specificity, 0.97 recall, 0.029 false rejection rate and 0.00048 false acceptance rate. Furthermore, the findings of our work show that Fréchet distances perform better than the Euclidian distance for ECG data classification in the context of multiclass classification problems.

3.2 Introduction

The ECG is graphical display that is used to measure the electrical activity of the heart. Each heartbeat in the ECG is represented by three complex waves known as P, QRS, and T waves (see Figure 3.1). The ECG is typically analyzed by time intervals and segments. To explain, the P wave represents the electrical depolarization of the atria of the heart, the QRS interval represents the time required for a stimulus to spread through the ventricles (ventricular depolarization), and the T wave represents the resting state of the heart (ventricular repolarization) [1] . In practice, the ECG is the simplest and fastest test to detect cardiac abnormalities. However, recently the ECG based human identification has gained a great momentum as a new approach in human recognition.

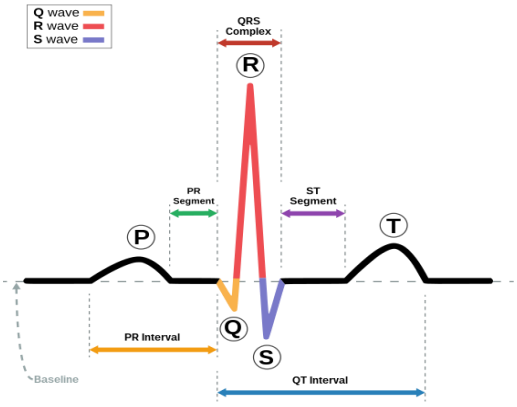

Figure 3.1: Normal components of a heartbeat

The potential use of ECG as biometric modality has shown excellent results in several studies [1]. Specifically, the ECG signal has many characteristics which makes it an appropriate way for human identification compared to the existing biometric modalities such as face, fingerprint, and iris. For instance, the ECG captures unique traits of an individual, it exists in all living human, and it can be continually and non-invasively recorded [2].

Generally, ECG based biometric systems are categorized into two main groups: fiducial point and non-fiducial point. Previous studies have reported promising findings on various issues related to feature extraction, classification, applications fields and ECG databases [1] [3] [4] [5] [6]. However, some problems still exist. Specifically, problems on dynamic feature extraction and multiclass classification were not addressed.

Feature extraction is the process of obtaining significant information from the ECG signal for identification purposes. Such informative features can be fiducially or non-fiducially extracted [1]. However, the ECG is a time varying signal, and it usually has large temporal, morphological, amplitude and spectral variations. Most importantly, it has been demonstrated that the static features may not fully characterize the ECG signal [1] [7]. In addition, it is difficult to use only static features for human identification because the recorded data is more likely to be different whenever it is measured [1] [7]. To address this problem, the most appropriate way to characterize the ECG signal is by utilizing the dynamic change of ECG features as a distinguishing characteristic.

The ECG data classification is defined as the process of accurately assigning the transformed feature matrices into a specific class. On other words, it is a process of correctly identifying individuals using distance minimization algorithms [1]. That is, choosing the right distance measure is specifically important because it directly determines the corresponding identity. Hence,

it has a great influence on the overall performance of the identification system. However, in multiclass classification problems such as classifying symmetric positive definite feature matrices, it has been demonstrated that the geometrical space of symmetric positive definite matrix is not Euclidean [8] [9]. Geometrically, every symmetric positive definite matrix (e.g., a covariance matrix with zero eigenvalues) defines an ellipsoid. In order to measure the minimum distance between objects in such space (e.g., finding the minimum distance between ECG feature matrices) algorithms based on Fréchet distances have been proposed [10] [9] [11]. It has been proven that Fréchet based classifiers perform better than Euclidean based classifiers when it comes to classifying symmetric positive definite matrices [10].

In general, this paper focuses on modeling the dynamic change of ECG features for identification purposes and has the objective to test the feasibility of ECG classification using non-Euclidean distances. In section 3.3, we provide a brief literature of the existing methods for ECG biometrics. In section 3.4, we outline the corresponding algorithms of our proposed methodology. In section 3.5, we present and analyze the experimental results of our proposed methodology. In section 3.6, we discuss the main findings of the research with comparison to the state of art methods. Section 3.7 outlines some future work directions and section 3.8 summarizes and concludes the paper.

3.3 Literature Review

Currently, much research on ECG based human identification have been conducted. Several papers have demonstrated the feasibility of utilizing the ECG characteristics for identification purposes [1] [12] [13]. Dong et al. [7] have proposed an ECG identification system based on modeling the QRS complex dynamics in the form of constant radial basis functions (RBFs). Using the L_1 norm as a classifier utilized for identity recognition, Dong's et al. method has achieved 97.42% identification accuracy. In contrast, Choi et al. [14] have proposed a methodology using

ECGs that were acquired from mobile sensors. Choi's et al method is based on extracting eight fiducial points including five amplitude and three temporal features. In addition, they used nine different classifiers for authentication. Accordingly, the support vector machine (SVM) classifier has shown the best performance with 95.99% identification accuracy. On the other hand, Kang et al [15] have developed a non-fiducial algorithm which is based on utilizing the cross-correlation (CC) method to obtain the degree of similarity between randomly selected heart beats.

Moreover, Selfie [16] has proposed a technique by utilizing the ECG amplitude and slope features for biometric authentication. Such method is based on comparing the ECG morphological features using normalized Euclidean distances and assigning different thresholds for classification. Cherifi et al. [17] have proposed two algorithms which are based on combination of several methods including autocorrelation (AC), discreet cosine transform (OCT), fast Fourier transform (FFT) and principal component analysis (PCA). Both of Cherifi's et al. algorithms relay on extracting non-fiducial features from detecting multiple heart beats; thus, the accuracy of such algorithms highly depends on the number of heart beats that are selected for human authentication [17]. Fatimah et al. [18] have investigated the feasibility of utilizing the ECG for human identification using a single heartbeat. Both fiducial and non-fiducial features of 12 subjects were extracted and combined into different sets. Namely, Kruskal-Wallis method was used to select the relevant heart beats for identity recognition. Relatively, the identification process was performed using various classifiers including SVM, k nearest neighbor (kNN) and ensemble bagged trees (EBT). Consequently, Fatimah et al. [18] algorithm has achieved 98.5% identification accuracy using the SVM classifier.

Furthermore, Chu et al [19] have introduced the parallel multi-scale one-dimensional residual network (PMODRN) technique. The PMODRN is based on utilizing the multi scale conventional

neural networks (CNN) method to extract parallel heartbeat feature vectors followed by authenticating individuals using the template matching algorithms. Accordingly, Chu et al. work has obtained 98.24% identification accuracy. Cordeiro et al. [3] have presented the domain specific architecture (DSA) method which depends on extracting 24 fiducial features and defining user-specific threshold via utilizing distance measurements. Hence, the ECG based authentication using the DSA method is conditionally obtained when the Euclidean distance between two sets of ECG features is above certain threshold. Relatively, Cordeiro et al. [3] method has achieved 100% identification accuracy. Kim et al. [20] have developed a machine learning based biometric authentication system using the RR- interval framing method (RRIF) and designing a decision tree (DT) based multi-variable regression model. Such method has obtained 95% authentication accuracy. Hammad et al. [21] have proposed a multimodal biometric authentication system based on fusing the ECG and fingerprint characteristics. Features of both modalities were extracted and fused using the CNN method, in addition; Q-Gaussian multi support vector machine (QG-MSVM) method was utilized for the authentication process. Technically, Hammad's et al. authentication system has shown 98.66% identification accuracy. Also, in our previous works [22] [23], we have initially tested the potential use of ECG for human identification using the Fréchet classifiers. Specifically, we presented the preliminary results of utilizing the Fréchet distances for ECG based human identification [22] .

In this paper we propose an automatic methodology for ECG based human identification by utilizing the dynamic change in ECG features along with using Fréchet classifiers for multiclass classification of ECG data. The main contributions of this paper include:

1) Modeling the dynamic change in the ECG power spectral density (PSD) using several data windowing techniques as a unique characteristic that is used to identify individuals. Since

ECG is believed to have distinctive patterns, the dynamic change in the frequency components may further prove the uniqueness of the biological signal [5]. To accomplish our objective, we utilize the PSD dynamics as a unique non-fiducial feature that is modeled to differentiate between multiple ECGs belonging to different individuals.

2) It has been demonstrated that ECG fiducial features are difficult to be used for human identification because they vary significantly. To address this issue, we also propose a technique to model the dynamic change in the ECG temporal, amplitude, and distance features for identification purposes. We achieve this goal via obtaining a cross feature matrix that is utilized to model the dynamic change in the QRS fiducial features. Most importantly, the proposed dynamic features can be generally utilized to model nonstationary signals because they provide continues information on feature changeability.
3) In this study, each subject is considered one class. To correctly classify the above-mentioned feature matrices to the appropriate class, the Fréchet distance measures perform better than the Euclidian distance for ECG data classification. Therefore, this paper proves that Fréchet classifiers can be utilized in multiclass classification problems.

3.4 Materials and Methods

In this study, we propose a methodology for ECG based human identification using both fiducial and non-fiducial features. We developed our methods to identify individuals based on the minimum Fréchet distance between features of randomly selected ECG data. In our non-fiducial approach, we choose various time windows and apply Short Time Fourier Transform (STFT) to extract the ECG frequency components followed by creating a feature matrix. In our fiducial approach, we select multiple consecutive heart beats and extract the QRS amplitude, temporal, and distance features followed by creating a cross feature matrix. In both approaches, each subject is

considered an independent class and in order to identify individuals, we perform multiclass classification by finding the minimum distance between the abovementioned feature matrices.

3.4.1 Human identification based on the dynamic change in ECG spectral components

In general, static features that are extracted from multiple time segments or heartbeats and stacked in feature vectors or feature matrices may not adequately characterize the ECG signal because it is a time varying pattern with large variations. One of the appropriate ways to address this variation is to model dynamic features that have much informative details about the ECG variability. In Figure 3.2 we show the general block diagram of our non-fiducial method that is based on tracking the consecutive change in ECG spectral features.

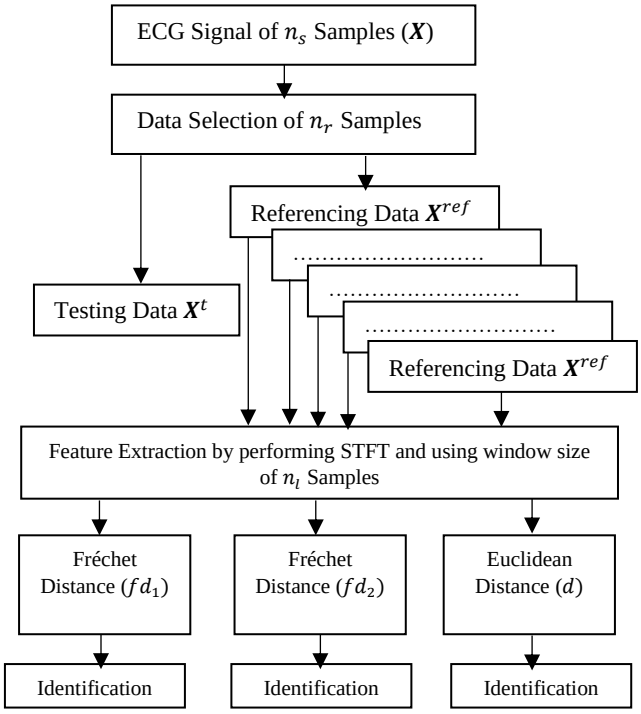

Figure 3.2: The block diagram of the proposed non fiducial methodology

3.4.1.1 Reference and Test data selection

In this paper, we use filtered ECGs of 62 subjects from the public ECG ID database which was originally recorded for biometric purposes. Each ECG was measured using a single lead at 500

sampling frequency and for a duration of 20 second. The public ECG ID database has ECG records of 90 subjects but do not provide any information about the exact time, date and the personal health condition in which the ECGs were recorded. However, all the ECG recordings were taking over six-month period. Therefore, we only chose ECG records of 62 subjects whom their ECG waveforms is similar to the normal shape of a heartbeat that is shown in Figure 3.1.

The process of selecting the reference and test data from the main ECG records using data windowing techniques is random. Each of the ECG records has 10000 samples which is enough information to randomly choose many continues data windows [24], for the referencing and testing purposes. To explain, let $\boldsymbol{X} = [x_1, x_2, \ldots\ldots\ldots, x_{n_s}]$ be any ECG signal with a total of many n_s samples. We first normalize the ECG data to reduce any possible similarity between the frequency components of multiple ECGs [4] [6]. Specifically, the samples are normalized according to the maximum and minimum values of the recorded ECG samples [22]. Then, we randomly select two sets of ECG data from **X** which are labeled as $\boldsymbol{X}^{ref} = [x_1^{ref}, x_2^{ref}, \ldots\ldots\ldots, x_{n_r}^{ref}]$ and $\boldsymbol{X}^t = [x_1^t, x_2^t, \ldots\ldots\ldots, x_{n_r}^t]$ where $n_r < n_s$. These randomly selected data windows are utilized for testing ($\boldsymbol{X}^t$) and referencing ($\boldsymbol{X}^{ref}$) purposes.

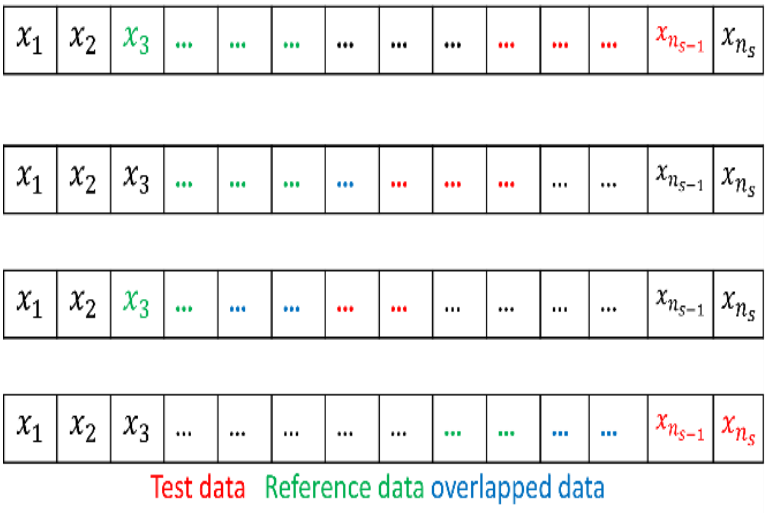

Figure 3.3: The randomization process of data selection

However, there is no agreement on the total number of ECG samples that are required for identification purposes [25]. Therefore, we arbitrarily select various n_r samples to provide a comparative analysis on the performance of the proposed method. Technically, equation (3.1) is used to find n_r such that:

$$n_r = \mathrm{r} \times n_s \tag{3.1}$$

where $0.2 \leq r \leq 0.5$

Moreover, the proposed method allows a maximum of 50% of overlapped samples between the randomly selected data. Figure 3.3 explains the data windowing technique for choosing different datasets. In addition, Figure 3.4 shows an example of randomly selecting the reference and test ECGs.

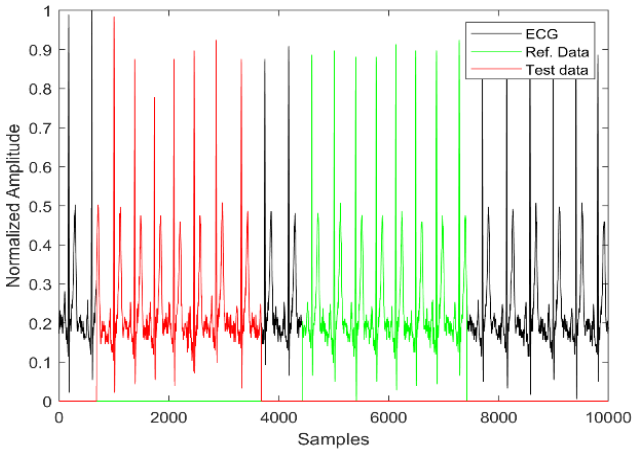

Figure 3.4: An example of randomly selecting the reference and test data (3000 samples each).

3.4.1.2 Extracting frequency components

In this stage, we apply STFT to extract the frequency components of consecutive ECG segments. STFT is a powerful general-purpose tool that is a useful method to define the time frequency distribution of signals [24]. STFT has better temporal and amplitude properties compared to the Fourier transform. In addition, STFT can be utilized to extract features of non-stationary biomedical signals such as the ECG. Moreover, although there are other methods such

as the wavelet transform which provides better time frequency resolution of non-stationary signals, the STFT has smaller computational time, because it is based on using fixed window length, which is advantageous property for increasing the identification time.

After randomly selecting the datasets, we divide the reference and test data into many n_w segments using a window of length n_l samples. However, since ECG is aperiodic signal, the optimal window length that tracks most of the change in the frequency components may differ among several ECGs. To address this problem, we choose three different window sizes to further examine the stability of our proposed method. To achieve our main goal on modelling the PSD dynamic change, we use an overlap of 50% between the adjoining samples. Consequently, we define here the following ECG time matrices:

$$X^{ref} = \begin{bmatrix} x^{ref}(1) & x^{ref}\left(n_l - \frac{n_l}{2} + 1\right) & x^{ref}(n_l + 1) \cdots & x^{ref}(n_r - n_l + 1) \\ \vdots & & \ddots & \vdots \\ x^{ref}(n_l) & x^{ref}\left(n_l + \frac{n_l}{2}\right) & x^{ref}(2n_l) \quad \cdots & x^{ref}(n_r) \end{bmatrix} \tag{3.2}$$

$$X^{t} = \begin{bmatrix} x^{t}(1) & x^{t}\left(n_l - \frac{n_l}{2} + 1\right) & x^{t}(n_l + 1) \cdots & x^{t}(n_r - n_l + 1) \\ \vdots & & \ddots & \vdots \\ x^{t}(n_l) & x^{t}\left(n_l + \frac{n_l}{2}\right) & x^{t}(2n_l) \quad \cdots & x^{t}(n_r) \end{bmatrix} \tag{3.3}$$

where n_l is the total number of ECG samples in each of the many n_w time segments such that:

$$n_w = 2 \times \left(\frac{n_r}{n_l}\right) - 1 \tag{3.4}$$

After that, we perform STFT on each time segment of the reference and test matrices. Namely, we perform STFT on each column of $X^{ref} \in R^{n_l \times n_w}$ and $X^{t} \in R^{n_l \times n_w}$. Let $\boldsymbol{X}_w \in R^{n_l \times 1}$ be any of the time segments in X^{ref} (or X^{t}), then its STFT is calculated using equation (3.5):

$$FR_w(k) = \sum_{m=0}^{n_{ft}} \boldsymbol{X}_w(m) e^{-j\left(\frac{2\pi}{n_{ft}}\right)km} \tag{3.5}$$

where (n_{ft}) is the STFT sampling points and $w = 1,2,3, \ldots . n_w$

Since we use sliding overlapped windows to extract the spectral information, each of the extracted spectrograms will contain some frequency components from the previous segment. To model the dynamic change in these frequency components between multiple time segments, we extract several consecutive spectrograms that represent how the spectral activity change from heartbeat to heartbeat. That is, this dynamic change in the frequency components from multiple time segments is utilized as distinguishing feature. Such characteristic is expected to be different from person to person. For instance, Figure 3.5 shows six consecutive time segments with 50% overlap and their corresponding spectrograms. The dynamic change in the power spectral density from heartbeat to heartbeat (the upper left image to the lower right image) can be seen as the increase or decrease in the intensity of the frequency components. This dynamic change is utilized to identify individuals.

Then, according to equation (3.5) we obtain two components for each STFT sampling point which are specifically the magnitude and phase. Since the phase components depend on several factors including the body state and the heart rate [25], we only select the magnitude components. Consequently, we define here the magnitude matrices of the frequency components:

$$A^{ref} = \begin{bmatrix} a_1^{ref}(0) & a_2^{ref}(0) & \cdots & a_{n_w}^{ref}(0) \\ \vdots & \ddots & & \vdots \\ a_1^{ref}(n_{ft}) & a_2^{ref}(n_{ft}) & \cdots & a_{n_w}^{ref}(n_{ft}) \end{bmatrix} \tag{3.6}$$

and

$$A^{t} = \begin{bmatrix} a_1^{t}(0) & a_2^{t}(0) & \cdots & a_{n_w}^{t}(0) \\ \vdots & \ddots & & \vdots \\ a_1^{t}(n_{ft}) & a_2^{t}(n_{ft}) & \cdots & a_{n_w}^{t}(n_{ft}) \end{bmatrix} \tag{3.7}$$

where $A^{ref} \in R^{(\frac{n_{ft}}{2}+1)\times n_w}$ has all the frequency components of the reference ECG data (X^{ref}) and $A^{t} \in R^{(\frac{n_{ft}}{2}+1)\times n_w}$ has all the frequency components of the test ECG data (X^{t}).

Note that because of the symmetry of STFT, we select half of the frequency components from each column of A^{ref} and A^{t}. However, the accuracy of extracting the dynamic change of ECG spectral activity highly affects the performance of the classification process. Therefore, we have performed multi-stage feature extraction technique to reach the best possible outcome via assigning various values to the n_r and n_l parameters. Namely, we extract many feature matrices for each subject according to Table 3.1. These multi feature matrices are then transferred to the classifiers.

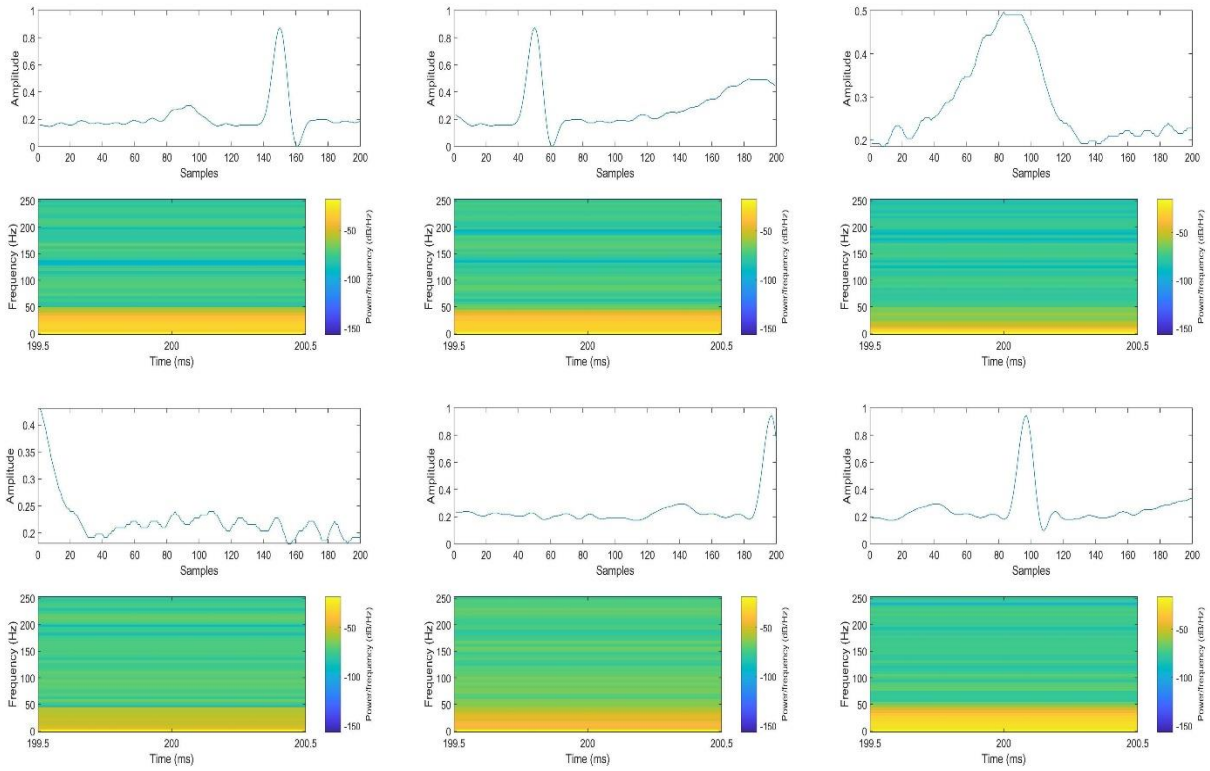

Figure 3.5:The spectrograms of consecutive heartbeats.

Table 3.1: Feature extraction based on selecting several data samples and STFT windows

Data Length	STFT window	Total Testing \ reference matrices
$n_{r1} = 0.2 \times n_s$ $n_{r2} = 0.3 \times n_s$ $n_{r3} = 0.4 \times n_s$ $n_{r4} = 0.5 \times n_s$	$n_{l1} = 100$ samples $n_{l2} = 200$ samples $n_{l3} = 250$ samples	$A^{ref}_{n_{r1},n_{l1}}, A^{ref}_{n_{r1},n_{l2}},$ ……. ……., $A^{ref}_{n_{r4},n_{l3}}$ $A^{t}_{n_{r1},n_{l1}}, A^{t}_{n_{r1},n_{l2}},$ ……. ……., $A^{t}_{n_{r4},n_{l3}}$

3.4.1.3 Fréchet distance measurements

This procedure involves correctly assigning the transformed feature matrices into a specific subject. To capture the dynamic change in the frequency components, we calculate the covariance matrices of the feature matrices using the following equations:

$$F^t = A^t A^{t^T} \tag{3.8}$$

$$F^{ref} = A^{ref} A^{ref^T} \tag{3.9}$$

where F^{ref} represents the covariance matrix of a reference feature matrix and F^t represents the covariance matrix of a test feature matrix.

These covariance matrices provide informative details on the dynamic change of the ECG frequency components. To identify subjects, we aim to find the minimum distance between F^{ref} and F^t. Technically, there several methods to compute the distance between matrices including the Euclidean distance and the Fréchet distance. However, choosing the adequate classifier relays on the geometrical characteristics of the matrices. Relatively, the covariance matrix is symmetric, and it is a positive definite if none of its eigenvalues is negative [8] . Also, it has been proven that the space of symmetric positive definite matrix is not Euclidean [10]. To minimize the distance between objects in non-Euclidian space, methods based on Fréchet distances have been proposed

[10]. Specifically, we use here the findings of Jahromi's work [10] to measure the minimum distance between F^{ref} and F^{t}, the covariance matrices of the ECG dynamic features. Namely, we use Fréchet distances as classifiers that are utilized for ECG based human identification. Technically, using equation (3.8), we obtain F^{t,p_i}, a single test covariance matrix, where $p_i = 1,2,3,\ldots,n_p$ is the subject number. Then, using equation (3.9), we obtain F^{ref,p_j}, a single reference covariance matrix of each subject involved in this study. To achieve our identification goal, we propose to find the Fréchet distances between a random test data of single person and a random reference data of all subjects. Specifically, we use equation (3.10) and (3.11) to calculate the Fréchet distances such that:

$$\boldsymbol{fd}_{\mathbf{1}}^{p_i} = \sqrt{Tr(F^{t,p_i}) + Tr(F^{ref,p_j}) - 2Tr(F^{t,p_i{}^{\frac{1}{2}}} F^{ref,p_j} F^{t,p_i{}^{\frac{1}{2}}})^{\frac{1}{2}}} \tag{3.10}$$

$$\boldsymbol{fd}_{\mathbf{2}}^{p_i} = \sqrt{Tr(F^{t,p_i}) + Tr(F^{ref,p_j}) - 2Tr(F^{t,p_i{}^{\frac{1}{2}}} F^{ref,p_j{}^{\frac{1}{2}}})} \tag{3.11}$$

where Tr refers to the trace of matrix and $p_j = 1,2,\ldots,n_p$ is the subject number with a total of n_p many subjects.

Moreover, we also provide a comparative analysis by comparing the results of Fréchet distances to the Euclidian distance. The later one is calculated using equation (3.12) where the summation is done over all the matrix entries.

$$d^{p_i} = \sqrt{\sum_{d_m=1}^{\frac{n_{ft}}{2}+1} \sum_{d_m=1}^{\frac{n_{ft}}{2}+1} \left(F^{t,p_i} - F^{ref,p_j}\right)^2} \tag{3.12}$$

Note that according to Table 3.1, we extract several test \ reference matrices. As explained above, the feature extraction step depends on the length of the selected ECG data and the length of the STFT window (see Figure 3.2). Consequently, using any of the above Fréchet classifiers, we technically define many distance vectors. To obtain the best identification performance, we

individually use these various feature matrices. Therefore, any of the above explained feature matrices and distance vectors can be written as F_{n_r,n_l}^{ref}, F_{n_r,n_l}^{t}, $\boldsymbol{FD}_{\mathbf{1},n_r,n_l}^{p_i}$ $\boldsymbol{FD}_{\mathbf{2},n_r,n_l}^{p_i}$ and $\boldsymbol{D}_{\mathbf{1},n_r,n_l}^{p_i}$. However, for simplicity, we used the general representation in equations (3.8), (3.9), (3.10), (3.11) and (3.12) respectively.

3.4.1.4 Classification and identification

After using equations (3.10), (3.11) and (3.12) we obtain $\boldsymbol{FD}_{\mathbf{1}}^{p_i} \in R^{n_p}$, $\boldsymbol{FD}_{\mathbf{2}}^{p_i} \in R^{n_p}$ and $\boldsymbol{D}^{p_i} \in R^{n_p}$. These three vectors contain n_p many distance measurements. As aforementioned, this is a multiclass classification problem where each subject is considered as an independent class. To correctly assign the test data to a specific subject (class), we perform classification by finding the minimum distance in each of these three vectors such that:

$$c_1^{p_i} = min_{p_j}\left(\boldsymbol{FD}_1^{p_i}\middle|_1^{n_p}\right) \tag{3.13}$$

where $c_1^{p_i}$ is the class obtained using the minimum distance in $\boldsymbol{FD}_{\mathbf{1}}^{p_i}$

$$c_2^{p_i} = min_{p_j}\left(\boldsymbol{FD}_2^{p_i}\middle|_1^{n_p}\right) \tag{3.14}$$

where $c_2^{p_i}$ is the class obtained using the minimum distance in $\boldsymbol{FD}_{\mathbf{2}}^{p_i}$

$$c^{p_i} = min_{p_j}\left(\boldsymbol{D}^{p_i}\middle|_1^{n_p}\right) \tag{3.15}$$

where c^{p_i} is the class obtained using the minimum distance in $\boldsymbol{D}^{p_i}$

After classification, the correct identification process is reached if $c_1^{p_i} = p_i$, $c_2^{p_i} = p_i$ and/or $c^{p_i} = p_i$. On other words, to correctly identify individuals the minimum distance must be obtained between a test data and a reference data that belong to one subject.

Most importantly, for each subject, the randomization process of reference and testing data selection is repeated 100 times which we refer to as the number of total experiments per subject (cross validation). Technically, in each experiment we repeat all that above explained process from

section 3.4.1.1 to section 3.4.1.4 respectively. This randomization process of the data selection aims to evaluate the robustness of our identification system over multiple repeated experiments because we aim to study the effect of the data length on the identification accuracy and other classification measures.

3.4.2 Human Identification based on the dynamic change in the QRS complex features

The QRS complex is the largest wave in the heartbeat, and it generally has most of the ECG significant information. Specifically, we use here the findings of our previous work on automatic QRS segmentation [26]. After correctly locating and segmenting QRS waves, we randomly select several consecutive QRS complexes that are utilized for identification purposes. In addition, we define here n_b as the number of heart beats that are selected for both testing and referencing purposes. Figure 3.6 shows an example of randomly selecting different QRS waves.

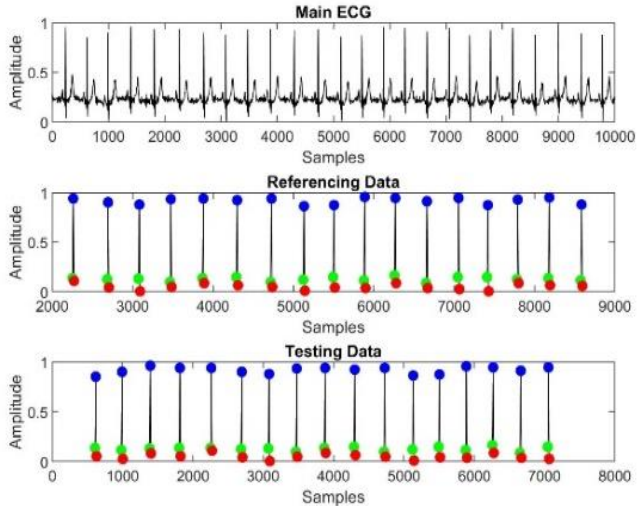

Figure 3.6: An example of randomly selecting the reference and test QRS waves.

3.4.2.1 QRS feature extraction

Several amplitudes, distance, morphological and temporal features can be extracted from each QRS [7] [18]. In this work, we propose to extract six fiducial features (n_f) and track their dynamic change among multiple heart beats. The consecutive variations of these features from heartbeat to

heartbeat is utilized as distinctive characteristic. The dynamic change between these features is expected to be different from person to person and it could provide significant information. Technically, we first align the QRS waves, then we extract temporal, amplitude, and distances features. These features include the time interval between R-Q peaks, the time interval between S-R peaks, the amplitude difference between R-Q peaks, the amplitude difference between R-S peaks, the distance between QRS waves and the distance between the first derivative of QRS waves. In addition, we normalize the above features to the personal heart rate to enhance the identification process.

Let n_b be the total number of heartbeats selected for the test / reference data, we obtain $\boldsymbol{Q} \in R^b$, $\boldsymbol{R} \in R^b$ and $\boldsymbol{S} \in R^b$ vectors. These three vectors contain the time localized QRS points for all the heart beats involved in the identification process. Accordingly, the time features ($\boldsymbol{F_1}$ and $\boldsymbol{F_2}$) are calculated using equation (3.16) and (3.17). the amplitude features ($\boldsymbol{F_3}$ and $\boldsymbol{F_4}$) are calculated using equation (3.18) and (3.19). Moreover, let M_{QRS} be the time matrix which has all the QRS waves and let M_{DQRS} be the matrix which has the first derivative of each column in M_{QRS}, then the distance features ($\boldsymbol{F_5}$ and $\boldsymbol{F_6}$) are calculated using equation (3.20) and (3.21).

$$\boldsymbol{F_1} = \boldsymbol{R_b} - \boldsymbol{Q_b} \tag{3.16}$$

$$\boldsymbol{F_2} = \boldsymbol{S_b} - \boldsymbol{R_b} \tag{3.17}$$

$$\boldsymbol{F_3} = \boldsymbol{X}(\boldsymbol{R_b}) - \boldsymbol{X}(\boldsymbol{Q_b}) \tag{3.18}$$

$$\boldsymbol{F_4} = \boldsymbol{X}(\boldsymbol{R_b}) - \boldsymbol{X}(\boldsymbol{S_b}) \tag{3.19}$$

$$\boldsymbol{F_5} = \sqrt{\sum_{b=1}^{n_b-1}(\boldsymbol{QRS_b} - \boldsymbol{QRS_{b+1}}))^2} \tag{3.20}$$

$$\boldsymbol{F_6} = \sqrt{\sum_{b=1}^{n_b-1}(\mathbf{D}\boldsymbol{QRS_b} - \boldsymbol{DQRS_{b+1}}))^2} \tag{3.21}$$

where $b = 1,2, \dots, n_b$ refers to the beat number

After using equations (3.16) to (3.21), we obtain $\boldsymbol{F_1} \in R^{n_b}$, $\boldsymbol{F_2} \in R^{n_b}$, $\boldsymbol{F_3} \in R^{n_b}$, $\boldsymbol{F_4} \in R^{n_b}$, $\boldsymbol{F_5} \in R^{n_b-1}$ and $\boldsymbol{F_6} \in R^{n_b-1}$ respectively. Consequently, we define here the QRS feature matrix:

$$A_{QRS} = \begin{bmatrix} f_1(1) & f_1(2)\cdots & f_1(n_b-1) \\ \vdots & \ddots & \vdots \\ f_{n_f}(1) & f_{n_f}(2)\cdots & f_{n_f}(n_b-1) \end{bmatrix} \tag{3.22}$$

where each column has features of a single QRS wave.

Note that the last two features are computed using the difference between two consecutive QRS complexes; therefore, the number of QRS waves utilized for creating the QRS feature matrix is less than the total number of selected heartbeats.

3.4.2.2 Creating the QRS cross feature matrix

The ECG is a time varying signal, and its fiducial features generally change according to many conditions such as work, body state and activity. Thus, it has been demonstrated that the large variability of ECG morphological, temporal and amplitude features make them hard to be utilized for human identification [7] [25]. However, tracking the dynamic change in these fiducial features could be utilized as significant feature. In this section, we aim to test the applicability of human identification using the dynamic variations of QRS features that are obtained from several consecutive heart beats.

Let $\boldsymbol{V_b} \in R^{n_f}$ and $\boldsymbol{V_{b+1}} \in R^{n_f}$ be the feature vectors for any two consecutive QRS waves in the matrix A_{QRS}, there are many methods to measure the similarity between these two vectors. Specifically, in this work we define the cross-feature matrix (CF_{QRS}) which shows how the QRS features change from heartbeat to heartbeat. The $CF \in R^{n_f \times n_f}$ is a square symmetric matrix and it is calculated using equation (3.23):

$$CF_{QRS} = \boldsymbol{V_b}\boldsymbol{V_{b+1}}^T \tag{3.23}$$

However, for each subject we randomly select multiple QRS waves, and we obtain $n_b - 1$ many feature vectors. Therefore, equation (3.23) can be generalized as:

$$CF_{QRS} = \sum_{b=1}^{n_b-1} \frac{\boldsymbol{V_b V_{b+1}}}{n_b - 1} \tag{3.24}$$

To address the variability of QRS features, $CF_{QRS} \in R^{n_f \times n_f}$ is defined as the average dynamic change in the QRS distance, amplitude, and temporal features of multiple consecutive heartbeats. Figure 3.7 shows multiple consecutive QRS waves of two different subjects where temporal, amplitude, and distance features have some variation. The degree of such variability can be expressed using equation (3.24) and it can be utilized as distinctive characteristic. Note that the cross-feature matrix is calculated based on the total number of selected QRS beats that are chosen from both the reference and test data. Since we set n_b to three different values, we obtain many cross-feature matrices for each subject. These multi cross feature matrices are transferred to the Fréchet classifiers.

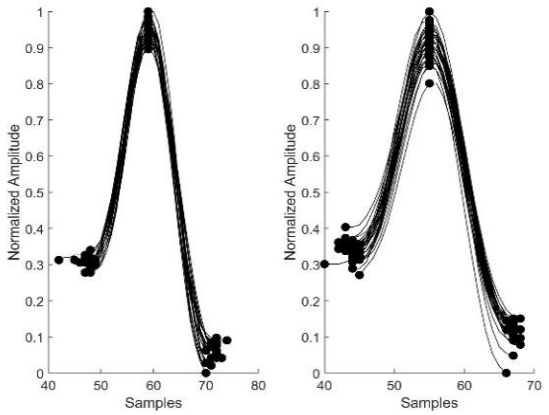

Figure 3.7: An example of the variability in QRS features.

3.4.2.3 Fréchet distance measurements

Similarly, we aim to identify individuals by correctly assigning the CF_{QRS} matrices into a specific person. Let CF_{QRS}^{t} be the matrix obtained from the test data and let CF_{QRS}^{ref} be the matrix

obtained from the reference data, we capture the dynamic change in the ECG fiducial features using equations (3.25) and (3.26):

$$F_{QRS}^{t} = CF_{QRS}^{t}\, CF_{QRS}^{t\,T} \tag{3.25}$$

$$F_{QRS}^{ref} = CF_{QRS}^{ref}\, CF_{QRS}^{ref\,T} \tag{3.26}$$

After using equations (3.25) we obtain $F_{QRS}^{t} \in R^{n_f \times n_f}$ which represents the covariance matrix of the test data. Similarly, using equations (3.26) we obtain $F_{QRS}^{ref} \in R^{n_f \times n_f}$ which represents the covariance matrix of the reference data. For each subject, these matrices are recorded and used as their unique signature. After that, we use equation (3.27) and (3.28) to find the Fréchet distances:

$$\boldsymbol{fd}_{\mathbf{1}}^{p_i} = \sqrt{Tr(F_{QRS}^{t,p_i}) + Tr(F_{QRS}^{ref,p_j}) - 2Tr(F_{QRS}^{t,p_i\frac{1}{2}} F_{QRS}^{ref,p_j} F_{QRS}^{t,p_i\frac{1}{2}})^{\frac{1}{2}}} \tag{3.27}$$

$$\boldsymbol{fd}_{\mathbf{2}}^{p_i} = \sqrt{Tr(F_{QRS}^{t,p_i}) + Tr(F_{QRS}^{ref,p_j}) - 2Tr(F_{QRS}^{t,p_i\frac{1}{2}} F_{QRS}^{ref,p_j\frac{1}{2}})} \tag{3.28}$$

Consequently, $\boldsymbol{FD}_{\mathbf{1}}^{p_i} \in R^{n_p}$ and $\boldsymbol{FD}_{\mathbf{2}}^{p_i} \in R^{n_p}$ vectors contain the Fréchet distances between single test matrix data and n_p many reference matrices.

3.4.2.4 Classification and identification

Similarly, we perform classification by finding the R-entry with smallest distance using equations (3.13) and (3.14) respectively. After classification, the correct identification process is obtained if the minimum Fréchet distance is measured between F_{QRS}^{t,p_i} and F_{QRS}^{ref,p_j} that belong to the same subject such that $c_1^{p_i} = p_i$ and/or $c_2^{p_i} = p_i$. We expect that the Fréchet distances between cross-feature matrices that belong to different subjects to be as large as possible. In contrast, we expect that the Fréchet distance between cross feature matrices that belong to the same subject to be as small as possible.

3.5 Experiments and Results

The performance of the proposed methodology has been evaluated using ECG data of 62 subjects (n_p) from the well-known ECG ID database. For each subject, the test and reference data are randomly selected for 100 times (n_{exp_i}). Note that we utilize randomized selection because the performance of our algorithms might be data dependent. By selecting reference and test data randomly, we can evaluate the performance range for different selections and ensure that minimum requirements are satisfied for arbitrarily chosen data in actual applications. Consequently, the total number of experiments is:

$$n_{exp} = n_{exp_i} \times n_p \tag{3.29}$$

For each experiment, we apply the proposed feature extraction technique, classification, and identification based on the minimum distance as explained above. As a result, we obtain the $ID \in R^{n_p \times n_p}$ matrix which contains the final identification results of all the experiments. Assuming that the rows represent the total number of subjects, and the columns represent the multiclass classification results, for each subject the elements of the ID matrix are defined as:

1) TP_{p_i} which is the diagonal element representing the total number of times the subject is identified in the many n_{exp_i} personal experiments (when the test data was selected from the relevant subject).
2) FN_{p_i} which is the total number of times the subject is not identified in the many n_{exp_i} personal experiments (the corresponding row elements because the system has incorrectly obtained a different class/es).
3) FP_{p_i} which is the total number of times the subject is identified in the many $n_{exp} - n_{exp_i}$ experiments (the corresponding column elements when the test data was selected from different subjects).

4) TN_{p_i} which is the total number of times the subject is not identified in the many $n_{exp} - n_{exp_i}$ experiments (the corresponding off diagonal elements when the test data was selected from different subjects).

As a result, we tested the applicability of our algorithm by measuring the average identification accuracy of the method and the personal identification accuracy. While the former measure shows the overall stability of our method to identify all the subjects, the later measure is more informative and precise in terms of the individual identification accuracy. To calculate these performance measures, we used equations (3.30) and (3.31) such that:

$$acc_{ave} = \frac{1}{n_p} \sum_{p_i=1}^{n_p} acc_{p_i} \tag{3.30}$$

where acc_{ave} is the average identification accuracy of the of method and acc_{p_i} is the personal identification accuracy:

$$acc_{p_i} = \frac{TP_{p_i}}{TP_{p_i} + FN_{P_i}} x100 \tag{3.31}$$

In addition, we evaluated the performance of our method by the following parameters:

Precision: it represents the ratio of truly identifying subjects with total number of identifications:

$$Precision = \frac{1}{n_p} \sum_{p_i=1}^{n_p} \frac{TP_{p_i}}{TP_{p_i} + FP_{p_i}} \tag{3.32}$$

Recall and it is also known as true positive rate (TPR): it represents the ratio of truly identifying subjects with total number of identification attempts:

$$Recall = \frac{1}{n_p} \sum_{p_i=1}^{n_p} \frac{TP_{p_i}}{TP_{p_i} + FN_{P_i}} \tag{3.33}$$

F score: a statistical measure to evaluate the model's accuracy:

$$F\ Score = \frac{2 \times\ Precision\ \times\ Recall}{Precision + \ Recal} \tag{3.34}$$

False Acceptance Rate (FAR) and it is also known as false positive rate (FPR): the ratio of falsely accepting subjects with the total number of rejection attempts:

$$FAR = \frac{1}{n_p} \sum_{p_i=1}^{n_p} \frac{FP_{p_i}}{TN_{p_i} + FP_{P_i}} \tag{3.35}$$

False Rejection Rate (FRR): the ratio of falsely rejecting subjects with the total number of identification attempts:

$$FRR = \frac{1}{n_p} \sum_{p_i=1}^{n_p} \frac{FN_{p_i}}{TP_{p_i} + FN_{P_i}} \tag{3.36}$$

Specificity: The ratio of truly rejecting subjects with a total number of rejection attempts:

$$Specificity = \frac{1}{n_p} \sum_{p_i=1}^{n_p} \frac{TN_{p_i}}{TN_{p_i} + FP_{p_i}} \tag{3.37}$$

3.5.1 Human Identification using the dynamic change in the ECG frequency components

The human identification based on the dynamic change in ECG frequency components has shown excellent results. However, the performance of the proposed method highly depends on several parameters including namely the length of STFT window, the length of ECG data and the type of classifier. Since the ECG recordings have substantial durations (e.g., each record has 10000 samples), we arbitrarily repeated the reference and test data selection 100 times.

As a result, the Fréchet based classifiers has significantly shown excellent performance at all the applied parameters as seen in Table 3.2. The table shows that the FD_2 classifier has slightly shown higher performance than the FD_1 classifier. Consequently, by applying equation (3.30) we obtained our highest performance of 97.03% average identification accuracy using the FD_2

classifier. Moreover, Figure 3.8 shows that the identification process depends on the length of the reference and test data. In this paper, our best findings are obtained at data length equal to 4000 and 5000 samples. As shown in Figure 3.8, the FD_2 classifier has the highest identification accuracy over all the three distance measurements. Also, we can clearly see that the best identification performance is achieved via using STFT windows size set to 200 samples and increasing the data length to 5000 samples. However, the optimal length of ECG data utilized for human identification varies according to the practical applications.

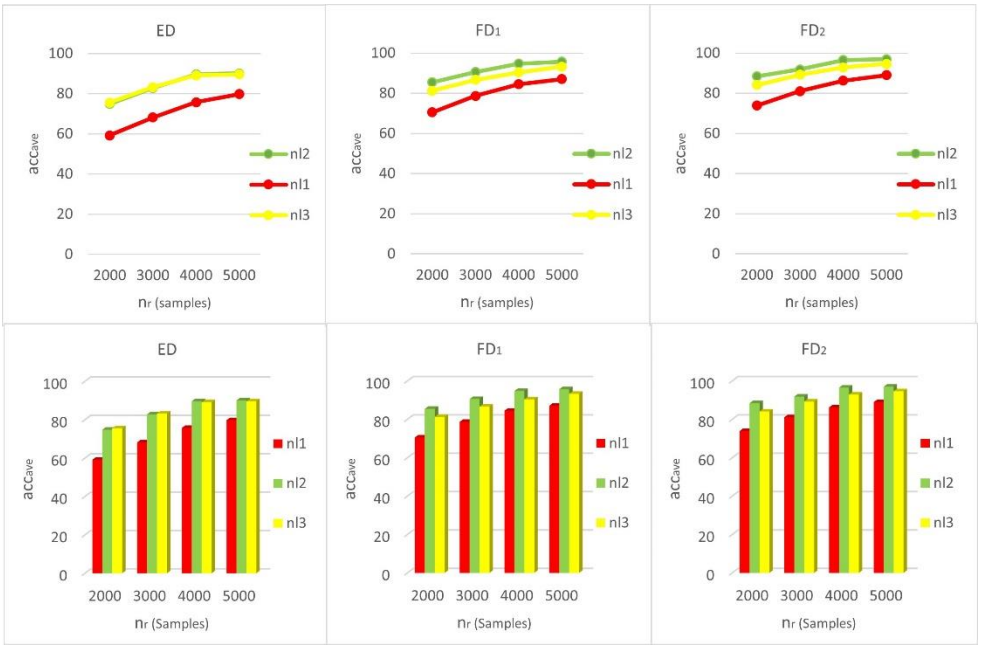

Figure 3.8: The average identification accuracy of our non-fiducial method

Moreover, we calculated the personal identification accuracy for all the 62 subjects using equation (3.31). As a result, the personal identification accuracy highly depends on the length of the STFT window. To accurately track the dynamic change in the ECG frequency components, the optimal window size should contain a full heartbeat. In addition, it is important to demonstrate that the size of the STFT window depends on the individual heart rate. In this paper, the optimal

STFT window size is in the range of 200 to 250 samples (e.g., using n_{l2} to n_{l3} from Table 3.1) because majority of the subjects are successfully identified with high acc_{p_i} as shown in Figure 3.9. Although some subjects are correctly identified using both above-mentioned parameters, Figure 3.9 shows that we achieve higher identification performance by setting the STFT window size to 200 samples.

Table 3.2: The identification accuracy of the non-fiducial methodology evaluated at all applied data lengths, STFT windows and different classifiers (n_{l1}= 100 samples, n_{l2}= 200 samples, n_{l3}= 250 samples, n_{r1}= 2000 samples, n_{r2}= 3000 samples, n_{r3}= 4000 samples, n_{r4}= 5000 samples.

Identification Accuracy (%)	Classifier	ED			FD_1			FD_2		
	STFT window (n_l) \ ECG Data Length (n_r)	n_{l1}	n_{l2}	n_{l3}	n_{l1}	n_{l2}	n_{l3}	n_{l1}	n_{l2}	n_{l3}
	n_{r1}	59.16	74.80	75.54	70.54	85.48	81.29	73.90	88.41	84.09
	n_{r2}	68.19	82.77	83.22	78.67	90.58	86.64	81.09	91.87	89.25
	n_{r3}	75.74	89.64	89.09	84.48	94.77	90.41	86.22	96.51	92.90
	n_{r4}	79.77	90.06	89.58	87.09	95.67	93.29	89	97.03	94.64

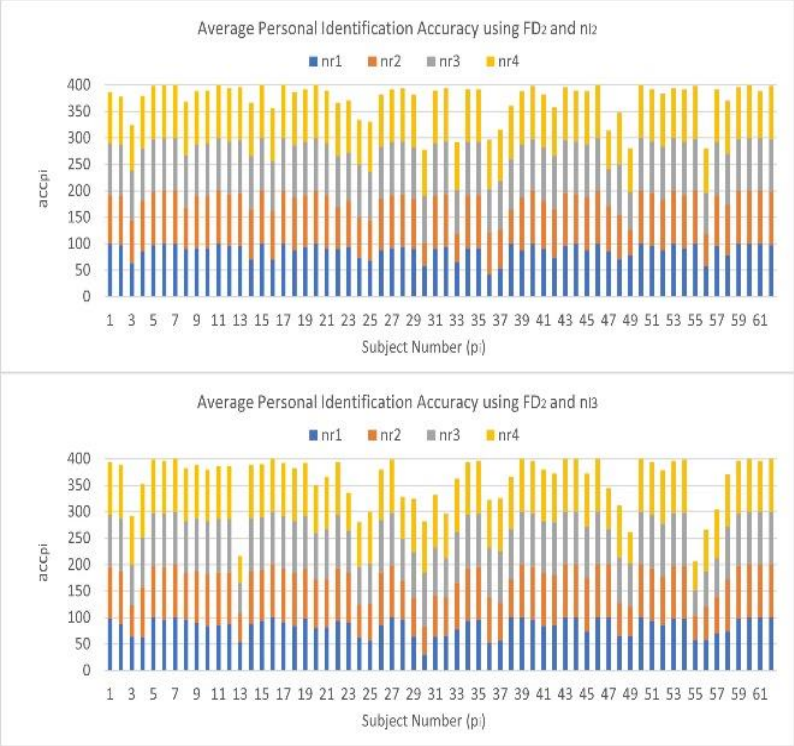

Figure 3.9: The personal identification accuracy using FD_2.

Furthermore, Table 3.3 and Figure 3.10 provide full details on identification accuracy using the FD_2 classifier. Table 3.3 shows that most of the subjects are accurately identified with acc_{p_i}

ranging from 91% to 100% when larger lengths of reference and test data are selected. In addition, Figure 3.10 shows that lowering the STFT window size than 200 samples (e.g., using 100 samples) or reducing the length of reference and test data (e.g., using 2000 or 3000 samples) decreases the identification accuracy. Most importantly, All the above illustrated findings prove that the Fréchet based classifiers are more robust to obtain the minimum distance between feature matrices than the Euclidean based classifiers.

Table 3.3: The total number of subjects identified per identification accuracy range using the dynamic change in the ECG frequency components at all applied data lengths, STFT windows and FD_2 classifier.

Total Subjects Identified	Identification Accuracy Range	0-50%			51-70%			71-80%			81-90%			91-100%		
	STFT window (n_l) \ ECG Data Length (n_r)	n_{l1}	n_{l2}	n_{l3}	n_{l1}	n_{l2}	n_{l3}	n_{l1}	n_{l2}	n_{l3}	n_{l1}	n_{l2}	n_{l3}	n_{l1}	n_{l2}	n_{l3}
	n_{r1}	9	1	1	11	8	15	15	5	4	17	12	13	10	36	29
	n_{r2}	7	2	1	9	3	9	11	6	6	7	4	4	28	47	42
	n_{r3}	1	0	1	13	1	3	4	2	7	10	5	5	34	54	46
	n_{r4}	2	0	1	6	0	2	5	1	4	12	7	4	37	54	51

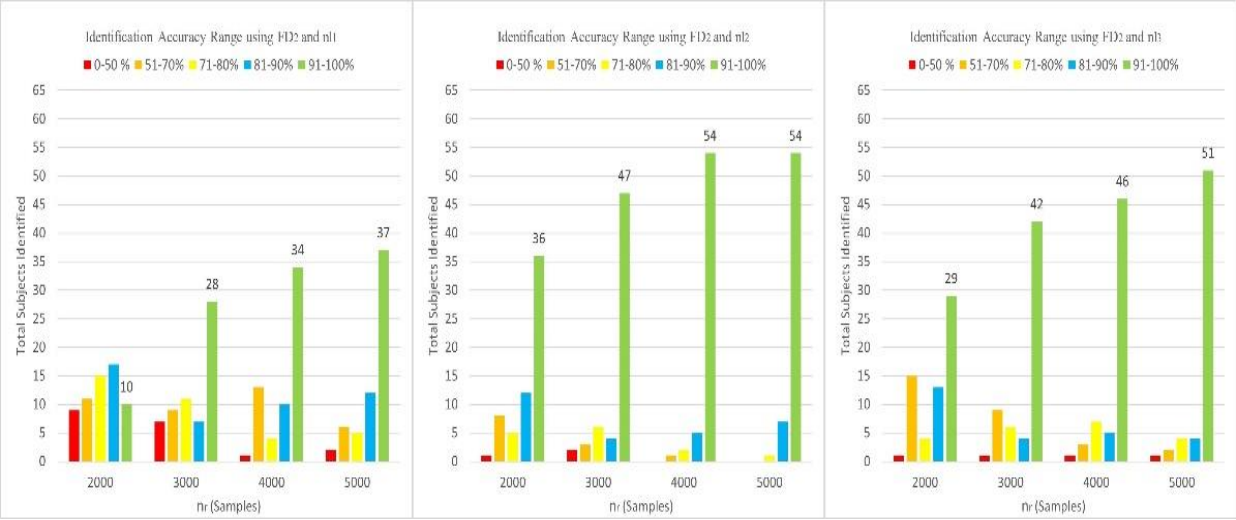

Figure 3.10: The total subjects identified per accuracy range via applying the FD_2 classifier

Furthermore, we evaluated the performance of the non-fiducial methodology in terms of precision, recall, F score, FAR, FRR and specificity which are calculated using equations (3.32) to (3.37) respectively. Consequently. Figure 3.11 shows the best performance findings which are achieved via applying the STFT window size of 200 samples. Specifically, the figure shows that we achieved the highest performance of

0.9719 precision, 0.9703 recall, 0.9711 F score, 0.0296 FRR, 0.00048 FAR and 0.9995 specificity via utilizing the data length of 5000 samples and applying the FD_2 classifier for identification.

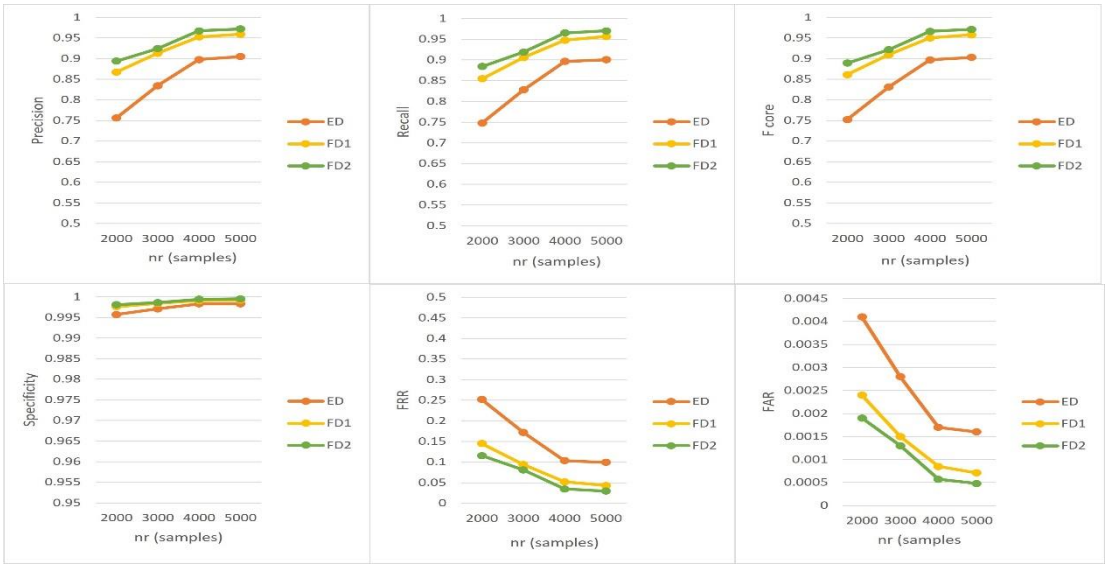

Figure 3.11:The performance of the non-fiducial methodology using STFT window size of 200 samples.

In addition, Table 3.4 shows the precision, recall, F score, specificity, FRR and FAR of the non-fiducial methodology evaluated at all applied data lengths, STFT windows and different classifiers. According to the table, increasing the data length from 2000 samples to 5000 samples significantly increases precision, recall, F score and specificity parameters at all applied STFT windows. In contrast, it decreases the FAR and FRR which is highly required result to reduce the overall error of the identification model. However, increasing or decreasing the STFT window size than 200 samples slightly decrease the precision, recall, F score and specificity parameters at all applied data lengths. In contrast, it increases the FRR and FAR. This is expected because the optimal number of STFT window size that can track the dynamic change in the ECG spectral features is different from subject to subject and it depends on the personal heart rate. Since ECG is nonstationary signal, the optimal window size should contain samples of a full heartbeat to accurately extract the dynamic features. Moreover, Figure 3.12 shows the FRR and FAR for all

Table 3.4: The overall performance of the non-fiducial methodology evaluated at all data lengths, STFT windows and different classifiers *(*n_{l1}= 100 samples, n_{l2}= 200 samples, n_{l3}= 250 samples, n_{r1}= 2000 samples, n_{r2}= 3000 samples, n_{r3}= 4000 samples, n_{r4}= 5000 samples).

Classifier	STFT window (n_l)	ECG Data Length (n_r)	Precision	Recall	F Score	FRR	FAR	Specificity
ED	n_{l1}	n_{r1}	0.6058	0.5916	0.5986	0.4083	0..0067	0.9933
		n_{r2}	0.6963	0.6819	0.689	0.318	0..0052	0.9947
		n_{r3}	0.7625	0.7574	0.7599	0.2425	0.004	0.996
		n_{r4}	0.801	0.7977	0.7993	0.2022	0.0033	0.9966
	n_{l2}	n_{r1}	0.7563	0.748	0.7521	0.2519	0.0041	0.9959
		n_{r2}	0.8343	0.8277	0.831	0.1722	0.0028	0.9971
		n_{r3}	0.8977	0.8964	0.897	0.1035	0.0017	0.9983
		n_{r4}	0.905	0.9006	0.9028	0.0993	0.0016	0.9983
	n_{l3}	n_{r1}	0.7651	0.7554	0.7602	0.2445	0.004	0.9959
		n_{r2}	0.8396	0.8322	0.8359	0.1677	0.0027	0.9972
		n_{r3}	0.8927	0.8909	0.8918	0.109	0.0018	0.9982
		n_{r4}	0.8973	0.8958	0.8965	0.1041	0.0017	0.9982
FD1	n_{l1}	n_{r1}	0.7215	0.7054	0.7134	0.2945	0.0048	0.9951
		n_{r2}	0.7944	0.7867	0.7905	0.2132	0.0035	0.9965
		n_{r3}	0.8502	0.8448	0.8475	0.1551	0.0025	0.9974
		n_{r4}	0.8756	0.8709	0.8733	0.129	0.0021	0.9978
	n_{l2}	n_{r1}	0.8675	0.8548	0.8611	0.1451	0.0024	0.9976
		n_{r2}	0.9129	0.9058	0.9093	0.0941	0.0015	0.9984
		n_{r3}	0.9526	0.9477	0.9501	0.0522	0.00085	0.9991
		n_{r4}	0.9592	0.9567	0.9579	0.0432	0.00071	0.9992
	n_{l3}	n_{r1}	0.8195	0.8129	0.8162	0.187	0.0031	0.9969
		n_{r2}	0.8692	0.8664	0.8678	0.1335	0.0022	0.9978
		n_{r3}	0.9077	0.9041	0.9059	0.0958	0.0016	0.9984
		n_{r4}	0.9362	0.9329	0.9345	0.067	0.0011	0.9989
FD2	n_{l1}	n_{r1}	0.7513	0.7390	0.7451	0.2609	0.0043	0.9957
		n_{r2}	0.8164	0.8109	0.8137	0.189	0.0031	0.9969
		n_{r3}	0.8674	0.8622	0.8648	0.1377	0.0023	0.9977
		n_{r4}	0.8945	0.89	0.8922	0.11	0.0018	0.9982
	n_{l2}	n_{r1}	0.8941	0.8841	0.8891	0.1158	0.0019	0.9981
		n_{r2}	0.9245	0.9187	0.9216	0.0812	0.0013	0.9986
		n_{r3}	0.9674	0.9651	0.9662	0.0348	0.00057	0.9994
		n_{r4}	0.9719	0.9703	0.9711	0.0296	0.00048	0.9995
	n_{l3}	n_{r1}	0.847	0.8409	0.8439	0.159	0.0026	0.9973
		n_{r2}	0.8971	0.8928	0.8948	0.1074	0.0018	0.9982
		n_{r3}	0.9316	0.929	0.9303	0.0709	0.0012	0.9988
		n_{r4}	0.9491	0.9464	0.9478	0.0535	0.00087	0.9991

the subjects at all applied classifiers, STFT window size of 200 samples and data length of 5000 samples. As a result, the FD_2 and FD_1 classifiers have significantly shown the minimum errors

compared to the Euclidean classifier. Most importantly, all the highest performance measures in Table 3.4 are achieved via using the Fréchet classifiers at all the applied STFT windows and data lengths. This shows that the Fréchet distances significantly perform better than the Euclidean distance when it comes to finding the minimum distance between features matrices.

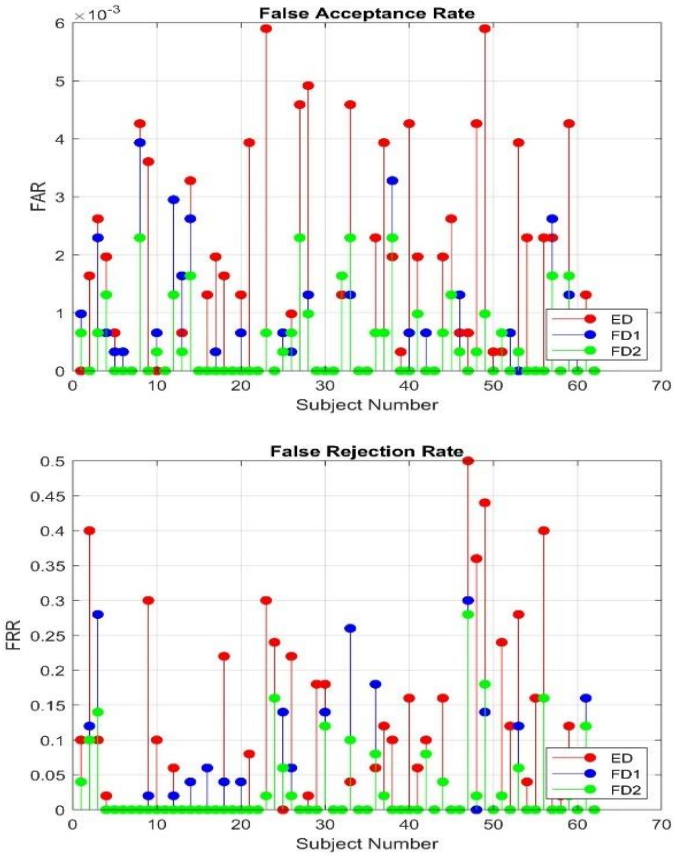

Figure 3.12: The FAR and FRR for all subjects using n_{r4} and n_{l2}

3.5.1.1. The performance evaluation using ROC, PR, AUC, and Cross validation

The non-fiducial methodology has been also evaluated using the receiver operating characteristic curve (ROC) which shows the performance of our classification models. Technically, ROC represents the tradeoff between the true positive rate (recall) and false positive rate (FAR). Consequently, the $\boldsymbol{FD_2}$ classifier has achieved the best results at all applied data lengths and STFT windows. In Figure 3.13, we show our best results using STFT window size of 200 samples. According to the figure, the $\boldsymbol{FD_2}$ classifier gives the closest curves to the top-left

corner followed by the $\boldsymbol{FD_1}$ and the Euclidean classifiers. In addition, we calculated the area under the curve (ROC AUC) with the best findings of 0.9849 at data length of 5000 samples.

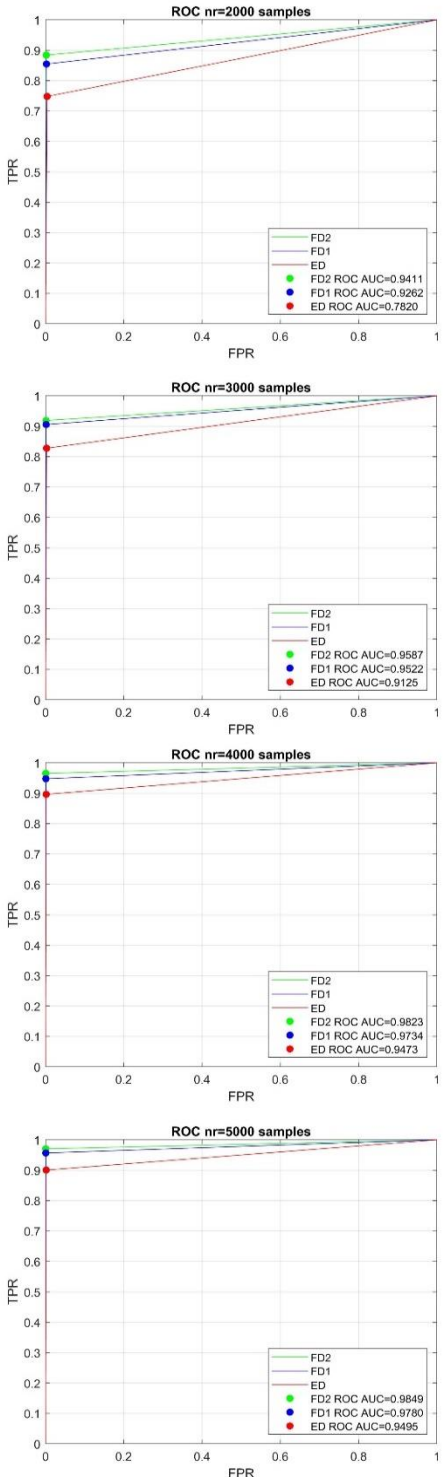

Figure 3.14: The ROC curves using n_{l2}

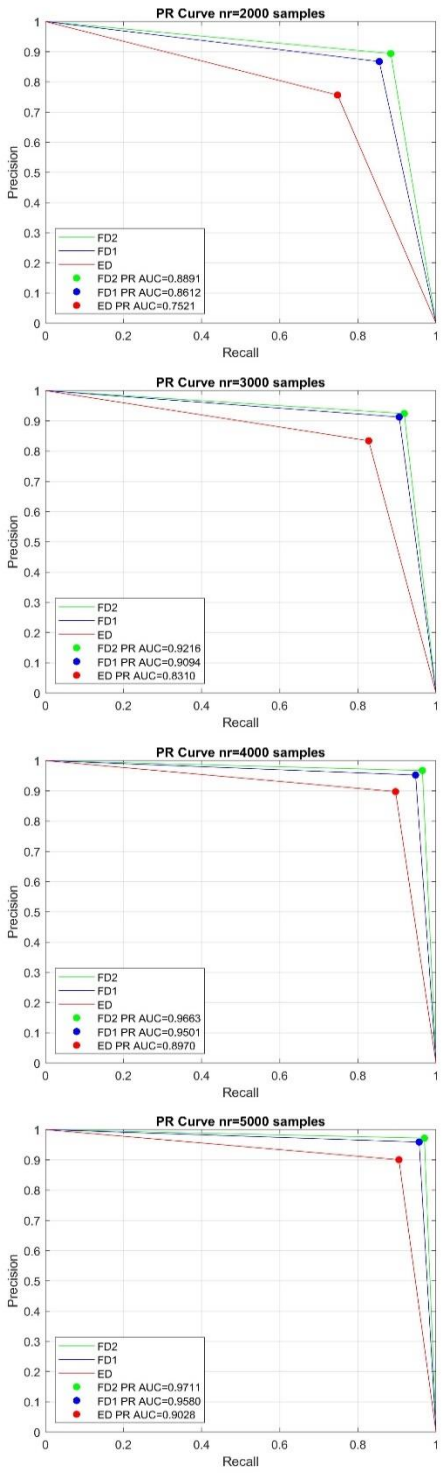

Figure 3.13: The PR curves using n_{l2}

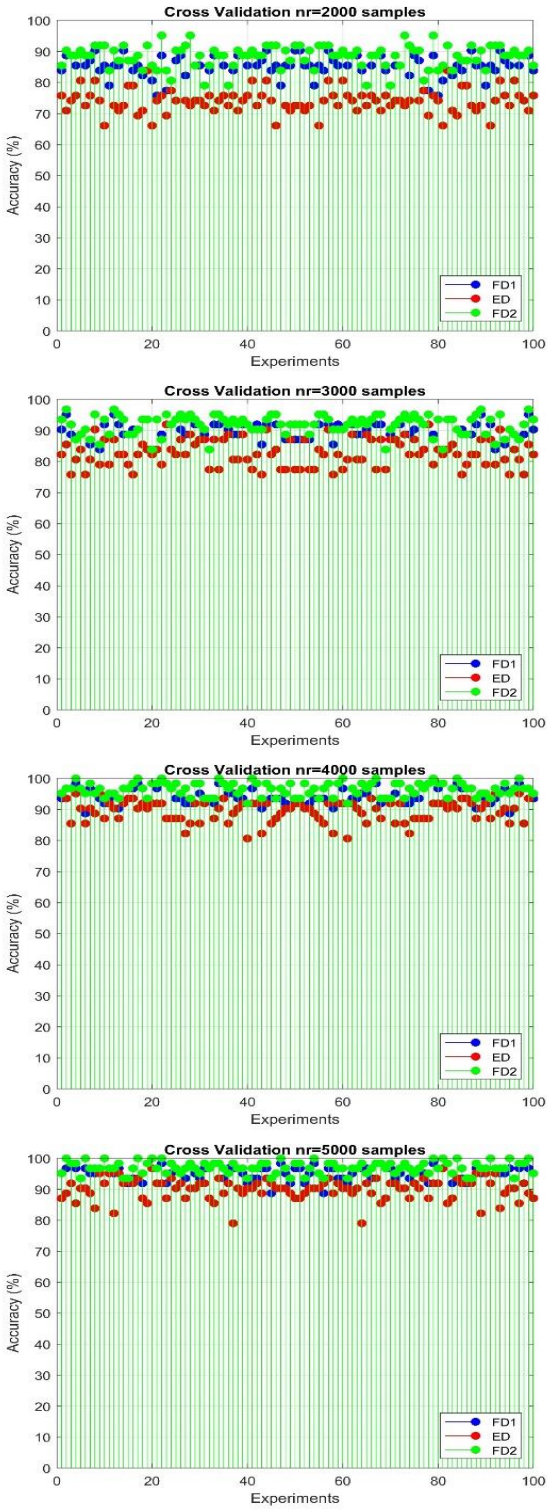

Figure 3.15: The cross-validation results using n_{l2}

Moreover, the performance of our non-fiducial method was examined using the precision-recall curves (PR) with the $\boldsymbol{FD_2}$ classifier achieving the closest curves to the top-right corner with PR AUC = 0.9711 as shown in Figure 3.14.

Furthermore, as mentioned above, for each subject we repeated the process of randomly selecting the refence and test data 100 times at all applied data lengths and STFT windows. In Figure 3.15, we present our best cross validation results. The figure clearly shows that for all subjects, the FD classifiers have significantly performed better than Euclidean classifier to obtain higher personal identification accuracy. In summary, Figures 3.13, 3.14 and 13.5 prove that the Fréchet classifiers can be utilized for to minimize the distance between ECG features for identification purposes.

3.5.2 Human Identification using the dynamic change in the QRS features

Human identification based on the dynamic change in QRS features has shown good results. In this paper, we set the total number of randomly selected QRS waves that are involved in the identification process to $n_{b1} = 14$, $n_{b2} = 15$ and $n_{b3} = 16$ respectively. Consequently, the FD_2 classifier has slightly shown higher performance than the FD_1 classifier as shown in Table 3.5. Generally, algorithms based on fiducial features have lower identification accuracy than algorithms based on non-fiducial features [1]. As a result, by applying equation (3.31) we obtained our highest performance of 82.01% average identification accuracy using the FD_2 classifier. In addition, Figure 3.16 shows that the identification process depends on the total number of QRS complexes that are utilized for extracting the dynamic feature. Specifically, our best performance was obtained using cross feature matrices of 16 consecutive QRS waves.

Table 3.5:Human identification accuracy using the dynamic change in the QRS features and Fréchet Classifiers

Classifier	No. QRS beats	Identification Accuracy (%)
FD_1	n_{b1}	69.11
	n_{b2}	73.3
	n_{b3}	77.11
FD_2	n_{b1}	74.11
	n_{b2}	77.74
	n_{b3}	82.02

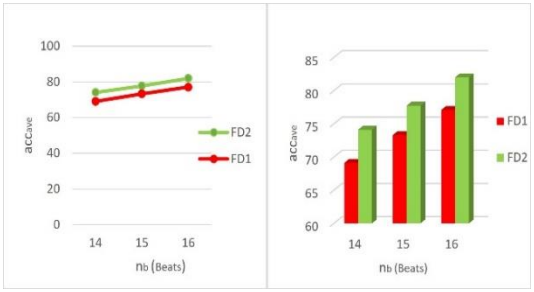

Figure 3.16: The average identification accuracy of our fiducial method

Moreover, we calculated the personal identification accuracy which highly depends on the degree of changeability in the temporal, amplitude, and distance features. Generally, larger changes in these features results in reducing the personal identification accuracy. Therefore, this method is ultimately individual based, but it can be utilized for identifying most of the subjects as seen in shown in Figure 3.17.

Figure 3.17:The personal identification accuracy using FD_2.

Nevertheless, Table 3.6 provides full details on the identification accuracy using the FD_2 classifier. The table shows that most of the subjects are accurately identified with personal identification accuracy ranging from 70% to 100% specifically when the number of selected QRS waves is increased. In addition, Figure 3.18 shows that selecting lower number of QRS waves (e.g., using n_{b1} or n_{b2}) decreases the identification accuracy. Hence, it decreases the overall performance of the identification method. Most importantly, these findings also prove that Fréchet based classifiers are stable for obtaining the minimum distance between feature matrices.

Table 3.6: The total number of subjects identified per identification accuracy range using the dynamic change in the QRS complexes and the FD_2 classifier.

Accuracy Range	No. QRS beats	Total subjects Identified
>70%	n_{b1}	28
	n_{b2}	25
	n_{b3}	17
71-80%	n_{b1}	14
	n_{b2}	13
	n_{b3}	16
81-100%	n_{b1}	20
	n_{b2}	24
	n_{b3}	29

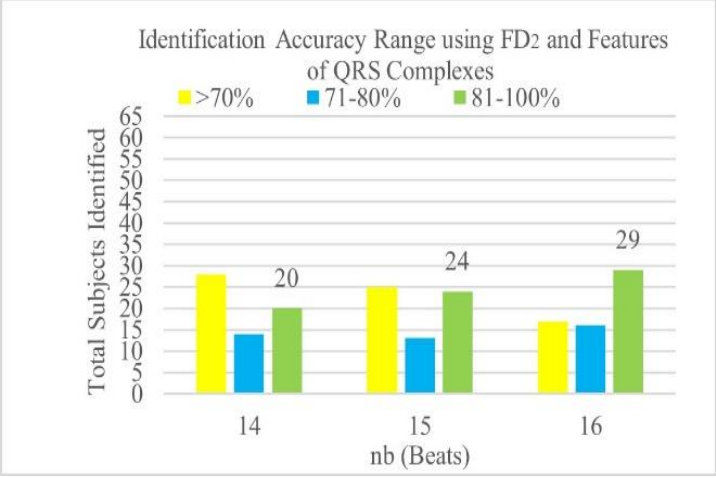

Figure 3.18: The total subjects identified per accuracy range via applying the FD_2 classifier.

Furthermore, we evaluated the performance of the fiducial methodology in terms of precision, recall, F score, FRR and FAR which are calculated using equations (3.32) to (3.36) respectively. As a result, we achieved the highest performance of 0.8294 precision, 0.8201 recall, 0.8247 F score, 0.1798 FRR and 0.0029 FAR via utilizing fiducial features of 16 consecutive heartbeats as shown in Table 3.7. The table shows that increasing the number of QRS complexes used for dynamic feature extraction increases the overall performance of the methodology and it decreases the FAR and FRR. In general, the proposed fiducial methodology has shown good results and it can be utilized as secondary identification tool in multibiometric systems that are based on biomedical signal.

Table 3.7: The performance of the fiducial methodology using Fréchet classifiers (*n_{b1}* = 14 QRS complexes, n_{b2} = 15 QRS complexes n_{b3} = 16 QRS complexes).

Classier	No. of QRS beats (n_b)	Precision	Recall	F Score	FRR	FAR
FD_1	n_{b1}	0.7099	0.6911	0.7003	0.3088	0.005
	n_{b2}	0.7492	0.733	0. 741	0.2669	0.0043
	n_{b3}	0.7846	0.7709	0.7777	0.229	0.0037
FD_2	n_{b1}	0.7546	0.7411	0.7478	0.2588	0.0042
	n_{b2}	0.7874	0.7774	0.7824	0.2225	0.0036
	n_{b3}	0.8294	0.8201	0.8247	0.1798	0.0029

In addition, the performance of the proposed fiducial methodology was evaluated using the ROC and PR curves. Consequently, Figure 3.19 displays the ROC curves, and it shows the *FD2* classifier achieving the closest curves to the top-left corner with the best AUC of 0.9086 using 16 heartbeats. Also, Figure 3.20 displays the PR curves, and it shows the *FD2* classifier achieving the closest curves to the top-right corner with the best AUC of 0.8248.

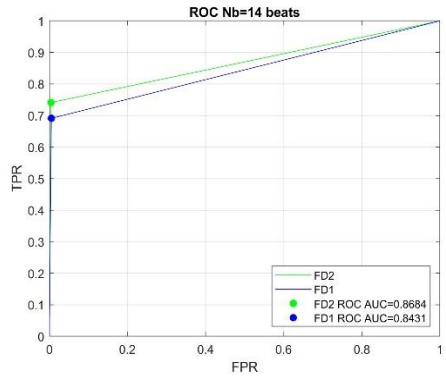

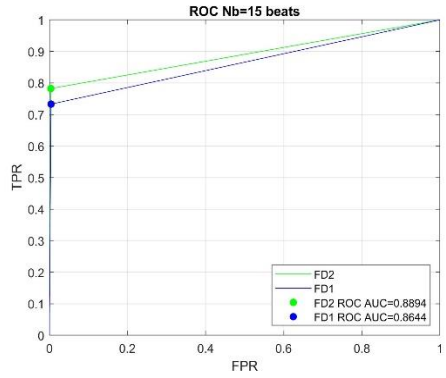

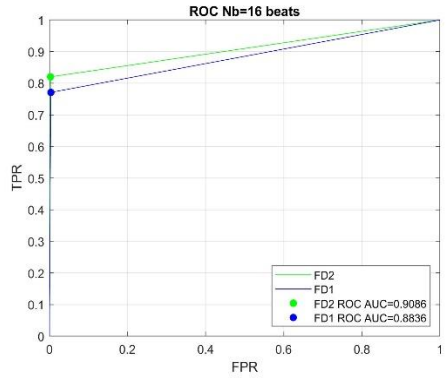

Figure 3.20: The ROC curves using n_{b3}

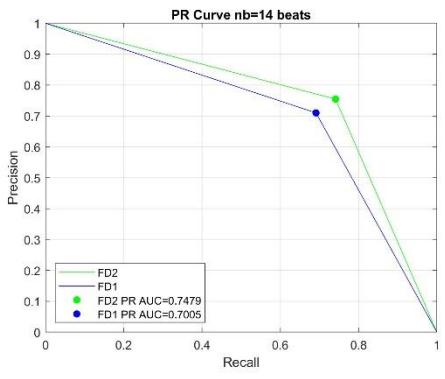

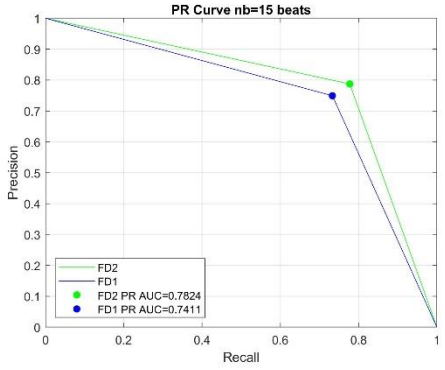

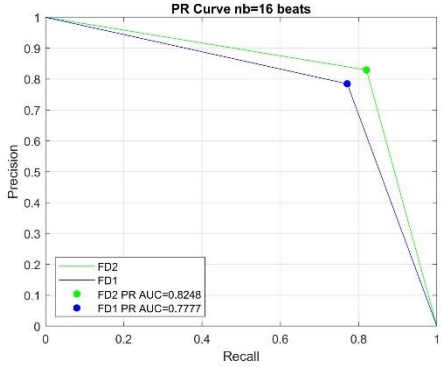

Figure 3.19: The PR curves using n_{b3}

3.6. Discussion

Generally, the performance of the ECG based human identification systems highly depends on the types of features and classifiers utilized for individual recognition. However, majority of the existing studies use static ECG features which in general have large variations [1]. In this study, our findings indicate that by obtaining an optimal STFT widow size for tracking the dynamic change in the ECG frequency components, majority of the subjects are correctly identified with higher identification accuracy. Also, our findings suggest that increasing the ECG data selected

for referencing and testing purposes increases the overall performance of the methodology, which is evaluated in terms of average identification accuracy, precision, recall, F score, specificity, FRR and FAR. Additionally, we also tested the feasibility of utilizing the dynamic change in the QRS morphological, amplitude and distance features for human identification purposes and we have achieved good results. Moreover, our findings indicate that the dynamic change in the QRS features remain stable and consistent for majority of the subjects. However, such characteristic is ultimately individual based, and it can be helpful as a supportive method.

Table 3.8 shows performance comparison with the state-of-the-art methods. The table shows that our non-fiducial method has shown excellent results compared to some of the approaches in the literature [14] [13] [20]. The method of Dong et al. [7] that is based on modelling QRS dynamics has shown good performance and it exceeded our performance. In comparison, our work has less mathematical complexity and it requires less computational time than the method presented in [7]. The work of authors in [12] exceeded the performance of our work by only 0.09%. However, the reported performance in [12] was based on using fiducial features which generally have larger variations as aforementioned. In addition, the fiducial features need to be extracted manually which requires segmentation. In comparison to [12], our best performance of 97.03% was obtained using non fiducial features which are automatically extracted. Method [19] which is based on conventional neural networks (CNN) reported 98.24% accuracy. However, it is well known that CNN based methods [21] are slow and they require several layers to obtain good results while our approach requires only to convert the ECG signal into only one domain of feature extraction. Although method [18] reported 98.5%, the development of an ECG biometric system considering only lower size of data (12 subjects) may limit the practical use of such systems in real world.

Table 3.8: Summary of the previous state of art and the proposed methodology on the ECG based human identification

Authors	Year	Database	Features	Classification	Subjects	Accuracy
Proposed	2022	ECG-ID	PSD Dynamics	FD	62	97.03%
Dong et al. [7]	2020	PTB	QRS Dynamics	DL , L_1 norm	52	97.42%
Fatimah et al. [18]	2020	ECG-ID	QRS morphological features, AR and L_4 norm	SVM, KNN, EBT	12	98.5%
Chu et al. [19]	2019	ECG-ID	Multi-level CNN features	CNN	90	98.24%
Kim et al. [20]	2019	PhBa and DCRI	RIFF	ML, DT	70	95%
Hammad et al. [21]	2019	PTB and CYBHi	CNN (ECG and fingerprint)	QG-MSVM	263	98.66%
Choi et al. [14]	2016	Private	Heartbeat morphological features	SVM	175	95.99%
Pal et al. [12]	2018	PTB	Heartbeat morphological features	PCA, KPCA, EDIST	100	97.12%
Hanilci et al. [13]	2019	PTB	AC, DCT, Cepstral features	MFCC, 2D CNN	42	90.48%

Abbreviations of data bases, features and classifications
PSD: Power spectral density; FD: Fréchet distance; PTB: Physikalisch-Technische Bundesanstal; DL: Deterministic learning; SVM: Support vector machine; K-Nearest neighbour; EBT: Ensemble bagged trees; CNN: Convolutional neural networks; PhBa: Physiobank; DCRI: Diabetes complications research initiative; RRIF: R-R Interval frame; ML: Machine learning: Decision tree; CYBHi: Check your bio signals here initiative; QG-MSVM: Q-Gaussian multi support vector machine; PCA: Principle Components Analysis; KPCA: Kernel principle components analysis; EDIST: Euclidean distance; AC: Autocorrelation coefficients; DCT Discrete Cosine transform; MFCC: Mel-frequency cepstral coefficients.

Some of the possible real-world deployment of our proposed method include enhancing security for multibiometric systems and in security control applications benefiting from continues biometric monitoring (e.g., companies, banks, and government buildings. However, there are also some limitations to the proposed method because the identification process depends on measuring the minimum distance between a test data and the reference data of all subjects that are enrolled in the identification system. Although the average identification time in this work is about 2.5 seconds which may be suitable for some applications, the real-world deployment of our method on large scale of databases could increase the average identification time which may limit practicability of our proposed methods to small population.

Most importantly, the main contribution of this paper include:

1. Proving that the ECG dynamic features can be utilized for human identification. Namely, the findings of this paper suggest that the dynamic change in the ECG frequency components is a unique biometric characteristic. We provided complete analysis, and we showed that higher identification accuracy can be achieved via selecting the appropriate STFT window size/s. In addition, we proved this hypothesis using different ECG data lengths ranging from 2000 samples to 5000 samples and over multiple randomly repeated experiments .
2. Proving that the Fréchet classifiers are more reliable and stable than the non-Euclidean based classifiers to find the minimum distance between feature matrices. We showed that the minimum distance between the symmetric positive definite matrices of the ECG frequency components is achieved via using Fréchet distance measures instead of using Euclidean distance. This hypothesis is proved using different ECG data lengths and STFT windows.

3.7 Feature Work

There are few open problems that can be considered for future research as extension to the work that has been done in this paper. For instance, testing the applicability of our method using ECGs from multiple days to further investigate the uniqueness of this biological signal. In addition, addressing the variability of ECG spectral features using multi resolution analysis methods such as applying wavelet decomposition methods. Moreover, in our future work we will focus on classification of the ECG refencing data according to several parameters including mainly the heartbeat morphology and the personal health status. Specifically, clustering the ECG data into different groups will help to reduce the screening time of the identification process and it will make our algorithm more adaptable with significant change in the ECG features.

3.8 Conclusion

One of the main problems in ECG based identification problems is to extract the best of the ECG features. To address this problem, we have proposed a methodology to extract dynamic ECG features and utilize them as a significant characteristic. In this study, each subject is considered a separate class who has his/her own unique dynamic features. Moreover, our method is based on extracting feature matrices; therefore, we utilized the Fréchet classifiers to obtain the minimum distance because they perform better than the Euclidean distance when it comes to finding minimum distance between matrices, specifically, in a multiclass classification problem. Our experiments show that the proposed framework works well using on ECG ID database with 97.03% average identification accuracy, 0.9719 precision, 0.9995 specificity, 0.9703 recall and 0.0297 FRR and 0.00048 FAR. In conclusion, the results of this paper prove that ECG is a unique biological signal. Finally, our findings suggest that modelling non fiducial dynamic ECG features along with designing non-Euclidean based classifiers can be utilized for human recognition.

References

[1] M. Ingale, N. Cordeiro, S. Thentu, P. Y, and N. Karimian, "ECG Biometric Authentication: A Comparative Analysis," *IEEE Access* vol. 8, pp. 117853-117866, 2020.

[2] V. Chandrashekhar, P. Singh, M. Paralkar, and O. K. Tonguz, "Pulse ID: The Case for Robustness of ECG as a Biometric Identifier," *2020 IEEE 30th International Workshop on Machine Learning for Signal Processing (MLSP),* pp. 1-6, 2020.

[3] R. Cordeiro, D. Gajaria, A. Limaye, T. Adegbija, K. N., and F. Tehranipoor, "ECG-Based Authentication Using Timing-Aware Domain-Specific Architecture," *EEE Transactions on Computer-Aided Design of Integrated Circuits and Systems,* vol. 9, no. 11, pp. 3373-3384, 2020.

[4] H. Li and A. Jeremic, "Semi-supervised Distributed Clustering for Bioinformatics - Comparison Study," 2017, vol. 4, pp. 259-264.

[5] H. Ko *et al.*, "ECG-Based Advanced Personal Identification Study With Adjusted (Qi * Si)," *IEEE Access*, vol. 7, pp. 40078-40084, 2019.

[6] A. Biran and A. Jeremic, "ECG based Human Identification using Short Time Fourier Transform and Histograms of Fiducial QRS Features," in *Proceedings of the 13th International Joint Conference on Biomedical Engineering Systems and Technologies* Malta, 2020.

[7] X. Dong, W. Si, and W. Yu, "Identity Recognition Based on the QRS Complex Dynamics of Electrocardiogram," *IEEE Access,*, vol. 8, pp. 134373-134385, 2020.

[8] R. Bhatia, "Positive definite matrices," *Princeton University Press*, 2009.

[9] R. Bhatia and J. Holbrook, "Riemannian geometry and matrix geometric means," *Linear algebra and its applications*, vol. 413, no. 2, pp. 594–618, June 2006.

[10] M. Jahromi, "Frechet Means with Respect to the Riemannian Distances: Evaluations and Applications " McMaster University 2014

[11] F. Hiai and D. Petz, "Riemannian metrics on positive definite matrices related to mean," *Linear Algebra and its Applications*, vol. 430, no. 11, pp. 3105–3130, 2009.

[12] A. Pal and Y. N. Singh, "ECG biometric recognition," in *international conference in math and computer*, Singapore, 2018.

[13] A. Hanilci and H. Gurkan, "ECG biometric identification method based on parallel 2-D convolutional neural networks,"," *Journal of Innovative Science and Engineering*, vol. 3, no. 1, pp. 11-22, 2019.

[14] H. Choi, B. Lee, and Y. Yoon, "Biometric Authentication Using Noisy Electrocardiograms Acquired by Mobile Sensors," *IEEE Access*, vol. 4, pp. 1266-1273, 2016.

[15] S. J. Kang, S. Y. Lee, H. I. Cho, and H. Park, "ECG Authentication System Design Based on Signal Analysis in Mobile and Wearable Devices," *IEEE Signal Processing Letters*, vol. 23, no. 6, pp. 805-808, 2016.

[16] S. I. Safie, "ECG slope features for Biometric Authentication," in *IEEE 5th International Conference on Smart Instrumentation, Measurement and Application (ICSIMA)*, Songkhla, 2018, pp. 1-5.

[17] D. Cherifi, C. Adjerid, B. Boukerma, B. Zebbiche, and N.-A. A., "ECG features extraction using AC/DCT for biometric," in *2nd International Conference on Bio-engineering for Smart Technologies (BioSMART)*, Paris, 2017.

[18] B. Fatimah, G. Priyanka, S. R., and N. Rekha, "Analysis of ECG for biometric identification," in *11th International Conference on Computing, Communication and Networking Technologies (ICCCNT)*, Kharagpur, 2020.

[19] Y. Chu, H. Shen, and k. Huang, "ECG Authentication Method Based on Parallel Multi-Scale One-Dimensional Residual Network With Center and Margin Loss," *IEEE Access*, vol. 7, pp. 51598-51607, 2019.

[20] S. Kim, C. Y. Yeun, and P. D. Yoo, "Enhanced Machine Learning-Based Biometric Authentication System Using RR-Interval Framed Electrocardiograms," *IEEE Access*, vol. 7, pp. 168669-168674, 2019.

[21] M. Hammad, Y. Liu, and K. Wang, "Multimodal Biometric Authentication Systems Using Convolution Neural Network Based on Different Level Fusion of ECG and Fingerprint," *IEEE Access*, vol. 7, pp. 26527-26542, 2019.

[22] A. Biran and A. Jeremic, "Non-Segmented ECG bio-Identification using Short Time Fourier Transfrom and Frechet Mean Distance," in *42nd Annual International Conference of the IEEE Engineering in Medicine and Biology Society*, Montreal, 2020, pp. 5506-5509.

[23] A. Biran and A. Jeremic, "Segmented ECG Bio Identification Using Fréchet Mean Distance and Covariance Matrices of Fiducial QRS Features," in *In Proceedings of the 14th International Joint Conference on Biomedical Engineering Systems and Technologies*, 2021.

[24] A. V. Oppenheim and R. W. Schafer, *Discrete-Time Signal Processing*. New Jersey: Prentie-Hall, Inc, 1989.

[25] S. Lin, C. Chen, C. Lin, W. Yang, and C. Chiang, "Individual identification based on chaotic electrocardiogram signals during muscular exercise," *The Institution of Engineering*, 2014.

[26] A. Biran and A. Jeremic, "Automatic QRS Detection and Segmentation using Short Time Fourier Transfrom and Feature Fusion," in *33rd Canadian Conference on Electrical and Computer Engineering*, London, 2020.

Chapter 4

4 The Feasibility of Human Identification from Multiple ECGs using Maximal Overlap Discrete Wavelet Transform (MODWT) and Weighted Majority Voting Method (WMVM)

4.1 Abstract

The electrocardiography (ECG) has been a subject of research interest in human identification because it is a promising biometric trait that is believed to have discriminatory characteristics. However, features of ECGs that are recorded at different times are more likely to vary significantly. To address the variability of ECG features over multiple records, we propose a new methodology for human identification using ECGs recorded on different days. To demonstrate the applicability of our method, we use the publicly available ECG ID dataset. The main goal of this work is to extract the most significant and discriminative wavelet components of the ECG signal followed by utilizing the ECG spectral change for human identification using multi-level filtering technique. Our proposed multi-channel identification system is based on using the Maximal Overlap Discrete Wavelet Transform (MODWT) and its inverse (the IMODWT) to create multiple filtered ECG signals. The discriminative feature that we utilize for human identification is based on modeling the dynamic change of the frequency components in these multiple filtered signals. To reach the best possible identification performance, we use the Weighted Majority Voting Method (WMVM) for ECG classification. We evaluated the robustness of our proposed method

over several random experiments and obtained 92.29% average identification accuracy, 0.9495 precision, 0.9229 recall, 0.0771 FRR and 0.0013 FAR. These results indicate that filtering some of the ECG wavelet components along with performing data fusion technique can be utilized for human identification.

4.2 Introduction

In recent years, physiological signals have showed great potential in human recognition [1] [2] [3]. In addition, it has been demonstrated that physiological signal-based identification systems are more robust against counterfeit than the existing conventional and traditional biometric systems [4] [5]. Therefore, researchers have presented various methods to investigate the possibility of human recognition via biomedical signals [6] [7] [8]. Specifically, among different biomedical signals, the electrocardiogram (ECG) has been widely studied as a new approach in human identification. It has been shown that the ECG based biometric systems achieve satisfactory identification accuracy in wide range of applications [3]. In fact, the ECG has some key advantages including mainly its hidden nature and its liveness assurance which make it preferable than other means of biometric modalities such as face, fingerprint and iris [3] [5] since they can be damaged or stolen. Additionally, the ECG has several characteristics that are required for any biometric modality. In general, a biometric trait should satisfy the following requirements to be used for human recognition [9] [10]:

1) Universality: the trait should be present in all living population.
2) Uniqueness: major differences in trait characteristics should be derived among different people.
3) Collectability: the trait should be quantitatively measurable and easily accessible.

4) Acceptability: the degree in which the trait is user friendly, and it should be widely acceptable by many subjects.
5) Resistance to Circumvention: the trait should be resistant to the various spoofing attacks.
6) Permanence: the extent in which the trait features should remain stable over time.

The ECG satisfies most of the abovementioned requirements because it is by instinct a vital sign and it is present in all living population [11] [12] [13]. In addition, it has been proven that the ECG has unique patterns among various individuals [3] and it can be easily recorded using a single lead [14] [15]. Moreover, the ECG can be hardly forged duo to its biological nature and liveness indicator [16]. However, stability of ECG features is one of the most controversial characteristics because it has been demonstrated that cardiac signals are highly affected by many geometrical, individual, and technical factors [5] [17].

To illustrate, geometrical attributes such as heart size, cardiac muscle thickness, heart shape and the number of cardiac cells involved in the electrical activity directly dictate the routes of the electrical current inside the heart [5] [18] [19] . On the other hand, personal characteristics including mainly the health status, age and weight could cause changes in the heart position and orientation [20]. Hence, these factors shift the electrical current orientation, and they also change the conductivity of the heart [5] [20]. Additionally, the electrode features such as the type, quantity, degree of dryness and position may cause some changes in the electrical properties of the electrodes [5] [18] [20]. Consequently, all these previously mentioned factors create morphological variations in the ECG signals which are highly remarkable in ECGs that are recorded on different times [18]. This changeability of the ECG features is usually categorized as intra-subject variability and inter-subject variability [21]. Where the former one refers to the

variations within or between ECGs of a single subject, the later one refers to the variations of ECGs of different subjects [3] [5].

In fact, the inter-subject variability is highly desired for human identification because the uniqueness of the ECG signal can be explained through finding the core differences between cardiac signals of different individuals [5] [20] . On the other hand, the intra-subject variability could be beneficial because the dynamic change between ECG features of a single subject can be modeled to create individual based biometric signature [3] [18]. Hence, a perfect biometric trait should have a very high inter-subject variability. In contrast, it should have very low intra-subject variability [3] [16] [5]. However, the stability of these parameters over time, permanence, remain the main challenge in using multiple ECGs for human identification.

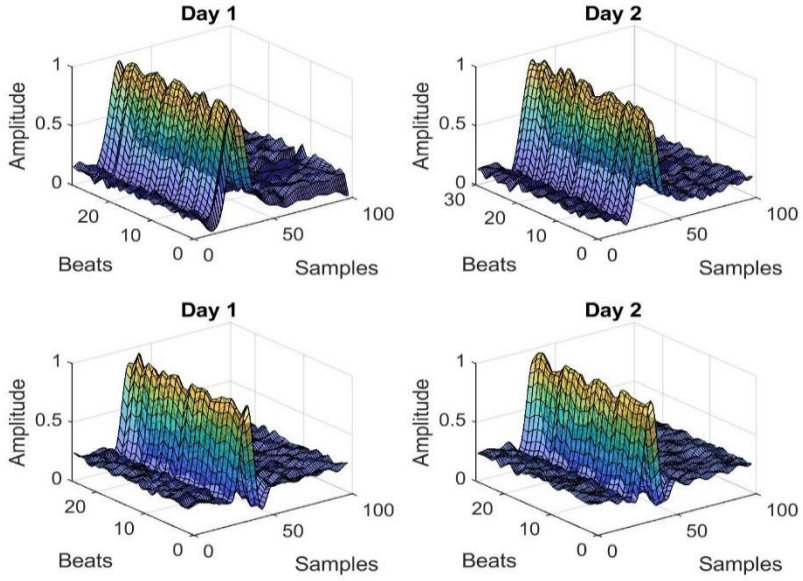

Figure 4.1: The variability of morphological features using ECGs recorded on different days of two subjects.

The variability of ECG features can be clearly noticed when analyzing the fiducial and non-fiducial characteristics of such biomedical signal. For example, in Figure 4.1 we show the heart beats of two subjects from the ECG-ID database. Obviously, the inter-subject variability can be observed by the various morphologies that form the personal heartbeats of these two individuals.

On the other hand, the intra-subject variability can be noticed as the significant fluctuations in the amplitude of the QRS complexes. In addition, Figure 4.2 shows the intra-subject variability which can be seen as the rapid changes in the ECG frequency components when the data are recorded on different days. Moreover, Figure 4.3 shows the various morphological bundles of the ECG heartbeat such as the right bundle branch block beat, the left bundle branch block beat and, normal beat [22].

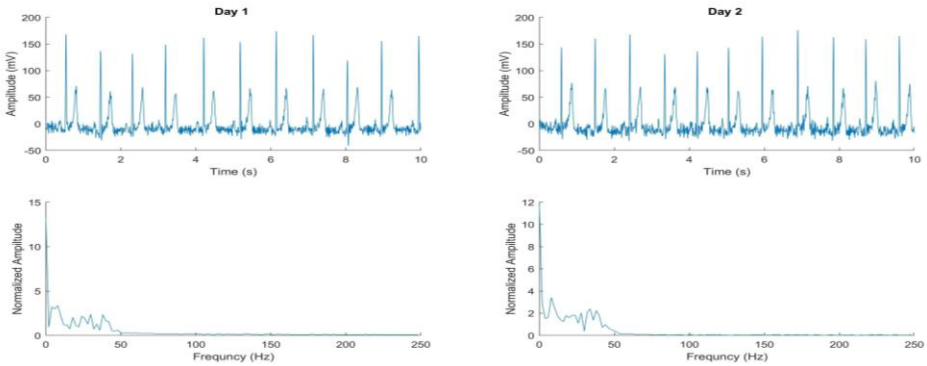

Figure 4.2: The variability of spectral features using ECGs recorded on two different days of one subject.

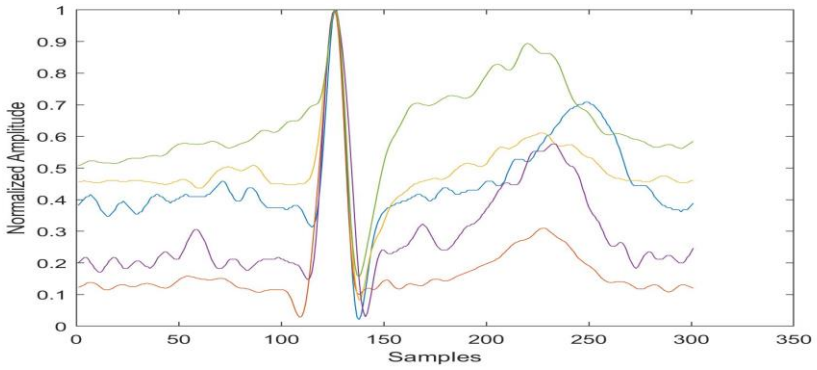

Figure 4.3: Figure 3. Normal heart beats of five different subjects from the ECG ID database

All the previously presented factors reflect that utilizing the cardiac signal for human recognition does not only depend on choosing the appropriate features, but also it relays on categorizing the variability of ECG features over time [23]. In this work, we focus on investigating the feasibility of human identification using ECGs that are recoded at two different days.

Specifically, we selected the ECG-ID data because it was originally recorded for biometric purposes. For each subject, two 20-second ECG recordings were chosen. These ECG signals were recorded over a six-month period [24] [25]. The original ECG-ID data have ECG recordings of 90 subjects; however, we only choose signals of 62 subjects who have normal ECG waveforms, where the QRS complex has the highest amplitude. The remaining subjects were excluded because their T wave is tall and higher than the QRS complex. In addition, we designed our method to decompose the ECG using SYM4 which generally detects the QRS features. Therefore, including all the database and treating it equally without changing the mother wavelet or classifying the reference data according to the heartbeat morphology, will affect the performance of our methodology because there is a significant difference between features of normal heartbeats and other types of heart beats with larger T waves.

4.3 Literature Review

The use of ECG in various clinical diagnosis applications has significantly demonstrated different characteristics of such human cardiac signal. Therefore, the potential use of ECG for human identification was derived by the motivation to utilize such features to create a new biometric modality. According to the best of our knowledge, the first attempt to utilize the ECG for human recognition was presented by Biel.et al [1]. The authors used 12 fiducial heartbeat features and reported 95% identification accuracy. However, most of the ECG based human identification systems are increasingly being presented in the last decade.

Dar et al. [26] have presented a method based on discrete wavelet transform (DWT) for human recognition. Technically, the preprocessing stage in [26] involved removal of baseline wonder and power interference followed by normalization of the signal with R peak detection. The DWT was applied using Har wavelet coefficients at five level decomposition to extract the ECG

features. Additionally, the Best First Search (BFS) method was performed for feature reduction and the k nearest neighbor method was utilized for feature classification. Consequently, DAR et al [26] reported 82.03% identification accuracy.

On the other hand, Morteza et. Al. [27] used the Daubechies wavelet (Db3) coefficients at five level decomposition for ECG feature extraction. In the classification stage, the Euclidean distance between the test data and the mean of 100 training data was performed for ECG classification. As a result, the authors in [27] reported 100% identification accuracy using ECG data of 21 subjects. Lee et al. [28] proposed an algorithm based on a time frequency representation of the ECG data. Both the robust principal components analysis network (RPCANet) and DWT methods were utilized for feature extraction. The support vector machine (SVM) was used for ECG classification [28]. Similarly, Arwa et al. [29] introduced a wavelet-based method which utilizes the ECG power and energy features for personal identification. The authors reported that their method can identify individuals with 83.3% recognition accuracy using Euclidean and linear discriminant analysis (LDA) classifiers.

Abdeldayem et al. [30] have presented an algorithm based on modeling the Spectro-temporal dynamic characteristics of the ECG signal using short time Fourier transform (STFT) and Morse wavelets for feature extraction. At the processing stage, the band pass filter was applied to remove any frequencies other than 0.05-40 Hz, which is generally the normal frequency range of the ECG [30] The authors in [30] used the 2D convolutional neural networks (CNN) for ECG feature classification and they reported an average identification rate of 97.86%. Ciocoiu et al. [31] introduced a comparative study on four different spatial representation of the ECG data using the STFT, Gramian angular field, the recurrence plot and state-space representation algorithms. Ciocoiu et al. method is based on converting the temporal ECG data into 2D/3D images followed

by applying CNN for image classification and individual authentication. The best reported identification accuracy Ciocoiu et al. work is 99.01%. Similarly, Choi et al. [32] presented a method by converting the ECG data into 2D resized spectrograms that are classified for user identification. Choi et al. reported that their method achieved 93% average identification performance.

Moreover, Kim et al. [33] proposed a method which is based a generalized likelihood ratio test (GLRT) and composite hypothesis testing. As result, Kim et al [33] reported 93% detection probability for user authentication. Tan et al. [34] introduced a sparse representation learning framework that utilizes the time frequency distribution of the ECG signal for biometric purposes and they reported 98% average identification accuracy. Their work was based on using the statistical n-best adaptive Fourier decomposition (SAFD) method for reducing the intra subject variability and increasing the inter-subject variability of ECG features.

Furthermore, the research investigations in [35] reported that the QRS complex exhibits significant features among different individuals and such features can be utilized for human authentication. The authors in [36] and [23] have shown that the ECG signal reveal various and unique patterns. The research findings in [37] showed that ECG based biometric identification highly relays on the type of methods that are utilized for feature selection (fiducial vs non fiducial methods). The work in [7] also showed that deep learning networks such as CNN can be employed to extract discriminatory features among multiple ECGs. Generally, utilizing the ECG for human identification depends on many factors including mainly, noise filtering, features selection, features extraction, ECG classification and addressing the variability of the ECG data [3] [23] [2].

In this paper, we focus on identifying individuals using multiple ECGs. These multiple ECGs are recorded on different days, and they are more likely to have some sorts of feature variability.

Based on our previous work in [38], modeling the dynamic change in ECG spectral features and using Fréchet based distance measurement for ECG classification has shown excellent results on individual recognition. However, when we select the ECG data from different days, the identification performance decreases significantly. This is expected because of the above-mentioned reasons on the variability of ECG features. To solve this problem, the main contributions of this paper include:

1) Addressing the variability of ECG features at the preprocessing stage by decomposing the signal and performing data filtering methods. Unlike the previous works where the processing stage involved noise removal and signal correction [30] [32] [31] [26], in this paper we focus on partitioning the signal variability according to its wavelet components. The variability of the ECG features can be analyzed by decomposition the signal into its wavelet components [39]. To accomplish our objective, we show that filtering some of the high frequency wavelet components in a set of parallel process can be modeled for human identification. The main advantage of this process is to reduce the variability ECG feature at the fundamental wavelet components while keeping majority of the signal information [40].
2) Proposing a new technique for data fusion at the classification stage to reach true identification. To achieve our goal, we show that utilizing the minimum Fréchet distances between filtered versions of multiple ECGs can be modeled to create weighted scoring technique based on majority voting for reaching correct identification. The main advantage of our proposed weighted majority voting includes using the minimum distance between multiple ECGs a unique feature that has an effective role in decision making [41].

4.4 Materials and Methods

In this work, we propose a method for individual identification using multiple ECGs that are recorded on two different days. The general flowchart of our proposed methodology is shown in Figure 4.4.

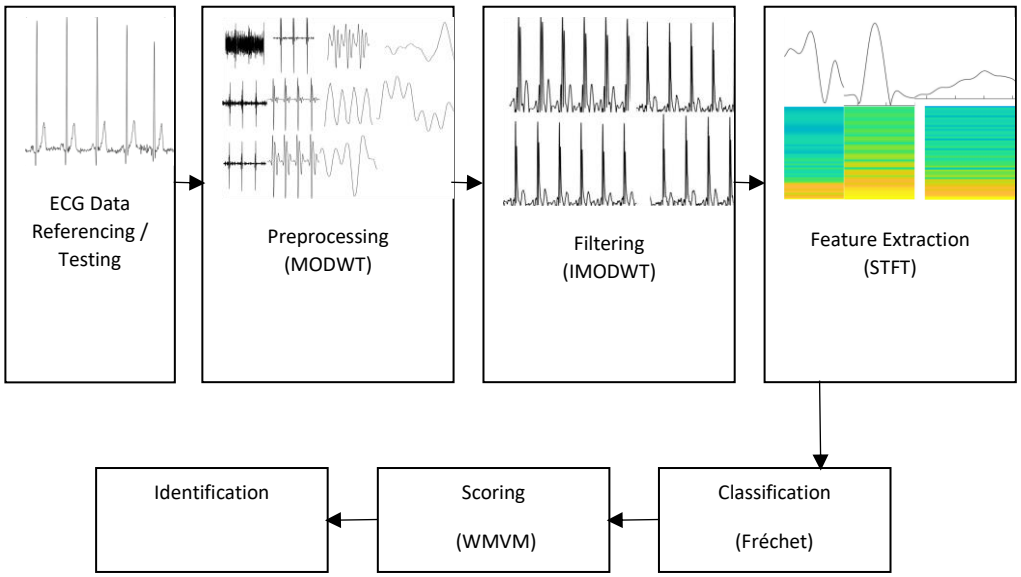

Figure 4.4: The flowchart of the proposed methodology

4.4.1. The ECG referencing and testing data

As mentioned above, we use the public ECG ID database of 62 subjects because it was originally recorded for biometric purposes [25]. For each subject, we selected two ECG recordings. The public ECG ID data do not have information about the exact time and date in which the ECGs were recorded. However, all the ECG recordings were taking over six-month period. We grouped the ECG ID data into two categories which are the referencing data and testing data. To achieve our goal of identifying individuals using multiple ECGs, we use the ECGs from the former group for referencing purposes and we use the ECGs from the latter group for testing purposes.

4.4.2 Preprocessing using Maximal Overlap Discrete Wavelet Transform (MODWT)

The Maximal Overlap Discrete Wavelet Transform (MODWT) like the Discrete Wavelet Transform (DWT) is a linear filtering process which is used to decompose a signal into a set of time dependent wavelet and scaling coefficients [39]. However, MODWT is non orthogonal transform compared to DWT [39]. The MODWT basic idea relays on using the values that are removed from DWT by down sampling. Therefore, MODWT is highly redundant transform compared to DWT since it is defined for all samples sizes. Like the DWT, the MODWT is utilized to perform multiresolution analyses (MRAs) and the redundancy of the MODWT enables instantaneous comparison between the original time series and its decomposition at each level. Most Importantly, the MODWT coefficients of various scales are approximately uncorrelated. Thus, it is a useful transform to partition the variability of the signal [39].

The ECG is a nonstationary signal, and its features are often localized in time and frequency [22]. Therefore, it is better to analyze such signal using wavelets because they are utilized to decompose the signal and provide sparser representation [3]. However, choosing the most appropriate wavelet function depends on the ECG features of interest [2]. Specifically, the QRS complex is the prominent wave of the ECG; therefore, we selected the sym4 as an analyzing wavelet to decompose the ECG into time-varying frequency (scale) components. In addition, the QRS complex can be easily segmented compared to the P and T waves since they require expert labeling to achieve proper segmentation [42] [43]. The sym4 wavelet resembles the QRS complex and it is an appropriate choice to detect most of the ECG information [14].

In Figure 4.5 we show a comparison between the sym4 wavelet and the QRS complex. The figure shows that the sym4 resembles the QRS complex. Although, sym4 is generally utilized to detect QRS features, it also can detect non QRS features by changing the scale and translation

parameters [44]. In this paper, the wavelet coefficients are computationally returned based on utilizing different versions of the analyzing wavelet. The small scales, compressed versions of SYM4, are utilized to detect the high frequency components of the signal. In contrast, the large scales, stretched versions of SYM4, are utilized to detect the low frequency components of the signal [45] [44].

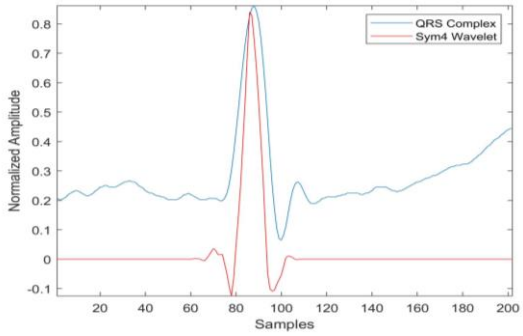

Figure 4.5: ECG analysis using sym4 wavelet

In signal processing, real world biological signals such as the ECG are sampled over finite interval of discrete times [46]. Therefore, the ECG data can be written as discrete function $f(x)$ recorded at n_l samples. The $f(x)$ can be expressed as a linear combination of two main functions which are a scaling function $\phi(x)$ and an analyzing wavelet $\psi(x)$ at varying scales and translations[39]. The linear representation of $f(x)$ can be written as:

$$f(x) = \sum_{k=0}^{n_l-1} c_k \, 2^{-\frac{J_0}{2}} \, \phi(2^{-J_0} x - k) + \sum_{j=1}^{J_0} f_j(x) \tag{4.1}$$

where

$$f_j(x) = \sum_{k=0}^{n_l-1} d_{j,k} \, 2^{-\frac{j}{2}} \, \psi\left(2^{-j} x - k\right) \tag{4.2}$$

and J_0 is the number of levels of wavelet decomposition.

According to equations (4.1) and (4.2), the MODWT returns n_l many scaling coefficients (c_k) and $J_0 \times n_l$ many detail coefficients($d_{j,k}$). However, the detail coefficients are generated at each level j such that $j = 1,2, \ldots, J_0$, but the scaling coefficients are generated only at the final decomposition level J_0. Therefore, $\boldsymbol{X}$ can be written as:

$$\boldsymbol{X} = \sum_{j=1}^{J_0} \boldsymbol{W_j} + \boldsymbol{V_{J_0}} \tag{4.3}$$

where $\boldsymbol{X}$ is the ECG data, $\boldsymbol{W_j}$ consists of the detail coefficients at scale j and $\boldsymbol{V_{J_0}}$ are the final level scaling coefficients.

In this work we set J_0 to 10 to provide a redundant MRAs of the ECG signal. In Figure 4.6 we show the 10 level wavelet coefficients of a random ECG signal. The figure shows the details coefficients for scales 2^1 to 2^{10}. In addition, it shows the final level scaling coefficients. These coefficients permit an easier analysis of the ECG because they provide sparser (reduced) representation of the signal. These wavelet components are likely to have some variations when it is extracted from multiple records. To address the variability of ECG features, we filter some of the wavelet components to obtain the most significant information.

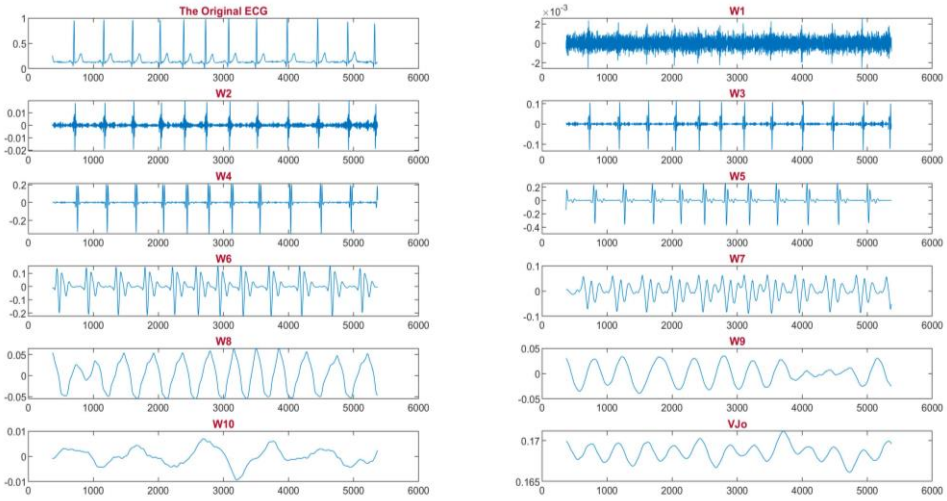

Figure 4.6: The ten level wavelet coefficients of the ECG using MODWT

4.4.3 Filtering and Reconstruction using the Inverse Maximal Overlap Discrete Wavelet Transform

The ECG is an aperiodic random signal whose value at any instant is unknown and it is generally unpredictable [22]. In addition, the ECG features exhibit some changes over time; specifically, the mean and variance of the ECG are function of time, and they can vary significantly from heartbeat to heartbeat [46]. The variability of ECG features is caused by physiological and non-physiological factors which we explained in the introduction [3] [5]. Consequently, it has been demonstrated that utilizing the ECG for human recognition highly requires to build identification systems that are adaptable to the variability of ECG features [23]. To achieve our objective, we developed a multi-channel wavelet-based filtering system because we expect that by filtering some of the wavelet components, the variability of ECG features will reduce, and the performance of the identification process will increase.

In fact, all the ECG wavelet-based features including the high frequency and the low frequency components can be useful for the identification process [38] [45]. Therefore, we designed our filtering systems which is utilized to remove different wavelet components at different levels of the filtering process [46]. The proposed system is designed to filter the high frequency components in a set of parallel processes. The main goal here is to remove some of the components which may have high variability between ECGs that are recorded at different times. To illustrate, we applied a windowing technique based on short time Fourier transform (STFT) to see how the variance of detail coefficients at each scale changes over time. In addition, each window contains an ECG time segment that approximately has a full heartbeat. According to

Figure 4.7, the variance of detail coefficients at scales 1 to 4 (the high frequency wavelet components of the ECG signal) have significant change across multiple heartbeats compared to the variance of details coefficients at scales 5 to 10 (the low frequency wavelet components of the ECG signal). However, the change in the variance over time of the detail coefficients at scales 1 to 4 is subject based. Therefore, filtering different high frequency wavelet components of the ECG signal in a set of parallel process helps to reduce the variability of ECG features.

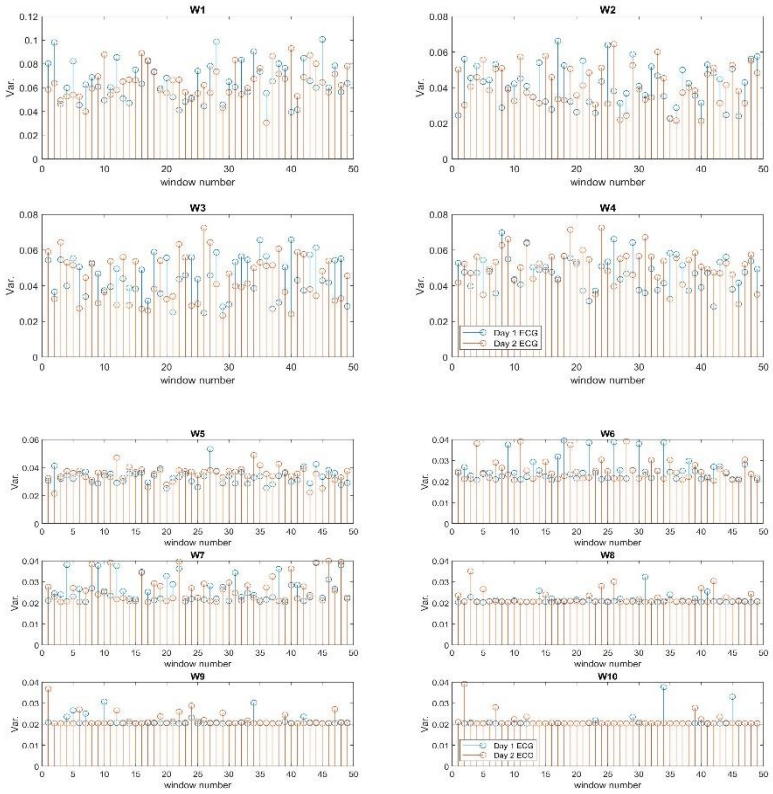

Figure 4.7: The variance in the frequency components of the ECG wavelet components over multiple records from one subject.

However, our filtering system is not designed to filter the low frequency components, which are calculated by utilizing larger scales of the analyzing wavelet, because we expect that such components have most of the ECG permanent information (see Figure 4.7). Technically, because we eliminated some of the wavelet information, the reconstructed signals are named as filtered ECGs [39]. Since we apply different levels of filtration, we create different types of filtered ECGs

[40]. The main goal here is to find the most significant wavelet components of the ECG signal which are utilized to create our multi-channel identification system.

In Figure 4.8, we show our Parallel High Frequency Filtering System (PHFFS) which consists of five channels. In addition, Table 4.1 shows the wavelet coefficients that are removed at each level of the filtering system. The PHFFS removes the detail coefficients from levels $\boldsymbol{W_1}$ to $\boldsymbol{W_4}$ in a parallel process. Moreover, the PHFFS consists of an additional channel which removes the detail coefficients of levels $\boldsymbol{W_1}$ to $\boldsymbol{W_4}$ (Figure 4.8).

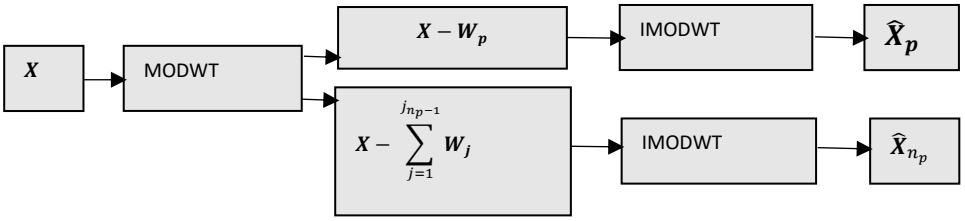

Figure 4.8: The block diagram of the Parallel High Frequency Filtering System

Table 4.1: Reconstruction of the ECG signal using the multichannel wavelet- based filtering system

Filtering Channel p	Removed Coefficients using PHFFS system	Filtered Signal Notation
1	W_1 , V_{J_0}	$\hat{X}_1$
2	W_2 , V_{J_0}	$\hat{X}_2$
3	W_3 , V_{J_0}	$\hat{X}_3$
4	W_4 , V_{J_0}	$\hat{X}_4$
5	W_1 , W_2 , W_3 , W_4 , V_{J_0}	$\hat{X}_5$

Then, the ECG is reconstructed using the Inverse Maximal Overlap Discrete Wavelet Transform (IMODWT) at each level of these filtering processes .[39] Therefore, the output of the PHFFS consists of several filtered ECGs. According to Table I, the PHFFS constructs five types of filtered ECGs which are defined as $\boldsymbol{\widehat{X}_1}$, $\boldsymbol{\widehat{X}_2}$, $\boldsymbol{\widehat{X}_3}$, $\boldsymbol{\widehat{X}_4}$ and $\boldsymbol{\widehat{X}_5}$. Each of these signals is independently analyzed for the identification process and it is utilized as a unique personal identifier. In Figure 4.9, we show an example of all the reconstructed signals. Generally, the high

frequency components of the ECG have slightly larger statistical variation than the low frequency components [47]. This variation may influence the overall identification performance for some individuals. Therefore, we apply the PHFFS to remove multiple wavelet components and investigate the applicability of the identification system using reduced amount of the signal information [40].

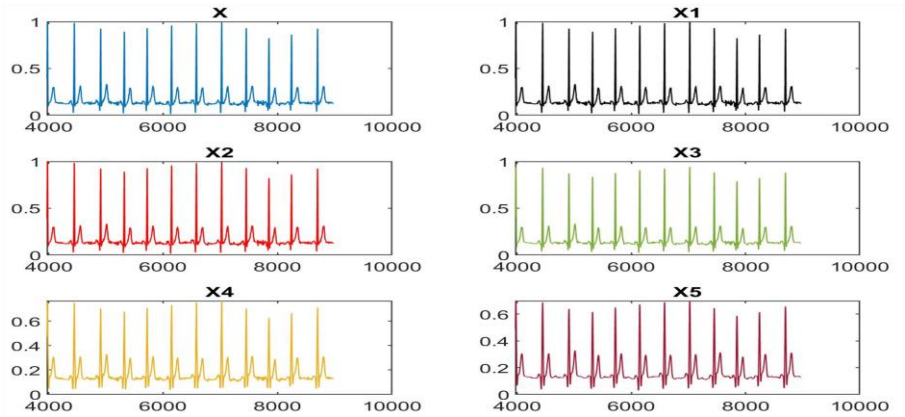

Figure 4.9: Multiple filtered versions of the ECG using the PHFFS.

4.4.4 Spectral Feature Extraction (STFT)

The feature extraction stage involves utilizing significant characteristics from the ECG for human identification. Since ECG is a random time varying signal, it generally has intra feature variability between multiple heartbeats [4] [22]. Therefore, the most appropriate way to utilize the ECG for human identification does not only depend on filtering some of the wavelet components, but also it involves tracking the dynamic change of features among multiple heartbeats [2]. In our previous work [38], we introduced a new feature that is based on modeling the dynamic change of ECG spectral components. Such feature, which is extracted from the main signal, has shown excellent results for individual recognition. Differently, in this work we extract the dynamic change of the spectral components in each of the filtered ECG signals.

The complete process of extracting the dynamic change of the ECG frequency components can be found in [38]. In short, let $\boldsymbol{X^r}$ be the referencing ECG from day 1, we divide each of the filtered signals (e.g., $\boldsymbol{\hat{X}_p^r}$) into multiple short segments and we create the time matrix $\hat{X}_p^r$. Then, we apply STFT on each row of $\hat{X}_p^r$ and we obtain the frequency matrix $\hat{F}_p^r$. The $\hat{F}_p^r$ matrix contains the spectral activity of multiple overlapped time segments of the filtered ECG $\boldsymbol{\hat{X}_p^r}$. Thus, it represents the dynamic change of the frequency components between several consecutive heart beats. Namely, we utilize this change as unique characteristic for individual recognition. Similarly, let $\boldsymbol{X^t}$ be a testing ECG from day 2, we obtain the spectral feature matrix $\hat{F}_p^t$ using the same procedure. For each subject, the process of randomly selecting a testing data is repeated many times to evaluate the performance of our method.

4.4.5. Classification using Fréchet Distance

ECG classification for human identification purposes is the process of correctly assigning a class for the transformed feature matrices [16] [30] [47] [9] [44]. Technically, the procedure for choosing the right classifier highly depends on the geometrical characteristics of the feature matrix [38]. We also refer here to our previous findings on the robustness of utilizing the Fréchet distance for correctly classifying the covariance matrices of the ECG dynamic features [38]. In short, let n_{sb} be the total number of subjects, we use equation (4.4) n_{sb} many times to compute the Fréchet distance (fd) between a single testing feature matrix of random subject and the reference feature matrices of all subjects such that:

$$fd_p = \sqrt{Tr\left(\hat{A}_{p,m}^t\right) + Tr\left(\hat{A}_{p,n}^r\right) - 2Tr\left(\sqrt{\hat{A}_{p,m}^t}\sqrt{\hat{A}_{p,n}^r}\right)} \tag{4.4}$$

where

$$\hat{A}_{p,n}^r = \hat{F}_{p,n}^r \, \hat{F}_{p,n}^{r\,T} \tag{4.5}$$

$$\hat{A}^{t}_{p,m} = \hat{F}^{t}_{p,m}\,\hat{F}^{t}_{p,m}{}^{T} \tag{4.6}$$

where $1 \leq m \leq n_{sb}$ is the index of one subject, $n = 1,2,3, \ldots\ldots, n_{sb}$ refers to the subject number with a total of n_{sb} many subjects and p is the index of the filtering channel (see Table 4.1)

In this work, the scaling coefficients ($\boldsymbol{V_{J_0}}$) are larger than the detail coefficients which may make the feature matrices to be singular [46]. Consequently, these two square roots in equation (4.4) ($\sqrt{\hat{A}^{t}_{p,m}}$ and $\sqrt{\hat{A}^{r}_{p,n}}$) may not exist. To address this problem, we removed the scaling coefficients in all the filtered channels (see Table 4.1). However, the scaling coefficients may have distinctive information and it can be used in other biometric applications such as ECG data clustering. According to equation (4.4), we use the referencing data of all subjects to obtain the Fréchet distance; however, the scaling coefficients could be utilized to address this problem by clustering the referencing data to reduce the computational time of classification. After finding the Fréchet distances, we use equation (4.7) to classify the testing data to a specific class (person) such that:

$$c_p = min_n \left(\boldsymbol{FD_p}\big|_{1}^{n_{sb}}\right) \tag{4.7}$$

where $\boldsymbol{FD_p}$ is a vector that has n_{sb} many individual Fréchet distances.

In addition, equation (4.8) returns the minimum Fréchet distance:

$$d_p = min \left(\boldsymbol{FD_p}\big|_{1}^{n_{sb}}\right) \tag{4.8}$$

where d_p is the minimum Fréchet distance that is obtained by using filter p.

Since our PHFFS consists of p many filtering channels, we obtain $\boldsymbol{C_p} \in R^{n_p}$ which is a vector that has n_p many classes where each filtering channel returns one class. In this work, the total number of classes is equivalent to the total number of subjects. We also obtain $\boldsymbol{D_p} \in R^{n_p}$ which is

a vector that has n_p many minimum Fréchet distances. For each subject, we repeated all the previously explained process many times by changing the testing ECG data to examine the stability of our method. After that, the $\boldsymbol{C_p}$ and $\boldsymbol{D_p}$ vectors are transmitted to the data fusion algorithm.

4.4.6 Decision fusion using Weighted Majority Voting Method

Data fusion is a process of combining information that are collected from multisensory system to form a final decision [41]. The use of multisensory data has been widely applied in many fields including medical applications [48]. In general, the data collected from multisensory system are incomplete or overlapping which may cause improper decision making. Therefore, data fusion is an essential step that improves the overall performance of a multi-sensors system [49] [50] [51].

In this work, we utilize the reconstructed ECG signals as information collected from multiple detectors. To reach a common final decision, we aim to combine the multiple decisions that are obtained from the wavelet-based filtering channels [41]. As explained in the previous stage, $\boldsymbol{C_p}$ is a vector that has a maximum of n_p many identities which are selected using n_p minimum Fréchet distances (see Figure 4.10). Each of these filtering channels picks one identity and it also returns the corresponding minimum Fréchet distance.

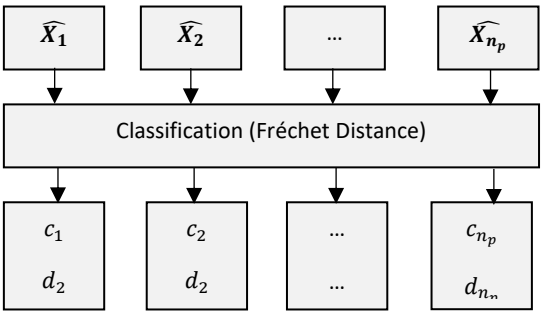

Figure 4.10: The outcome of the classification

We propose here a scoring technique to reach a final decision using the weighted majority voting method (WMVM) [40] [41]. Our technique is based on computing a weighted score for

each person picked by the classification process. For each person in $\boldsymbol{C_p}$ (e.g., person n), the scoring weight is calculated using the following equation:

$$wsc_n = \sum_{p=1}^{n_p} \frac{\frac{1}{d_p}}{\sum_{p=1}^{n_p} \frac{1}{d_p}} \times v_{p,n} \tag{4.9}$$

where $v_{p,n}$ is the vote given for person n using filter p such that:

$$v_{p,n} = \begin{cases} 1 & if \ \ c_p = n \\ 0 & if \ \ c_p \neq n \end{cases} \tag{4.10}$$

Consequently, we obtain $\boldsymbol{WSC} \in R^{n_i}$ where $n_i \ \leq \ n_p$ is the total number of identities selected by the classification process. In Figure 4.11 we show an example of three experiments. The left side of the figure shows the minimum Fréchet distances obtained from each of the filtering channel, and the right side of the figure shows the corresponding identities that are picked by each filter. If the number of picked subjects is equivalent to the number of filters, each person is a given a weighted score that is based mainly on the corresponding minimum Fréchet distance. Therefore, the identity with smallest distance will be picked as a final decision.

However, if more than one filtering channel picked a similar identity as seen in Figure 4.11, a higher weighted score is calculated for that person according to equations (4.9) and (4.10) respectively. In data fusion, adding a measurement based higher score for decisions which have been made using multi sensor system depends on the statistical parameters of the corresponding measurement [41]. To illustrate, Figure 4.12 shows an example of the range of minimum Fréchet distance which are obtained after randomly choosing multiple testing data and applying equations (4.4), (4.5), (4.6) and (4.8) respectively. For any of the filtering channels if the range of the minimum distance is very low it will result in higher weighted scores which make the WMVM method very biased to one filter. In contrast, if the range of the minimum distance is very high it

will result in lower weighted scores which make the outcome of the corresponding filtering channel less effective to reach a final decision. According to Figure 4.12, the range of the minimum distances obtained from each filter is very close which make our scoring method sufficient to reach a true final decision.

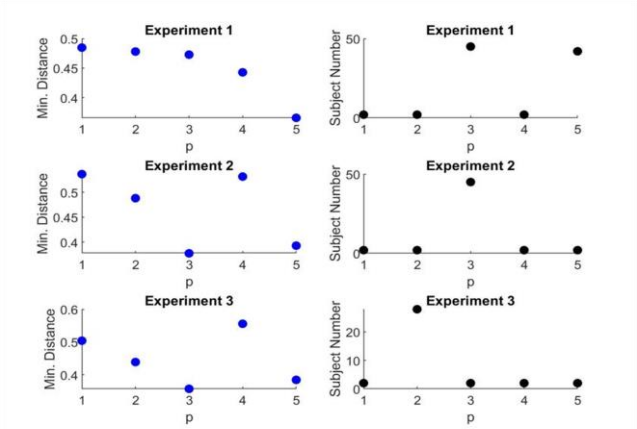

Figure 4.11:Three examples of the identities picked at each filtering channel based on the minimum Fréchet distance

4.4.7 Identification

In this stage, the identification step is a process of picking one identity from the multiple identities obtained by the classification process. As explained above, the WMVM assign a weighted score for each person selected by the classification process. To reach a final decision, the identity which has the higher weight is chosen such that:

$$c_f = max_n \left(\boldsymbol{WSC} \middle|_{1}^{n_i} \right) \tag{4.11}$$

where c_f is the final class (subject)

In short, features of multiple ECGs which belong to a same class might be different whenever it is recorded [19]. Utilizing the complete information of multiple ECGs (e.g., the wavelet components) might not adequately obtain the required minimum distance to reach the right class. The variability in the ECG features might be due to the variability in the individual bases of the ECG wavelet components [18]. Therefore, we developed our multichannel Fréchet based scoring

method to achieve the maximum possible similarity between multiple ECGs by parallelly filtering some of the wavelet components [39]. Finally, we combine the outcome of these multi-level filtering technique to reach a final class using equations (4.9), (4.10), and (4.11) respectively.

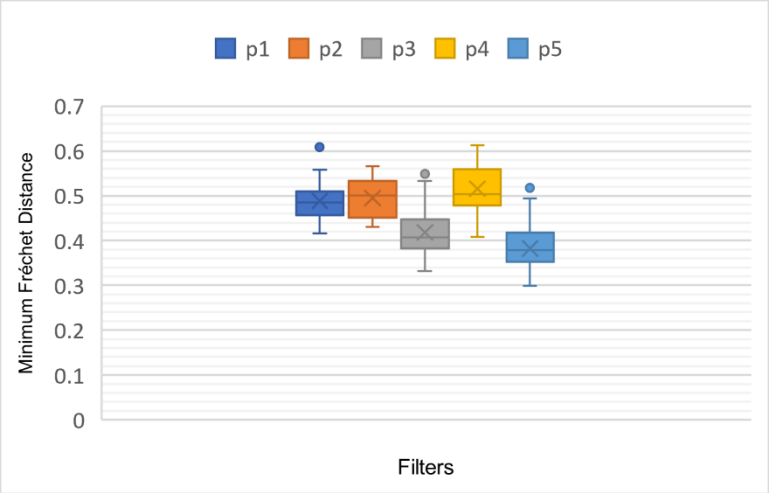

Figure 4.12: The range of minimum Fréchet distance using multiple testing data of one subject.

4.5 Experiment Setups

We have applied our proposed method using multiple ECGs of 62 subjects from the ECG ID database. The experiments set up are designed according to the following steps:

1. For each subject (m), starting from subject 1 to subject 62 (n_{sb}) :

   1.1 A random test data $\boldsymbol{X_m^t}$ is selected from day 2-ECG.

   1.2 Next, the five filtered test ECGs are created using equations 1 to 3 and they are labeled as $\boldsymbol{\hat{X}_{1,m}^t}$, $\boldsymbol{\hat{X}_{2,m}^t}$, $\boldsymbol{\hat{X}_{3,m}^t}$, $\boldsymbol{\hat{X}_{4,m}^t}$ and $\boldsymbol{\hat{X}_{5,m}^t}$.

   1.3 Then, the five spectral feature matrices are computed from each of the filtered test ECGs and labeled as $\hat{F}_{1,m}^t$, $\hat{F}_{2,m}^t$, $\hat{F}_{3,m}^t$, $\hat{F}_{4,m}^t$ and $\hat{F}_{5,m}^t$.

   1.4 After that, for each subject (n) starting from subject 1 to subject 62,

      1.4.1 A random reference data $\boldsymbol{X_n^r}$ is selected from day 1-ECG.

1.4.2 Next, step 1.2 is repeated to create the five filtered reference ECGs and labeled as $\widehat{\boldsymbol{X}}_{\boldsymbol{1,n}}^{\boldsymbol{r}}$, $\widehat{\boldsymbol{X}}_{\boldsymbol{2,n}}^{\boldsymbol{r}}$, $\widehat{\boldsymbol{X}}_{\boldsymbol{3,n}}^{\boldsymbol{r}}$, $\widehat{\boldsymbol{X}}_{\boldsymbol{4,n}}^{\boldsymbol{r}}$ and $\widehat{\boldsymbol{X}}_{\boldsymbol{5,n}}^{\boldsymbol{r}}$.

1.4.3 Then, step 1.3 is repeated to extract the five spectral feature matrices and labeled as $\hat{F}_{1,n}^{r}$, $\hat{F}_{2,n}^{r}$, $\hat{F}_{3,n}^{r}$, $\hat{F}_{4,n}^{r}$ and $\hat{F}_{5,n}^{r}$.

1.5 After that, the Fréchet distance between each test feature in step 1.3 and its corresponding many refence features in step 1.4.2 is calculated using equation (4.4). In addition, the results are stored in the following distance vectors $FD_{1,m} \in R^{n_{sb}}$,$FD_{2,m} \in R^{n_{sb}}$,$FD_{3,m} \in R^{n_{sb}}$,$\mathrm{FD}_{4,\mathrm{m}} \in R^{n_{sb}}$ and $FD_{5,m} \in R^{n_{sb}}$.

1.6 Then using equation (4.7), the classification process is performed based on the minimum Fréchet distance in each of the five distance vectors that are obtained from step 1.5. and the results are stored in the $\boldsymbol{C_p} \in R^{n_p}$ vector.

1.7 Also, the values of the corresponding five minimum distances are stored in the $\boldsymbol{D_p} \in R^{n_p}$ vector.

2. Next, equations (4.9), (4.10) are used to find a weighted score for each identity that is picked by step 1.6.
3. After that, the final level classification is performed using equation (4.11).
4. Next, steps 1 to 3 are repeated 50 times (n_{exp}) for each subject.
5. Finally, we obtained the $ID \in R^{n_{sb} \times n_{sb}}$ matrix which contains the final classification results of all the experiments, according to Figure 4.13, the rows of the ID matrix represent the actual identities (the true subjects), and the columns represent the rate of predicted identities to the total number of experiments per row (the identities that are obtained by the classification process).

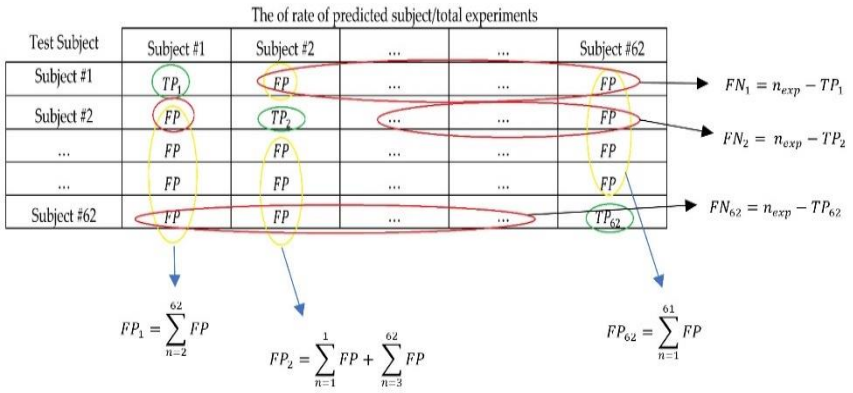

Figure 4.13:The output of the classification process using WMVM

In addition, for each subject (row), the elements of the ID matrix are defined as:

i. TP_m which is the diagonal element ($id_{m,m}$) representing the total number of times the m^{th} subject is truly identified using WMVM (when the test data was selected from the m^{th} subject).

ii. FN_m which represents the total number of times the m^{th} subject is falsely not identified using WMVM when the test data was selected from the m^{th} subject (the corresponding row elements except the diagonal element). The FN_m is calculated using equation (4.12):

$$FN_m = n_{exp} - TP_m \tag{4.12}$$

iii. FP_m which represents the total number of times the m^{th} subject is falsely identified using WMVM when the test data was selected from different subjects (the corresponding column elements except the diagonal element). The FP_m is calculated using the equation (4.13):

$$FP_m = id_{m.m} - \sum_{n=1}^{n_{sb}} id_{m,n} \tag{4.13}$$

iv. TN_m which represents the total number of times the m^{th} subject is truly not identified using WMVM when the test data was selected from different subjects (the corresponding off diagonal elements). The TN_m is calculated using the equation (4.14):

$$TN_m = \left(n_{exp} - 1\right) \times n_{sb} - FP_m \tag{4.14}$$

4.6 Results

4.6.1 Identification results based on using the wavelet filters individually

We examined the performance of our method in terms of the personal identification accuracy using equation (4.15) such that:

$$acc_{p,m} = \frac{TP_{m,p}}{n_{exp}} x100 \tag{4.15}$$

where $acc_{p,m}$ is the personal identification accuracy of the m^{th} subject using the p^{th} filter, exp is the experiment number with a total of n_{exp} many random experiments and $TP_{m,p}$ is the number of times that the m^{th} the subject is correctly identified using the p^{th} filter.

In addition, we evaluated the average identification accuracy of each filter using equation (4.16):

$$acc_p = \frac{1}{n_{sb}} \sum_{m=1}^{n_{sb}} acc_{p,m} \tag{4.16}$$

where acc_p is the average identification accuracy of the p^{th} filter.

The personal identification accuracy using our filtering system has shown good results. Consequently, Figure 4.14 shows full details of the personal identification accuracy at each filter. In addition, Table 4.2 shows that most of the subjects are identified with an identification accuracy ranging from 91% to 100% with best findings of 42 subjects. Furthermore, Figure 4.15 shows the average identification accuracy using each filter individually with the best findings of 85.55% for

filter p_2. These results indicates that all the ECG wavelet components are informative; however, utilizing only a single filtering channel does not appropriately identify majority of the subjects. Therefore, fusing the information obtained from of all these filters is a mandatory task to achieve the best possible performance.

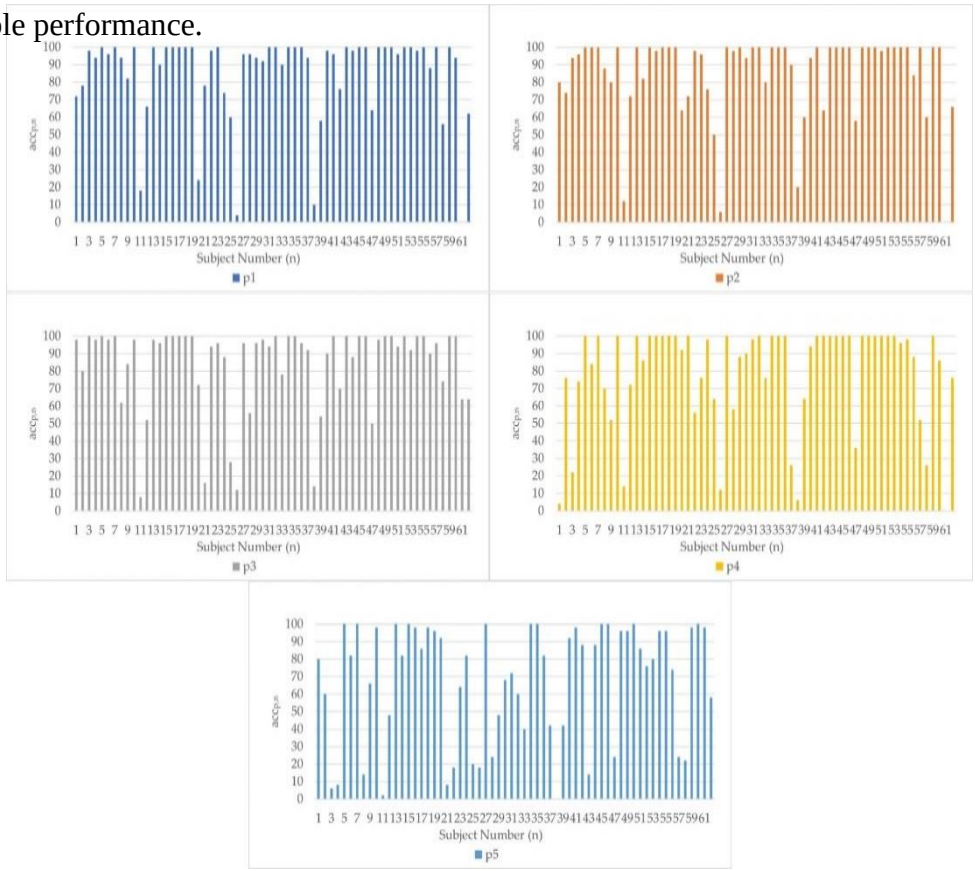

Figure 4.14: The personal identification accuracy using each filter individually

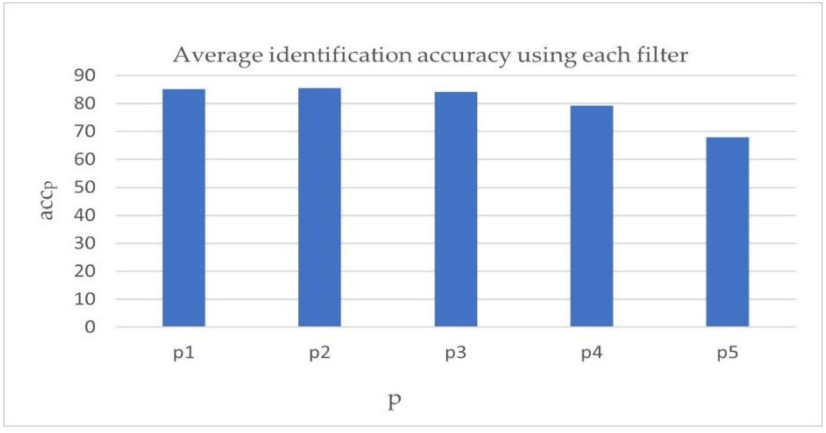

Figure 4.15: The Average identification accuracy using each filter individually

Table 4.2: Total subjects identified per accuracy range using each filter

Personal Identification Accuracy	91- 100 (%)	81- 90 (%)	71- 80 (%)	Less than 70%	MODWT Filter
Total Subjects Identified	42	4	5	11	p_1
	40	4	7	11	p_2
	40	5	4	13	p_3
	34	6	6	16	p_4
	24	8	5	25	p_5

4.6.2 Identification Results based on data fusion using the WMVM

We evaluated the performance of our proposed method after we performed data fusion using the WMVM. The personal identification accuracy is calculated using equation (4.17):

$$acc_{wm,m} = \frac{TP_m}{n_{exp}}\ x100 \tag{4.17}$$

where $acc_{wm,m}$ is the personal identification accuracy of the m^{th} subject

In addition, we evaluated the average identification accuracy of our proposed method using equation (4.18):

$$acc_{wm} = \frac{1}{n_{sb}} \sum_{m=1}^{n_{sb}} acc_{wm,m} \tag{4.18}$$

Consequently, the personal identification accuracy has significantly increased as shown Table 4.3. After we combined the information using the WMVM, 53 subjects are identified with an identification accuracy ranging from 91% to 100%. In addition, Figure 4.16 shows the full details of the personal identification accuracy for each subject. Moreover, Table 4.4 shows the average identification accuracy of the proposed method.

According to Table 4.4, we excluded six subjects who have less than 80% identification accuracy (subjects with red and yellow bars in Figure 4.16). These subjects are excluded because

none of the filtering channel were able to identify them which indicate that their ECG features from multiple days have significant variability. As a result, our proposed method for ECG based human identification which is based on filtrating some of the wavelet components and applying the WMVM for data fusion has achieved 98.07% identification accuracy. These findings indicate that applying the WMVM is significantly useful since it accurately combines information obtained from multiple filtering channels to correctly reach the final class.

Table 4.3: Total subjects identified per accuracy range using the WMVM

Personal Identification Accuracy	91- 100 (%)	81- 90 (%)	71- 80 (%)	Less than 70%
Total Subjects Identified	53	3	2	4

Table 4.4: Average Identification Accuracy of the proposed method

Average Identification Accuracy	92.29%	97.24%	98.07%
Number of Subjects	62	58	56

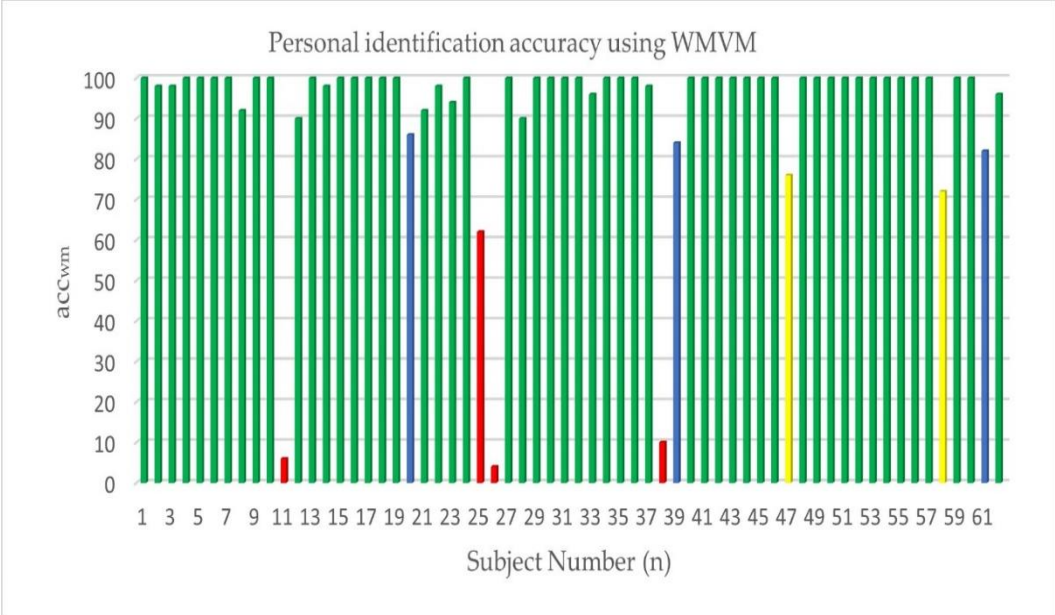

Figure 4.16: The personal identification accuracy using the WMVM

4.6.3 Performance evaluation of the proposed method

Moreover, we evaluated the general performance of our proposed method using the following parameters:

Precision: the rate of truly identifying subjects to the total number of identifications:

$$Precision = \frac{1}{n_{sb}} \sum_{m=1}^{n_{sb}} \frac{TP_{\mathrm{m}}}{TP_m + FP_{\mathrm{m}}} \tag{4.19}$$

Recall/True Positive Rate (TPR): the rate of truly identifying subjects to the total number of identification attempts:

$$Recall = \frac{1}{n_{sb}} \sum_{m=1}^{n_{sb}} \frac{TP_m}{TP_m + FN_m} \tag{4.20}$$

False Rejection Rate (FRR): the rate of falsely not identifying subjects to the total number of identification attempts:

$$FRR = \frac{1}{n_{sb}} \sum_{m=1}^{n_{sb}} \frac{FN_m}{TP_m + FN_m} \tag{4.21}$$

False Acceptance Rate (FAR) / False Positive Rate (FPR): the rate of falsely identifying subjects to the total number of rejection attempts:

$$FAR = \frac{1}{n_{sb}} \sum_{m=1}^{n_{sb}} \frac{FP_m}{TN_m + FP_m} \tag{4.22}$$

Accordingly, Table 4.5 shows the precision, recall, FAR and FRR parameters computed by performing classification at each filter. As a result, the best findings are achieved via applying the p_2 filter with 0.8631 precision, 0.8555 recall, 0.1445 FRR, and 0.0024 FAR. Consequently, after performing data fusion using the WMVM the precision \recall parameters have significantly increased and the FRR \FAR have significantly decreased. As a result, we achieved 0.9495

precision, 0.9229 recall, 0.0771 FRR and 0.0013 FAR. Additionally, Figure 4.17 shows the performance comparison using each filter individually and after performing data fusion using WMVM.

Table 4.5: Performance evaluation of the proposed method

Filter / data fusion	Precision	Recall	FRR	FAR
p_1	0.8624	0.8519	0.1481	0.0024
p_2	0.8631	0.8555	0.1445	0.0024
p_3	0.8680	0.8423	0.1577	0.0026
p_4	0.8069	0.7919	0.2080	0.0034
p_5	0.6787	0.6878	0.3213	0.0053
WMVM	0.9495	0.9229	0.0771	0.0013

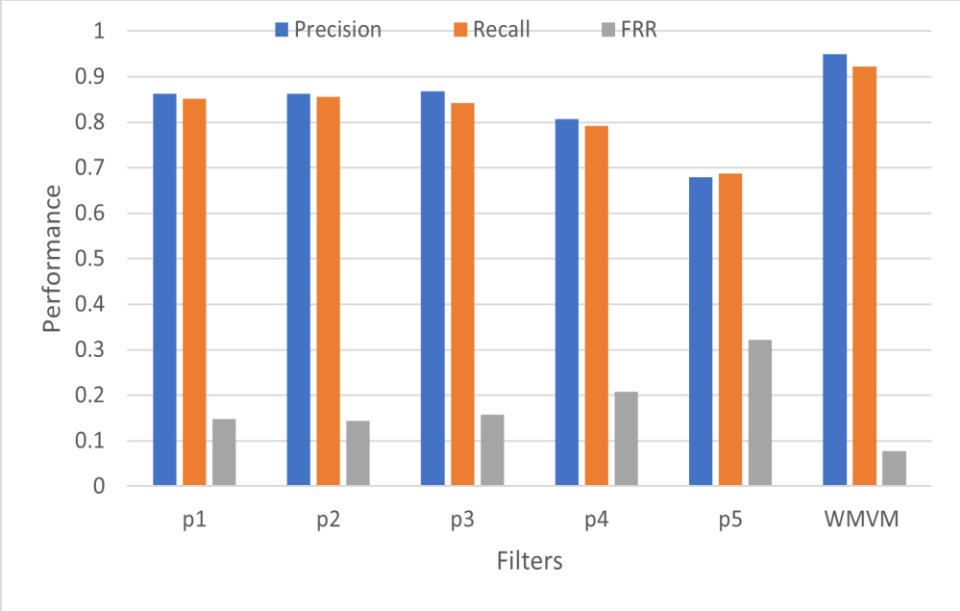

Figure 4.17: Performance evaluation of the proposed method.

Moreover, we evaluated the performance of the proposed method using the receiver operating characteristic curve (ROC), which shows the tradeoff between the true positive rate and false positive rate. Consequently, Figure 4.18 shows the ROC of the proposed method with the closest curve to the top left corner achieved via performing data fusion. In addition, we obtained our highest area under the curve (ROC AUC) that is equal to 0.9608 via applying the WMVM.

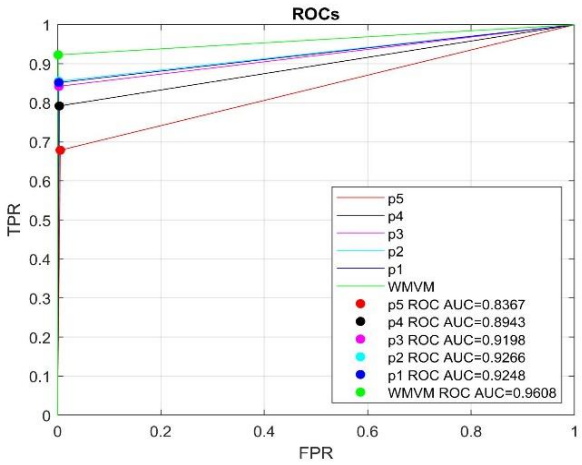

Figure 4.18: The ROCs of the Proposed

Furthermore, we analyzed the performance using the precision recall curve (PR) as shown in Figure 4.19. Consequently, the best results are also obtained after performing data fusion. According to Figure 4.19, the closest curve to the top right corner with PR AUC equal to 0.9362 is achieved via using the WMVM. As previously mentioned, we repeated the process of randomly selecting the test data 50 times for each subject. Consequently, Figure 4.20 shows the cross-validation results in terms of the average identification accuracy of each experiment. These results further shows that filtering some of the wavelet components and performing data fusion using the proposed voting method can be utilized to identify subjects from multiple ECGs.

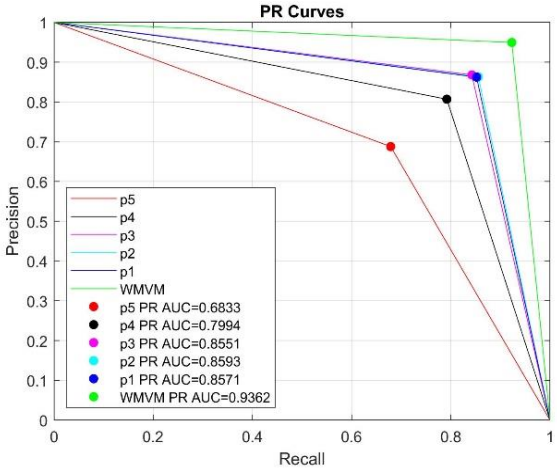

Figure 4.19: The PR curves of the Proposed Method

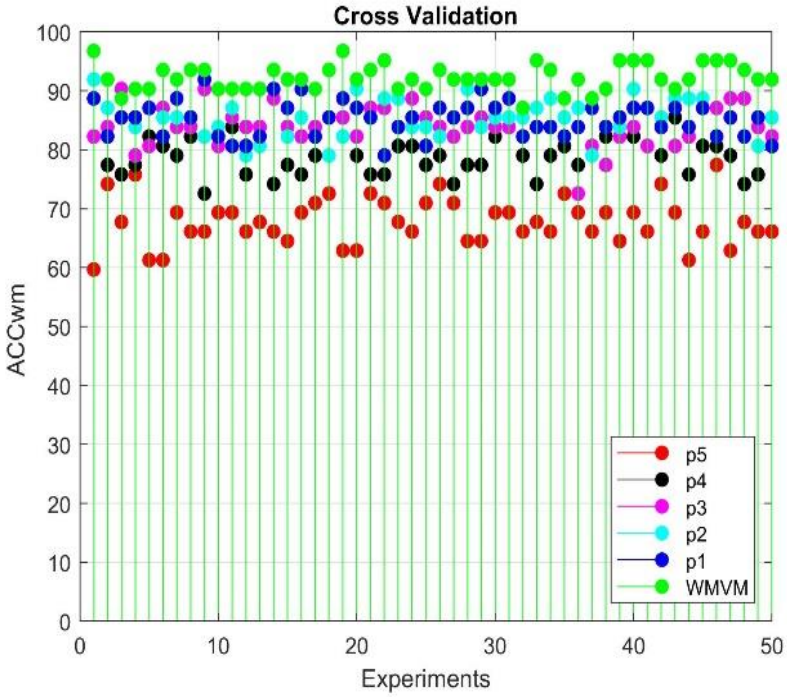

Figure 4.20: The cross-validation results

4.7 Discussion

In general, the use of ECG for human identification is challenging task that depends mainly on choosing the appropriate features and classifiers [22] [1] [2] [5]. Different studies have presented different ECG features which can be utilized for biometric purposes [3]. In our previous work we also proposed a study on the most appropriate features and classifiers [38]. However, the stability of ECG features remains the most challenging task for utilizing the cardiac signal as biometric modality for real applications [23]. Previous studies have achieved excellent identification results; however, topics regarding the variability of ECG features were not discussed [38] [22] [4] [52]. Therefore, we proposed a methodology to investigate the feasibility of human identification using multiple ECGs that are recorded at different days.

Table 4.5 shows performance comparison with the state-of-the-art methods and it summarizes the main algorithms that are used in these previous approaches. In comparison, the performance of our method has shown excellent results compared to some of the approaches in the literature [26] [29] [32] [33] . In addition, our performance slightly exceeded some of the recent methods in ECG biometrics which are based on time frequency analysis of the cardiac signal [28] [30] [34]. Although method [27] reported 100% accuracy, the authors used ECG data of 21 subjects which make the use of such method very limited due to the small data size. The method of Ciocoiu et al. [31], which is based on converting the ECG heartbeat segments into images and utilizing the CNN for classification, has slightly exceeded our performance. However, the performance of method [31] considering the variability of ECG features among multiple records was not reported. In comparison, this paper presents a contribution that is based on MODWT to address the variability of ECG features. In addition, we present our WMVM which is used to combine the multiple decisions obtained from our multi-channel filtering system to reach a single common decision for identification purposes. Finally, the experimental results show that our proposed method has shown excellent results up to 98.07% identification accuracy and with 53 subjects having a personal identification accuracy ranging from 90% to 100%.

In addition, to make our proposed method clinically applicable, the ECG can be utilized in multibiometric identification systems. The combination of the intrinsic characteristic of the ECG with the extrinsic characteristics of some of the existing biometrics such voice and iris can increase patient security in clinics. Additionally, clinics can benefit from deploying the ECG biometrics in telemedicine to update the personal records periodically for identification purposes. Generally, ECG records should be updated according to the personal health status and age to be utilized for human identification [20].

Table 4.6: Summary of the previous state of art and the proposed methodology on the ECG based human identificatio

Authors	Methodology	Accuracy
Dar et al. [26]	Proposed a multiresolution analysis of the DWT features using the Har wavelet coefficients of the heartbeats	82.3%
Lee et al. [28]	Proposed a time frequency representation of the ECG data using the robust RPCANet and DWT	97.5%
Arwa et. Al [29]	Developed a wavelet-based method to extract the ECG power and energy features and utilizing Euclidean and linear discriminant analysis (LDA) classifiers for identification	83.3%
Abdeldayem et. Al [30]	Proposed a methodology based the Spectro-temporal dynamic characteristics of the ECG signal using short time Fourier STFT, Morse wavelets and CNN.	97.86%
Choi et al. [32]	Introduced a method to convert the ECG data into 2D resized spectrograms that are utilized for identification	93%
Kim et al. [33]	Proposed a method based on likelihood ratio test (GLRT) and composite hypothesis testing	93%
Tan et. Al [34]	Presented a methodology that is based on the time frequency distribution of the ECG and the statistical n-best adaptive Fourier decomposition (SAFD)	98%
Proposed Method	Proposed a filtering system that is based on MODWT to test the ECG feasibility of human identification using multiple signals and performing weighted majority voting method (WMVM) for decision fusion	98.07%

However, there are some limitations to our methodology. Specifically, topics on optimizing the number of filters, ECG data clustering and personal ECG selection for enrolment purposes need to be addressed in future work. According to Figure 4.13, the number of MODWT filters that are required to correctly identify individuals is subject relevant, which may limit the applicability of our method due to the long computational time. However, optimizing techniques might address this problem to reduce the number of required filters. Also, implementing our method requires to cluster the ECG into different groups to further reduce the screening time since our method depends on finding the minimum Fréchet distance of one random testing data and all the referencing data. Therefore, clustering the ECG will address such problem. In our feature work we will address this problem by utilizing the MODWT scaling coefficients to cluster the ECG referencing data. Moreover, our method was evaluated based only on two ECG records per subject. therefore, the applicability of our method should be investigated on larger ECG records. Accordingly, future work should focus on selecting the most appropriate personal ECG records which may require to perform similarity measurements algorithm at the enrolment stage of the biometric system.

4.8 Conclusion

One of the main challenges to utilize ECG for human identification is to address the variability of ECG features across multiple records [5] [22]. To solve this problem, we proposed a methodology for human identification using multiple ECGs via applying data filtering and data fusion techniques. To model the changeability of ECG features over multiple records, we utilized the MODWT to create a multi-channel filtering system that is used for partitioning the variability of ECG features according to its wavelet components followed by removing different wavelet

components at different levels of the filtering system [39]. The proposed filtering system is utilized to identify subjects with reduced amounts of the signal information through filtering the wavelet components that may have significant change across multiple ECG records [40]. In addition, we proposed the WMVM technique which is utilized to combine information obtained from multiple filtering channels [41]. The WMVM is a scoring technique based on the minimum Fréchet distances and it utilized to obtain a common final decision for reaching correct identification. The experimental results have shown that our proposed method has achieved an identification accuracy ranging from 92.29% to 98,07%. In addition, we achieved 0.9495 precision, 0.9229 recall, 0.0771 FRR and 0.0013 FAR. In conclusion, ECG based human identification using multiple ECGs is feasible. However, it requires to implement methods that are adaptable with variability ECG features because it may adversely influence the performance of biometric applications.

References

[1] L. Biel, O. Pettersson, L. Philipson, and P. Wide, "ECG analysis: a new approach in human identification " *IEEE Transactions on,Instrumentation and Measurement,* vol. 50, no. 3, pp. 808–812, 2001.

[2] M. Ingale, R. Cordeiro, S. Thentu, Y. Park, and N. Karimian, "ECG Biometric Authentication: A Comparative Analysis," *IEEE Access,* vol. 8, pp. 117853-117866, 2020.

[3] A. N. Uwaechia and D. A. Ramli, "Comprehensive Survey on ECG Signals as New Biometric Modality for Human Authentication: Recent Advances and Future Challenges," *IEEE Access,* vol. 9, pp. 97760-97802, 2021.

[4] S. Dargan and M. Kumar, "A comprehensive survey on the biometric recognition systems based on physiological and behavioral modalities," *Expert Syst. Appl.,* vol. 143, no. 113114, 2020.

[5] J. Ribeiro Pinto, J. S. Cardoso, and A. Lourenço, "Evolution, Current Challenges, and Future Possibilities in ECG Biometrics," *IEEE Access*, vol. 6, pp. 34746-34776, 2018.

[6] D. Wang, Y. Si, W. Yang, G. Zhang, and J. Li, "A Novel Electrocardiogram Biometric Identification Method Based on Temporal-Frequency Autoencoding," *Electronics*, vol. 8, no. 6, p. 667, 2019.

[7] R. D. Labati, E. Muñoz, V. Piuri, R. Sassi, and F. Scotti, "Deep-ECG: Convolutional neural networks for ECG biometric recognition," *Pattern Recognit. Lett.* , vol. 126, pp. 78–85, 2019.

[8] J. Xu, G. Yang, K. Wang, Y. Huang, H. Liu, and Y. Yin, "Structural sparse representation with class-specific dictionary for ECG biometric recognition," *Pattern Recognit. Lett.*, vol. 135, pp. 44-49, 2020.

[9] N. Belgacem, F. Bereksi-Reguig, A. Nait-Ali, and R. Fournier, "Person identification system based on electrocardiogram signal using LabVIEW," *Int. J. Comput. Sci. Eng.*, vol. 4, no. 6, p. 974, 2012.

[10] J. Nelson, "Chapter 12 - Biometrics Characteristics," in *Effective Physical Security (Fourth Edition)*: Fennelly, Lawrence J., 2013, pp. 255-256.

[11] P. Pagliaro, C. Penna, and R. Rastaldo, "3 Cardiac Electrophysiology," in *Basic Cardiovascular Physiology: From Molecules to Translational Medical Science*: River Publishers, 2020, pp. 27-40.

[12] P. Pagliaro, C. Penna, R., and Rastaldo, "5 The Cardiac Cycle," in *Basic Cardiovascular Physiology: From Molecules to Translational Medical Science*: River Publishers, 2020, pp. 65-94.

[13] J. C. George and H. M. Paul, "Chapter 21 - Cardiovascular Physiology: Integrative Function," in *Pharmacology and Physiology for Anesthesia*. Philadelphia: W.B. Saunders, 2013, pp. 366-389.

[14] Y. A. Altay, A. S. Kremlev, and A. Margun, A,, "ECG Signal Filtering Approach for Detection of P, QRS, T Waves and Complexes in Short Single-Lead Recording," *2019 IEEE Conference of Russian Young Researchers in Electrical and Electronic Engineering (EIConRus),* pp. 1135-1140, 2019.

[15] A. Kharshid, H. S. Alhichri, R. Ouni, and Y. Bazi, "Classification of Short-time Single-lead ECG Recordings Using Deep Residual CNN," *2019 2nd International Conference on new Trends in Computing Sciences (ICTCS),* pp. 1-6, 2019.

[16] S. S. Abdeldayem and T. Bourlai, "A Novel Approach for ECG-Based Human Identification Using Spectral Correlation and Deep Learning," *IEEE Transactions on Biometrics, Behavior, and Identity Science,* vol. 2, no. 1, pp. 1-14, 2020.

[17] F. Agrafioti and D. Hatzinakos, "Ecg biometric analysis in cardiac irregularity conditions," *Signal, Image and Video Processing,* vol. 3, no. 4, 2009.

[18] R. Hoekema, G. J. H. Uijen, and A. van Oosterom, "Geometrical aspects of the inter-individual variability of multilead ECG recordings," *Proc. Comput. Cardiology,* vol. 26, pp. 499–502, 1999.

[19] R. Hoekema, G. J. H. Uijen, and A. van Oosterom, "Geometrical aspects of the interindividual variability of multilead ECG recordings," *IEEE Trans. Biomed. Eng,* vol. 48, no. 5, pp. 551–559, 2001.

[20] J. A. Schijvenaars, "Intra-individual Variability of the Electrocardiogram: Assessment and exploitation in computerized ECG analysis," *Ph.D. dissertation, Dept. Med. Inform., Erasmus Univ. Rotterdam,* 2000.

[21] P. Langley, E. J. Bowers, and A. Murray, "Principal Component Analysis as a Tool for Analyzing Beat-to-Beat Changes in ECG Features: Application to ECG-Derived Respiration," *IEEE Transactions on Biomedical Engineering,* vol. 57, no. 4, pp. 821-829, 2010.

[22] S. k. Berkaya, A. k. Uysal, E. S. Gunal, S. Ergin, S. Gunal, and G. M. B., "A survey on ECG analysis " vol. 43, pp. 216–235, 2018.

[23] S.-C. S.-C. Wu, P.-L. Hung, and A. L. Swindlehurst, "ECG biometric recognition: Unlinkability, irreversibility, and security," *IEEE Internet Things J.*, vol. 8, no. 1, pp. 487–500, 2021.

[24] A. P. Nemirko and T. S. Lugovaya, "Biometric human identification based on electrocardiogram," pp. 387–390., 2005.

[25] T. S. Lugovaya, "Biometric human identification based on electrocardiogram," *M.S. thesis, Faculty Comput. Technol. Inform., Saint Petersburg Electrotech. Univ., Saint Petersburg,* 2005.

[26] M. N. Dar, M. U. Akram, A. Usman, and A. Khan, "ECG biometric identification for general population using multiresolution analysis of DWT based features," *2015 Second International Conference on Information Security and Cyber Forensics (InfoSec),* pp. 5-10, 2015.

[27] M. E. Naraghi and M. B. Shamsollahi, "ECG based human identification using wavelet distance measurement," *2011 4th International Conference on Biomedical Engineering and Informatics (BMEI)*, pp. 717-720, 2011.

[28] J.-N. J. Lee and K.-C. Kwak, "Personal Identification Using a Robust Eigen ECG Network Based on Time-Frequency Representations of ECG Signals," *IEEE Access*, vol. 7, pp. 48392-48404, 2019.

[29] A. Elamin and M. Y. Esmail, "Wavelet-Based ECG Signal Analysis for Human Recognition," *2020 International Conference on Computer, Control, Electrical, and Electronics Engineering (ICCCEEE)*, pp. 1-7, 2020.

[30] S. S. Abdeldayem and T. Bourlai, "ECG-based Human Authentication using High-level Spectro-temporal Signal Features," *2018 IEEE International Conference on Big Data (Big Data)*, pp. 4984-4993, 2018.

[31] I. B. Ciocoiu and N. Cleju, "Off-Person ECG Biometrics Using Spatial Representations and Convolutional Neural Networks," *IEEE Access*, vol. 8, pp. 218966-218981, 2020.

[32] G. Choi, E. Bak, and S. Pan, "User Identification System Using 2D Resized Spectrogram Features of ECG," *IEEE Access*, vol. 7, pp. 34862-34873, 2019.

[33] H. Kim and S. Chun, Y, "Cancelable ECG Biometrics Using Compressive Sensing-Generalized Likelihood Ratio Test," *IEEE Access*, vol. 7, pp. 9232-9242, 2019.

[34] C. Tan, l. Zhang, T. Qian, B. S, and A. J. Pinho, "Statistical n-Best AFD-Based Sparse Representation for ECG Biometric Identification," *IEEE Transactions on Instrumentation and Measurement*, vol. 70, pp. 1-13, 2021.

[35] R. D. Labati, R. Sassi, and F. Scotti, "ECG biometric recognition:Permaence analysis of QRS signals for 24 hours continuous authentication," *Proc. IEEE Int. Workshop Inf. Forensics Secur. (WIFS),* pp. 31-36, 2013.

[36] O. Boumbarov, Y. Velchev, and S. Sokolov, "ECG personal identification in subspaces using radial basis neural networks," *Proc. IEEE IDAACS,,* pp. 446–451, 2009.

[37] Z. Hassan, S. O. Gilani, and M. Jamil, "Review of fiducial and non fiducial techniques of feature extraction in ECG based biometric systems," *Indian J. Sci. Technol.,* vol. 9, no. 21, pp. 850–855, 2016.

[38] A. Biran and A. Jeremic, "Non-Segmented ECG bio-identification using Short Time Fourier Transform and Fréchet Mean Distance.," in *Annu Int Conf IEEE Eng Med Biol Soc.* , 2020.

[39] C. R. Cornish, C. S. Bretherton, and D. B. Percival, "Maximal Overlap Wavelet Statistical Analysis With Application to Atmospheric Turbulence," *Boundary-Layer Meteorology,* vol. 119, pp. 339-374, 2006.

[40] S. Cruces, R. Martín-Clemente, and W. Samek, "Information Theory Applications in Signal Processing," *Entropy (Basel),* vol. 21, no. 7, 2019.

[41] B. Khaleghi, A. Khamis, F. O. Karray, and S. N. Razavi, "Multisensor data fusion: A review of the state-of-the-art," *Informartion Fusion,* vol. 14, no. 1, pp. 28–44, 2013.

[42] H. D. Hesar and M. Mohebbi, "A Multi Rate Marginalized Particle Extended Kalman Filter for P and T Wave Segmentation in ECG Signals," *IEEE Journal of Biomedical and Health Informatics,* vol. 23, no. 1, pp. 112-122, 2019.

[43] S. Modak, L. Y. Taha, and E. Abdel-Raheem, "A Novel Method of QRS Detection Using Time and Amplitude Thresholds With Statistical False Peak Elimination," *IEEE Access,* vol. 9, pp. 46079-46092, 2021.

[44] H. Chen and K. Maharatna, "An Automatic R and T Peak Detection Method Based on the Combination of Hierarchical Clustering and Discrete Wavelet Transform," *IEEE Journal of Biomedical and Health Informatics,* vol. 24, no. 10, pp. 2825-2832, 2020.

[45] T. H. Chowdhury, K. N. Poudel, and Y. Hu, "Time-Frequency Analysis, Denoising, Compression, Segmentation, and Classification of PCG Signals," *IEEE Access,* vol. 8, pp. 160882-160890, 2020.

[46] M. R. Howard, "Background: Signal and System Theory," in *Principles of Random Signal Analysis and Low Noise Design: The Power Spectral Density and its Applications*: IEEE, 2002, pp. 3-58.

[47] S. Banerjee and M. Mitra, "Application of Cross Wavelet Transform for ECG Pattern Analysis and Classification," *IEEE Transactions on Instrumentation and Measurement,* vol. 63, no. 2, pp. 326-333, 2014.

[48] S. R. Stahlschmidt, B. Ulfenborg, and J. Synnergren, "Multimodal deep learning for biomedical data fusion: a review," *Briefings in Bioinformatics,,* vol. 23, no. 2, pp. 1-15, 2022.

[49] D. W. and M. Kam, "Dependent Randomization in Parallel Binary Decision Fusion," *IEEE/CAA Journal of Automatica Sinica,* vol. 8, no. 2, pp. 361-376, 2021.

[50] W. Yang, B. Chen, and L. Yu, "Bayesian-Wavelet-Based Multisource Decision Fusion," *IEEE Transactions on Instrumentation and Measurement,* vol. 70, pp. 1-10, 2021.

[51] P. Shao, Y. Yi, Z. Liu, T. Dong, and D. Ren, "Novel Multiscale Decision Fusion Approach to Unsupervised Change Detection for High-Resolution Images," *IEEE Geoscience and Remote Sensing Letters,* vol. 19, pp. 1-5, 2021.

[52] S. H. Jambukia, V. K. Dabhi, and H. B. Prajapati, "Classification of ECG ignals using machine learning techniques: A survey," *Proc. Int. ConfAdv. Comput. Eng. Appl*, pp. 714–721, 2015.

Chapter 5

5 Discussion and Conclusion

5.1 Research Overview

There are many human traits that have been studied for the purpose of human identification. In this thesis, we developed multiple methods for investigating the feasibility of human identification using the public ECG ID database. In short, we utilized both the ECG fiducial and non-fiducial features as unique characteristics for identification purposes (Chapter 2). In addition, we developed a technique to study how these features change from heartbeat to heartbeat (Chapter 3). At the classification stage, we provided a comparative study on the importance of using the Fréchet distance for finding the minimum distance between feature matrices (Chapters 3 and 4). Lastly, we addressed the variability of ECG features obtained from multiple records along with performing data fusion techniques for application purposes (Chapter 4). Table 5.1 shows summary of our proposed methods for ECG based human identification.

5.2 Comparison between the Proposed Methods

5.2.1 Comparison between the Proposed Fiducial Approaches

In general, both proposed fiducial approaches have shown good results as shown in Figure 5.1. Consequently, method 1 has shown higher performance than method 4. However, there are many factors which affect the performance of these approaches such as 1) finding the exact location of fiducial points due to the lack of general rules that define boundaries of the cardiac waves, and 2) the amount of componential time that is required to extract the fiducial features as well the general time constraints [1]. Therefore, the findings of this thesis suggests that the proposed fiducial

methods can be used as a supportive tool to identify subjects who have clear wave boundaries and less variant fiducial features.

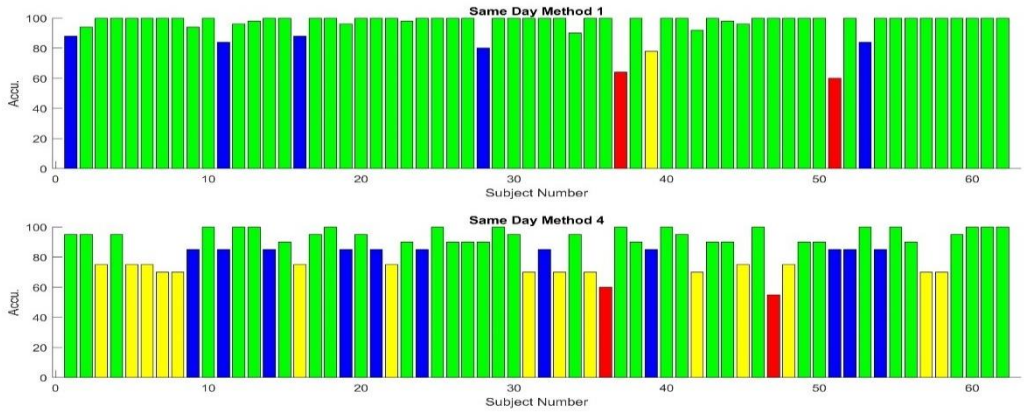

Figure 5.1: Comparison between the performance of the fiducial approaches (methods 1 and 4) in terms of the average personal identification accuracy

5.2.2 Comparison between the Proposed Non-Fiducial Approaches (Single ECG Record)

All the proposed non fiducial approaches have shown excellent results when the referencing and testing data are selected from a single ECG record (same day). In comparison, method 2 has shown higher performance than method 3 as previously reported in chapter 2, chapter 3, and Table 5.1. However, method 3 provides instantaneous information of the frequency components while method 2 provides general information of the frequency components. To present a fair comparison, we also tested the performance of method 5 using ECG data selected from a single record. Consequently, method 5 outperformed methods 2 and 3 as shown in Figure 5.2. However, method 5 requires larger computational time to identify individuals. In short, the findings of this thesis suggests that the proposed non fiducial methods can be used to identify subjects using single ECG record because the non-fiducial features are likely to be similar when it is measured within short time frame.

Table 5.1: Summary of our proposed methods for ECG based human identification and their performance

Paper No.	1		2		3
Method No.	1	2	3	4	5
Category	Fiducial	Non-Fiducial	Non-Fiducial	Fiducial	Non-Fiducial
Ref. and Testing Data	Same day	Same day	Same day	Same day	Different days
Preprocessing	Main filtered data	Main filtered data	Main filtered data	Main filtered data	Multiple wavelet filtered data
Feature Extraction	Matrices of stacked time and amplitude features	Matrix of frequency components from heartbeat to heartbeat	Matrix of the dynamic change in frequency components within the heartbeats	Matrices of dynamic time, distance, and amplitude features	Matrices of the dynamic change in frequency components within the heartbeats
Classification	Euclidean distance	Normalized Euclidean distance	Fréchet distance	Fréchet distance	Fréchet distance
Identification	Minimum distances and majority voting	Minimum distance	Minimum distance	Minimum distance	Minimum distances and weighted majority voting
No. of Subjects	62	62	62	62	56
Average Accuracy	96.42%	99.64%	97.03%	82.02%	98.07%
Average Identification Time	0.65 Sec	0.18 Sec	2.5 Sec	10 Sec	28 Sec
Precision	0.97	0.9965	0.9719	0.8294	0.9468
Recall	0.9642	0.9964	0.9703	0.8202	0.9807
FRR	0.0358	0.0035	0.0296	0.1798	0.0193
FAR	0.006	0.0001	0.0004	0.0029	0.0014

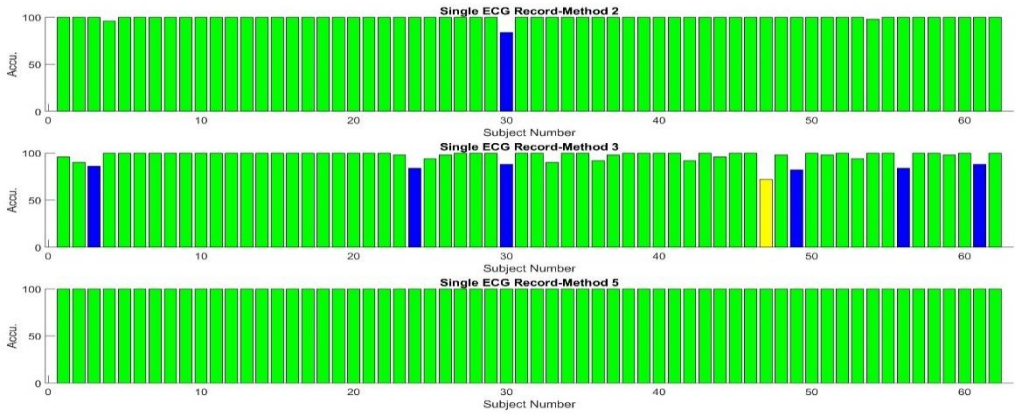

Figure 5.2: Comparison between the performance of the non fiducial approaches (methods 2, 3 and 5) in terms of the average personal identification accuracy using single ECG record.

5.2.3 Comparison between the Proposed Non-Fiducial Approaches (Multiple ECG Records)

Method 5 which is mainly based on identifying individuals using multiple ECG records has shown excellent performance as previously reported in chapter 4 and Table 5.1. To provide a fair comparison, we show in Figure 5.3 the performance of all the proposed non fiducial approaches considering that the referencing and testing data are selected from multiple ECG records. Unlike method 5 which addresses the variability of ECG features among multiple records, methods 2 and 3 are based on extracting features of unfiltered ECG data. Consequently, the average identification accuracy of methods 2 and 3 have significantly decreased to 47.29% and 46.59% respectively. This is expected because ECG features are more likely to be variable whenever it is extracted. Yet, methods 2 and 3 can be utilized to identify subjects who have less variant non-fiducial features (e.g., 23 subject using method 2 and 16 subjects using method 3). In short, the findings of this thesis suggests that method 5 can be used to identify subjects because it addresses the variability of non-fiducial features that are likely to be different when it is measured within long time frame.

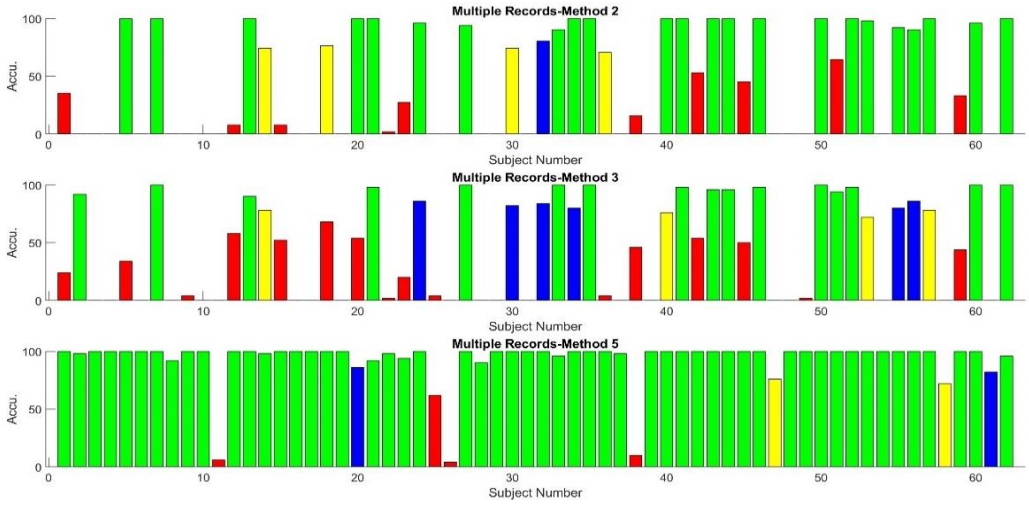

Figure 5.3: Comparison between the performance of the non fiducial approaches (methods 2, 3 and 5) in terms of the average personal identification accuracy using multiple ECG records.

5.3 Applications

The perspective use of ECG for human identification, which has been a subject of considerable research in the area of biometric recognition over the past decade, has shown promising results. In this thesis, we presented multiple methods that enclosed several aspects of ECG based biometric systems with the aim of real-world deployment. The potential impact of our methods extends to a board variety of application fields, ranging from security enhancement to gaming and auto industry. Some of the possible real-world applicability of our developed ECG biometric systems are include:

1. Enhancing security for multibiometric systems as supportive secondary tool (e.g., biometric applications based on fingerprint or iris).
2. Logging to single user applications for low security usage (e.g., phone).
3. In security control for applications benefiting from continues biometric monitoring (e.g., companies, banks and government buildings) [2].

4. In high security departments that require periodic data update in a short time frame ((e.g., companies, banks and government buildings).
5. Governmental applications that relay on data management and user services (e.g., Absher application in Saudi Arabia).
6. Other domains such as in electronic trading platforms for continuous identification, in gaming industry for identifying players and in auto industry for car sharing programs [3].

Despite the fact that ECG biometric application are highly beneficial since it is directly associated to intrinsic characteristics of the individual, yet few problems still exist. Specifically, the ECG permanence remain the biggest challenge for deploying it in real world applications.

5.4 List of Contributions

The contributions of this thesis are listed as follows:

1. Developing an ECG based biometric system to quickly identify individuals using non-fiducial characteristics of the cardiac signal.
2. Proposing an automatic method for QRS detection and segmentation.
3. Developing fiducial based methods to enhance the human recognition process for multibiometric systems.
4. Proposing a technique to compute ECG dynamic features to provide instantaneous information of the signal.
5. Utilizing non-Euclidean distances measures to calculate the minimum distance between feature matrices for classification purposes.
6. Addressing the variability of ECG features that are obtained from multiple records using data filtering methods.

7. Mathematically proposing a scoring technique for data fusing purposes to reach a final decision in multi-channel identification systems.

5.5 Future Work

There are few open problems that can be considered for future research as extension to the work that has been done in this thesis. In general, these problems are associated with the constraints on computational time and data volume. In short, the future work should focus on:

1. Clustering the ECG data into different groups to reduce the screening time.
2. Defining criteria on the appropriate number of ECG records that is required at the enrolment stage of the biometric system.
3. Optimizing the length of ECG data that is required for identification purposes according to real world applications.
4. Developing similarity measurement techniques to optimize the process of feature selection.
5. Optimizing the number of MODWT filtering channels to reduce the identification time.

Nevertheless, the biggest challenge for utilizing the ECG as biometric modality relate to its permanence which is open research question, and it requires a lot of time to collect large data base, finding volunteers and persuading ethics committee to prove the uniqueness of the ECG signal.

References

[1] D. P. Coutinho, H. Silva, H. Gamboa, A. Fred, and M. Figueiredo, "Novel fiducial and non-fiducial approaches to electrocardiogram-based biometric systems," *in IET Biometrics*, vol. 2, no. 2, pp. 64-75, February 2013.

[2] H. Plácido da Silva, A. Lourenco, F. Canento, A. Fred, and N. Raposo, *ECG Biometrics: Principles and Applications*. 2013.

[3] C. Carreiras, A. Lourenco, A. Fred, and R. Ferreira, ECG Signals for Biometric Applications - Are we there yet? 2014, *In Proceedings of the 11th International Conference on Informatics in Control, Automation and Robotics*, pp. 765-772.